AD-A179 512 INVESTIGATION OF PERIODIC PITCHING THROUGH THE STATIC STALL ANGLE OF ATTACK(U) AIR FORCE INST OF TECH WRIGHT-PATTERSON AFB OH SCHOOL OF ENGINEERING 1/2

UNCLASSIFIED E C STEPHEN MAR 87 AFIT/GAE/AA/87M-4 F/G 20/4 NL

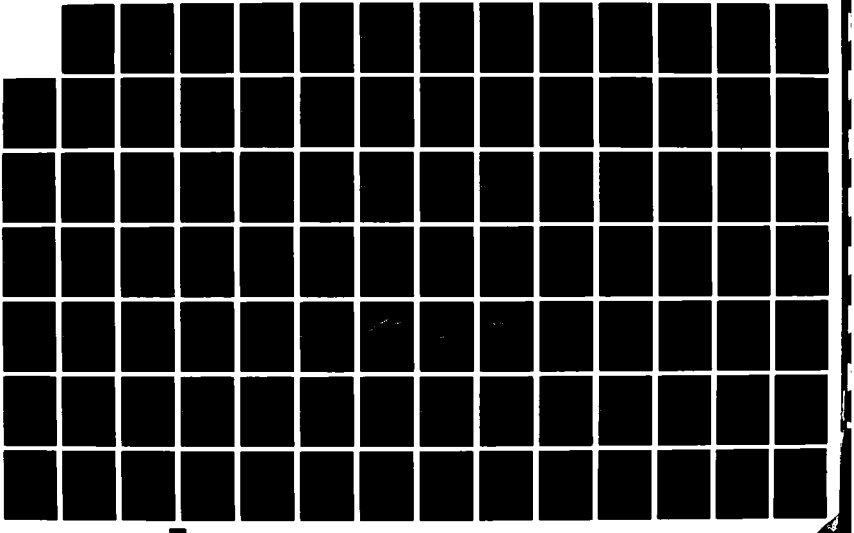

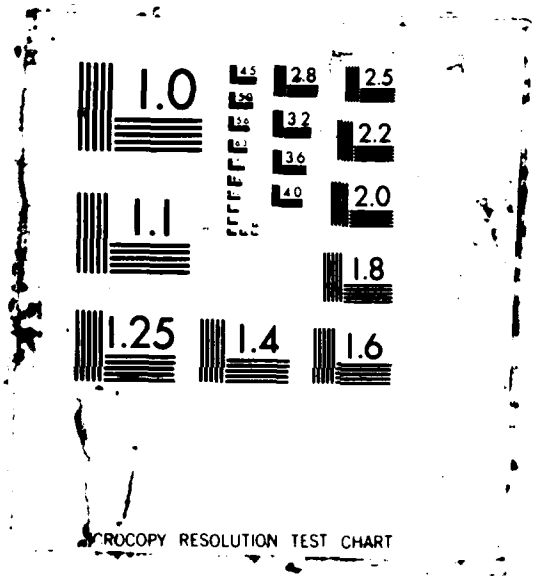
1.0
1.1
1.25
1.4
1.6
2.8
3.2
3.6
4.0
2.5
2.2
2.0
1.8
CROCOPY RESOLUTION TEST CHART

INVESTIGATION OF PERIODIC PITCHING HROUGH THE STATIC STALL ANGLE OF ATTACK

THESIS

Eric J. Stephen
Captain, USAF

AFIT/GAE/AA/87M-4

DEPARTMENT OF THE AIR FORCE
AIR UNIVERSITY
AIR FORCE INSTITUTE OF TECHNOLOGY

Wright-Patterson Air Force Base, Ohio

AFIT/GAE/AA/87M-4

INVESTIGATION OF PERIODIC PITCHING THROUGH THE STATIC STALL ANGLE OF ATTACK

THESIS

Eric J. Stephen
Captain, USAF

AFIT/GAE/AA/87M-4

Approved for public release; distribution unlimited

Unclassified
SECURITY CLASSIFICATION OF THIS PAGE

AD-A179 512

REPORT DOCUMENTATION PAGE

1a. REPORT SECURITY CLASSIFICATION: Unclassified	1b. RESTRICTIVE MARKINGS
2a. SECURITY CLASSIFICATION AUTHORITY	3. DISTRIBUTION/AVAILABILITY OF REPORT: Approved for public release; distribution unlimited
2b. DECLASSIFICATION/DOWNGRADING SCHEDULE	
4. PERFORMING ORGANIZATION REPORT NUMBER(S): AFIT/GAE/AA/87M-4	5. MONITORING ORGANIZATION REPORT NUMBER(S)
6a. NAME OF PERFORMING ORGANIZATION: School of Engineering; 6b. OFFICE SYMBOL (If applicable): AFIT/ENY	7a. NAME OF MONITORING ORGANIZATION
6c. ADDRESS (City, State and ZIP Code): AF Institute of Technology, Wright-Patterson AFB, Ohio 45433	7b. ADDRESS (City, State and ZIP Code)
8a. NAME OF FUNDING/SPONSORING ORGANIZATION; 8b. OFFICE SYMBOL (If applicable)	9. PROCUREMENT INSTRUMENT IDENTIFICATION NUMBER
8c. ADDRESS (City, State and ZIP Code)	10. SOURCE OF FUNDING NOS. — PROGRAM ELEMENT NO. / PROJECT NO. / TASK NO. / WORK UNIT NO.
11. TITLE (Include Security Classification): See box 19	
12. PERSONAL AUTHOR(S): Fric J. Stephen, B.S., Capt, USAF	
13a. TYPE OF REPORT: MS Thesis; 13b. TIME COVERED: FROM _____ TO _____; 14. DATE OF REPORT (Yr., Mo., Day): 1987 March; 15. PAGE COUNT: 144	
16. SUPPLEMENTARY NOTATION	

17. COSATI CODES			18. SUBJECT TERMS (Continue on reverse if necessary and identify by block number)
FIELD	GROUP	SUB. GR.	Dynamic Stall, Periodic Pitching, Stall, Constant Ramp Angle of Attack, Increased Lift
20	04		

19. ABSTRACT (Continue on reverse if necessary and identify by block number)

Title: Investigation of Periodic Pitching through the Static Stall Angle of Attack

Thesis Advisor: Fric J. Jumper, Lieutenant Colonel, USAF

Approved for public release: IAW AFR 190-1.
LYNN E. WOLAVER
Dean
Air Force Institute of Technology (AU)
Wright-Patterson AFB OH 45433

20. DISTRIBUTION/AVAILABILITY OF ABSTRACT: UNCLASSIFIED/UNLIMITED ☒ SAME AS RPT. ☐ DTIC USERS ☐	21. ABSTRACT SECURITY CLASSIFICATION: Unclassified
22a. NAME OF RESPONSIBLE INDIVIDUAL: Fric J. Jumper, Lieutenant Colonel, USAF	22b. TELEPHONE NUMBER (Include Area Code): (513) 255-3517; 22c. OFFICE SYMBOL: AFIT/ENY

DD FORM 1473, 83 APR — EDITION OF 1 JAN 73 IS OBSOLETE.

Unclassified
SECURITY CLASSIFICATION OF THIS PAGE

The flow over an NACA 0015 airfoil undergoing periodic pitching motions using constant pitch rate ramps was experimentally studied over a range of pitch rates and angles of attack. Surface pressure transducers coupled with a microcomputer-based data acquisition system were used to collect surface pressure data at a rate of 4000 samples per second. The data was reduced through numerical integration of the pressure data to provide graphs of the coefficients of lift, pressure drag and pitching moment versus time. Each point on the graphs represents an average of five runs. The results were compared according to their nondimensional pitch rates (defined as the product of one-half the chord length and the pitch rate divided by the freestream velocity). Data was collected in the range of nondimensional pitch up rates between .0104 and .0384 and the range of angles of attack between 0 and 30 degrees.

AFIT/GAE/AA/87M-4

INVESTIGATION OF PERIODIC PITCHING THROUGH THE STATIC STALL ANGLE OF ATTACK

THESIS

Presented to the Faculty of the School of Engineering

of the Air Force Institute of Technology

Air University

In Partial Fulfillment of the

Requirements for the Degree of

Master of Science in Aeronautical Engineering

Eric J. Stephen, B.S.

Captain, USAF

March 1987

Acknowledgment

The completion of this experimental thesis was only possible with help from several people. I would like to express my appreciation for their support and guidance. First I would like to thank Lieutenant Colonel Eric Jumper, my advisor for his direction and help in solving the problems that came up. His knowledge of and enthusiasm about the thesis topic were invaluable. I would also like to thank Professors Elrod and Hitchcock, who worked on my thesis committee, for their help in getting the thesis out quickly after my return from VKI. I would like to thank Jay Anderson for his technical support in building the airfoil motion control systems. Also for his help with the data collection set up. I would like to thank Major Garcia for lending his time and expertise in solving the interface problem between the computer and the printer. The printer provided the final piece to an independent work station. I would like to thank Robert and Roger, the technicians at the VKI, and Professor Carbonaro for his help in modifying the wind tunnel. Finally I would like to thank Sherri Pamer for her patience and support throughout the AFIT tour and Ralph Pamer for providing me with a place to stay and work during the short times at AFIT.

Table of Contents

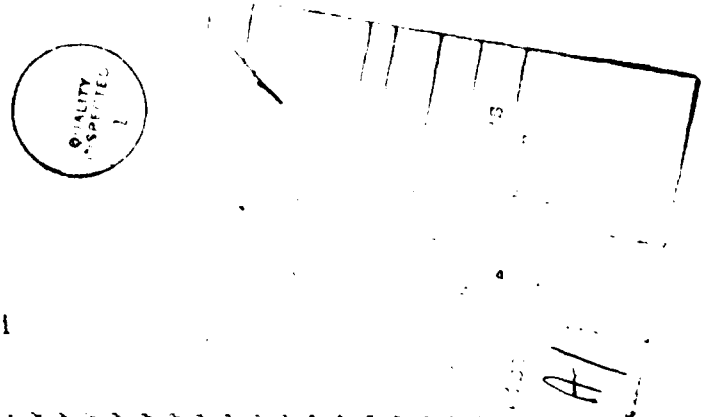

List of Figures

Figure

Page

List of Tables

List of Symbols

$\dot{\alpha}$	pitching rate of the airfoil
$\dot{\alpha}_{ND}$	nondimensional pitching rate
α_{ss}	static stall angle of attack
C_L	coefficient of lift
$C_{L_{MAX\ DYN}}$	maximum dynamic coefficient of lift
$C_{L_{MAX\ ST}}$	maximum static coefficient of lift
c	chord length
V_∞	the freestream velocity
$\alpha_{dyn\ stall}$	the angle at which dynamic stall occurs
α_{sep}	the at which flow separates from the quarter chord
p_{loc}	local pressure on the airfoil
p_{amb}	pressure outside the tunnel
p_{tran}	differential pressure sensed by the transducer
p_∞	the freestream static pressure
ρ_∞	the freestream air density
C_p	coefficient of pressure
C_D	coefficient of drag
C_M	coefficient of moment

Abstract

The effects of a periodic pitching motion on the flow around an NACA 0015 airfoil were studied. The periodic motions consisted of a rotation up at a constant rate followed by a constant pitch down at an higher rate. The pitch rate as well as the minimum and maximum angles of attack were variables in this study. Data was collected through surface pressure transducers connected to a microcomputer based data acquisition system. Data was collected at a rate of about 4000 samples per second and reduced on the same microcomputer system. The data was reduced by numerical integration of the pressure readings to produce coefficient of moment, drag ,lift curves versus the time. The curves seem to indicate that the airfoil can be pitched to angle 1.5 times its static stall angle without any signs of major flow separation. Also over a wide range of pitching rates the airfoil reaches the same value of C_L at 20 degrees angle of attack. Above twenty the maximum C_L and stall angle of attack are dependent on the pitch rate.Nondimensional pitch up rates from .01 to .038 were used in this study.

INVESTIGATION OF PERIODIC PITCHING THROUGH THE STATIC STALL ANGLE OF ATTACK

I. Introduction

Background

Dynamic stall is the process by which a pitching airfoil passes through its static stall angle of attack, α_{ss}, from below and continues to increase its lift with increasing angle of attack. Through this process, stall can be delayed up to tens of degrees. When the airfoil does stall, however, the stall can be more severe and can persist after the airfoil is returned to an angle of attack below α_{ss}. On the other hand, the coefficient of lift, C_L, has been shown to reach values up to four times the maximum static C_L before stall occurs. The extra lift provided by this process might be of some practical use and is worthy of further study.

The dynamic stall effect was first reported in the 1920's by pilots who realized unusually high lift in turbulent air (Ref 3). The effect has become an important topic in several areas of aerodynamic research. In turbomachinery, poor nozzle design, flow separation from the inlet cowling or boundary layers from adjacent aerodynamic

surfaces can cause the velocity to vary circumferentially at the inlet. The effect on the compressor blades has been compared to periodic motions involving rotation (Ref 4). Dynamic stall effects might be useful in explaining improvements in compressor performance under some conditions. With helicopters, dynamic stall is part of the phenomenon known as retreating blade stall. When a helicopter is in forward motion the advancing blade experiences a relative wind which is the vector sum of the blade rotation velocity and the helicopter forward velocity. The retreating blade experiences the sum of the forward velocity and minus the rotation velocity. The result is a decrease in the local angle of attack and relative air speed for the retreating blade. The combination requires the retreating blade to increase its angle of attack during rotation in order to maintain lift and keep the aircraft from rolling. In high performance helicopters increasing the angle of attack as the blade retreats causes the blade to be at an angle of attack well above α_{ss} for as much as half the revolution (Ref 11). Dynamic stall effects are also present in some cases of stall flutter as the fluttering section passes through α_{ss}. Finally, and most recently, in the field of aircraft supermaneuverability, dynamic stall effects might be used to allow aircraft to perform maneuvers in the post stall (PST) range (Ref 5).

The PST maneuver is initiated with a rapid pitch up to bring the aircraft into the post stall region where the pilot might remain for a few seconds to perform a maneuver. Even if the dynamic stall effect could not be exploited to this extent, it is important to understand the aerodynamic effects on a wing pitching through α_{ss}.

With several areas of applicability, a large number of studies have been completed to characterize and predict the dynamic stall process. In 1968 Ham (Ref 11) completed a study to explain the torsional oscillation of helicopter blades during the stall portion of their revolution. Through interferograms of the airfoil he showed that the mechanism of dynamic stall included the shedding of a large leading edge vortex. The leading edge vorticity tended to roll up into a dense accumulation on the order of the original wing bound vorticity. The vortex was then carried downstream with the free stream velocity. As the vortex passed over the airfoil it caused a large pitch down moment which he felt was responsible for the oscillations.

Knowing the vortex was present, Ham used potential flow theory to model the pitching airfoil. He used a flat plate for the airfoil and adjusted the strengths of the leading edge and trailing edge shed vortices to maintain stagnation at the leading and trailing edges respectively. A sinusoidal pitching motion was used and the vortices were

assumed to travel at the local flow velocity. Results of the theory versus the experiment showed that the peak values of lift and moment could be predicted accurately, but the model did not predict when the peaks would occur. Another problem with the model was that it required input from experimental results to tell when leading edge vortex separation occurred.

The prediction of when vortex shedding and subsequently stall occurs has been under investigation since the dynamic stall phenomenon was first reported. Kramer (Ref 20) found a relationship between the maximum static coefficient of lift and the maximum dynamic coefficient of lift.

$$C_{L_{MAX\ DYN}} = C_{L_{MAX\ ST}} + 0.36 \frac{c\,\dot{\alpha}}{V} \qquad (1)$$

This equation does not indicate when (at what angle of attack) stall occurs. If it is assumed, however, that the slope of the C_L versus angle of attack is linear and has the same value for both the static and dynamic cases, the above equation can be rearranged to provide an angle of attack for dynamic stall. Since Kramer's study the coefficients of the equation have been improved but the nondimensional parameter used to relate the static case to the dynamic case has remained the same. Most recently Daley (Ref 18) verified and extended the work of Deekens and Kuebler for an airfoil pitching at a constant rate. The new relationship is

$$C_{L_{MAX\ DYN}} = C_{L_{MA\ \ ST}} + 4.8\frac{c\dot{\alpha}}{V} \qquad (2)$$

Schreck (Ref 3) continued Daley's work by mounting several pressure transducers on the pitching airfoil to provide pressure profiles as well as lift versus time graphs for the dynamic stall process. Schreck's data shows very clearly that the assumption made earlier of a linear coefficient of lift versus angle of attack curve all the way up to stall is incorrect. Schreck's work was extended in Reference 1. The C_L versus angle of attack curves in Reference 1 (Fig 1) show some interesting characteristics. A slight "knee" occurs in the curve starting at about 23 degrees angle of attack. After this knee the curve behaves similar to what Chow (Ref 10) predicted analytically for a vortex passing over an airfoil. The pressure profiles seem to confirm the vortex passage by indicating a suction wave over the upper surface.

Another important parameter in describing the process is the angle of attack where quarter chord separation occurs. As shown in Reference 1, the difference between α_{sep} and $\alpha_{dyn\ stall}$ can be related by the same parameter used to relate α_{ss} to $\alpha_{dyn\ stall}$.

$$\alpha_{ss} - \alpha_{sep} = k\dot{\alpha}_{ND} \qquad (3)$$

With these empirical equations and the potential flow model, an accurate prediction of the coefficient of lift on

an airfoil pitching at a constant rate can be made. However, to be able to exploit the augmented lift provided by dynamic stall effects, the airfoil must enter and depart from the post stall region with a minimum of adverse drag and moment effects.

For the most part research involving airfoils moving in and out of the post stall region have been confined to sinusoidal pitching motions. While sinusoidal motion most accurately represents the motion of helicopter or compressor blades, most of the work on modelling dynamic stall has been accomplished on constant pitch rate airfoils. For a better understanding of the dynamic stall process on periodically pitching airfoils some work should be done with airfoils moving with *constant pitch rates*. A better understanding could provide an angle of attack profile that would capture the augmented lift by sustaining the extra lift provided by the pitching motion.

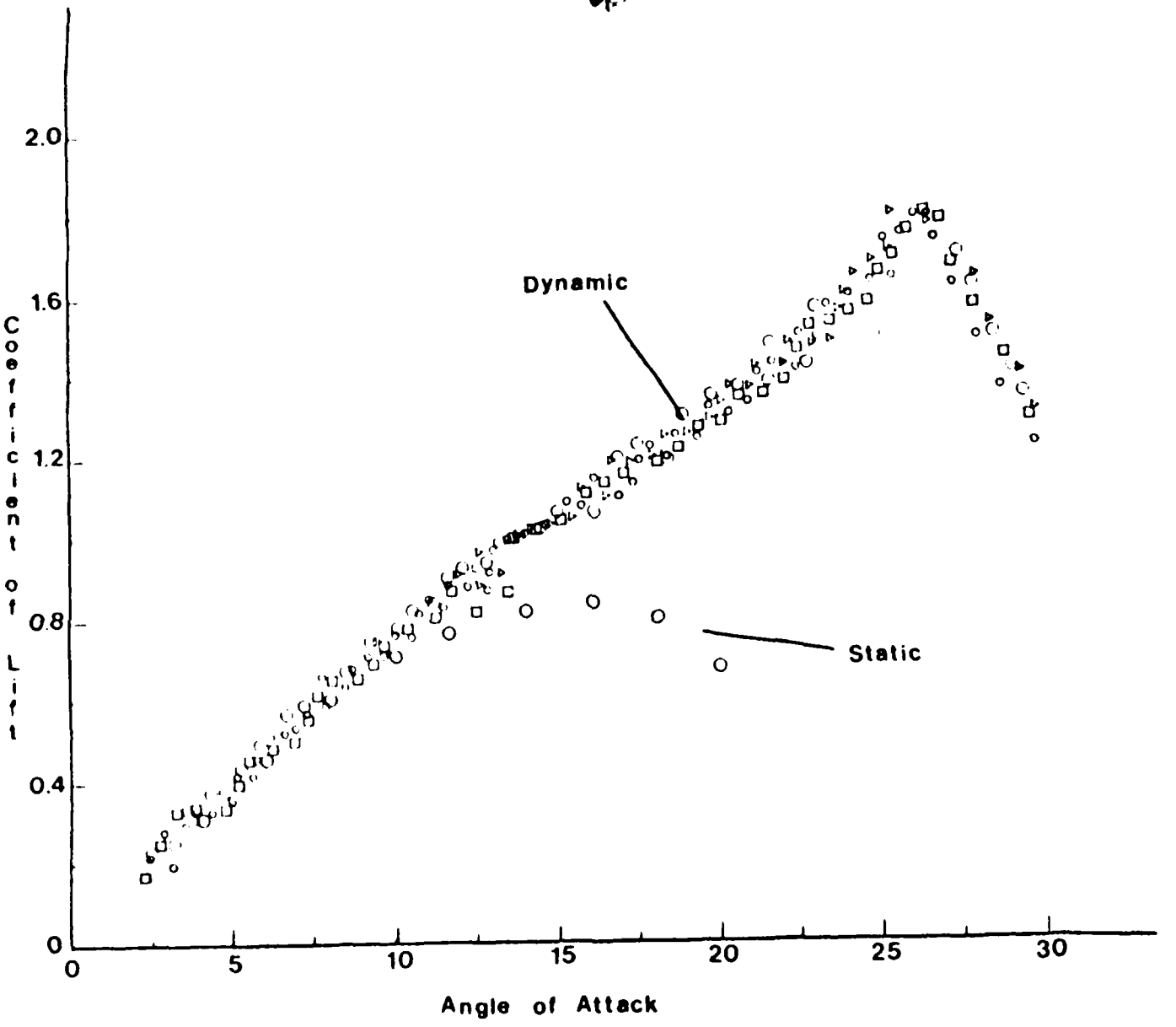

Figure 1. Lift Curve for $\dot{\alpha}_{ND}=0.02$

Objectives

The first objective was to study the effects of having constant pitch rates on periodic pitching motions into and out of the post static stall region. It was hoped that a motion could be found which would provide an average coefficient of lift which was higher than would be available for steady flow. Since the vortex separation was believed to be an integral part of the process which provides the excess lift, the plan was to try to provide the excess lift by pitching up, exciting vortex separation, terminating the motion and then pitching down in an attempt to reattach the flow before the influence of the shed vortex was lost.

The second objective was to justify work accomplished in the Air Force Institute of Technology, AFIT, Smoke Tunnel by attempting the same pitch motions in a wider tunnel at the von Karman Institute, VKI. While the model in both the AFIT and VKI tunnels spanned the width of the tunnels, simulating infinite aspect ratios, it was of interest to know how the experimental aspect ratio differences would affect the dynamic stall results.

II. Theory and Approach

This section is divided into six subsections . The first section describes the theory of dynamic stall that was used to make decisions about the direction of the investigation. The remaining sections describe the approach taken to different aspects of the experiment. These include discussions of force coefficient measurements and pitching motion control.

Dynamic Stall

Even though a discussion of the dynamic stall phenomenon was given in the background section, a more detailed description will be given here. Figure 1, which was tken from Reference 1, shows a coefficient of lift versus angle of attack for both static and dynamic cases. It will aid in the discussion. Up to 16 degrees angle of attack the dynamic lift varies roughly proportional to the angle of attack and with approximately the same slope as the static case, although the slope of the static curve has already started to decrease by 12 degrees. Work from Jumper, et. al. (Ref 1) suggests that the two slopes may only appear to be colinear. The pitching airfoil may have a positive lift coefficient a rotation onset even at zero angle of attack due to an "induced camber" from the motion. The induced

camber effect is outlined in Allaire (Ref 25).

The fact that the dynamic curve remains linear up to 16 degrees while the static curves begins to level off at 12 degrees may be attributed to several factors: the pitching motion of the airfoil; the Moore-Rott-Sears (MRS) criterion for separation, which allows reverse flow in the reference frame of a moving wall as long as the x-component of the velocity is positive in an inertial frame; mass ingestion, which accounts for the extra mass taken into the control volume by the pitching motion; and the effects of the wake. All these are discussed in Jumper et al (Ref 24).

The way these variables combine is not completely understood, but, in the case of constant-$\dot{\alpha}$ motion, the figure shows that after 16 degrees the curve levels off slightlybefore continuing to rise. Then somewhere between 20 and 25 degrees, separation at the quarter chord occurs (Ref 1). This separation is followed almost immediately by the shedding of a leading edge vortex.

The vortex convects over the airfoil at some fraction of but on the order of the freestream velocity. When the vortex starts its passage the suction peak near the leading edge collapses and a suction wave passes over the upper surface of the airfoil. The passage of the wave, while increasing the lift, causes a pitch down moment. The moment reaches a negative "peak" as the vortex passes the trailing

edge, slghtly lagging the maximum lift peak.

Since, in the series of experiments (Ref 3) upon which current work is based, the wing is allowed to continue to pitch up at a constant rate during the passage of the vortex, the angle of attack far exceeded the static stall angle at the point when the lift violently decreased (dynamic stall point). With continued pitching motion a train of alternating leading and trailing edge vortices are shed which cause other lift peaks, but none with the magnitude of the first.

With this model of the dynamic stall process the present investigation proposed to examine periodic motion of an airfoil into and out of the post stall region, using constant, but different, pitch rates for the up and down ramps. It was hoped that the periodic motions would provide an averaged lift that was higher than the maximum static lift. To provide for this, the airfoil was pitched up at one rate to try to excite the leading edge vortex separation then pitched down at a faster rate in an attempt to get the airfoil to an angle of attack where the flow could reattach. The maximum angle of attack as well as the pitch rates were varied to determine the effect on the formation of the vortex. The minimum angle was varied to determine the effect on flow reattachment.

Determination of Pressure Coefficients

For this investigation a NACA 0015 airfoil instrumented with 16 pressure transducers was used. This is the same model used by Daley, Schreck and Dimmick (Ref 18,3,8). Due to freestream irregularities and some noise, the signal from the transducers had a larger variance than had been experienced in the previous studies. Following the example of Schreck (Ref 3), these fluctuations were filtered out by using ensemble averaging of five runs at the same dynamic conditions, i.e., at the same angular rate and freestream velocity.

For this experiment the airfoil was sealed and the reference ports on the transducers were vented to the atmosphere through a shaft in the side of the airfoil. The transducers thus returned a voltage which was proportional to the pressure difference between the local pressure on the airfoil, p_{loc}, and the pressure outside the tunnel, p_{amb}. These voltages were transformed to digital counts via a Dual AIM-12 Analog-to-Digital(A/D) Converter and were stored on a disk. Knowing the characterisics of th A/D board and the transducer sensitivities, the difference in the pressure, Δp_{tran}, could be regained.

The coefficient of pressure for each location was determined from the definition

$$C_p = (p_{loc}-p_\infty)/((1/2)\rho_\infty V_\infty^2) \qquad (4)$$

where p_∞ is the freestream static pressure in the tunnel and ρ_∞ and V_∞ are the freestream density and velocity, respectively. As described in the last paragraph p_{loc} can be determined by

$$p_{loc} = \Delta p_{tran} + p_{amb} \qquad (5)$$

Substituting

$$C_p = \{\Delta p_{tran} + (p_{amb} - p_\infty)\} / \{(1/2)\ \rho_\infty V_\infty^2\} \qquad (6)$$

From Bernoulli's incompressible flow relation the denominator is equal to $p_o - p_\infty$, where p_o is the total pressure in the tunnel. So

$$C_p = \{\Delta p_{tran} + (p_{amb} - p_\infty)\} / \{p_o - p_\infty\} \qquad (7)$$

The determination of Δp_{tran} has already been discussed. The value of the denominator is the pressure difference measured by the pitot-static probe and the second term in the numerator can be measured by venting the pitot side of the probe to the atmosphere.

Accuracy of the Pressure Profile

The number of transducers in this case was limited to 16 by the capability of the data acquisition system. It was important that the transducers be well positioned to provide an accurate pressure profile. In McAllister, et. al. (Ref

2), the pressure profiles indicate that narrow pressure spikes occur near the leading edge. Therefore it is adequate to cluster the pressure transducers near the leading edge and allow greater separation toward the trailing edge. By this method the locations in Figure 2 were chosen.

Physical limitations of size precluded the use of a transducer nearer to the trailing edge. However, based again on results from McAllister, et. al., the coefficient of pressure at the trailing edge was calculated by extrapolating the values from the last two transducers on the upper surface (i.e., locations 8 and 9 on Figure 2).

Integration of the Force Coefficients

Following Schreck (Ref 3) integration of the force coefficient was accomplished by finding the area inside the polygonal lines joining the data points on the coefficient of pressure versus position curve. The normal coefficient was obtained from the pressure versus chordwise position and the chordwise coefficient was obtained from the pressure versus normal position curve. The coefficient of moment was determined by a similar method only a moment arm was multiplied by each section normal coefficient. Additions to the moment from chordwise forces were considered negligible. These coefficients were converted to lift and pressure drag using the cosine and sine of the angle of attack.

The Problem of Data Acquisition

Measurement of the physical parameters of the dynamic stall poses the problem common to unsteady flow measurement. The measurement system must provide accurate measurements and must react quickly. In this experiment the data is collected at a rate of about 4000 samples per second. Since there are 16 transducers, the requirements for each transducer are, at most, 300 samples per second. The rated frequency response of the transducers is approximately 9000 Hertz, far exceeding the experimental requirements.

Driving the Airfoil Motion

The pitching motion of the airfoil in this investigation consisted of a constant pitch up followed by a constant ramp down with perhaps some delay in the middle. Dimmick and Schreck (Ref 3,8) had used a planetary gearmotor to provide constant pitch rates for their projects, so the same motor was initially incorporated in this experiment. The slope of the ramp could be controlled by adjusting the voltage. The problem was to provide a constant ramp down after the ramp up. After consideration of a system of cams, a simpler solution using two microswitches was adopted. The microswitches were mounted in a circular track. A shaft which was connected to the airfoil passed through the center

of the circle. An arm made of flexible spring steel was attached to the shaft. As the shaft turned the arm would trip the microswitch. The microswitch was connected to a relay which switched the power supplied to the motor from one source to a second source of opposite polarity. The power supplies were independent so that the ramp up and ramp down could have different values. A variable delay was built into the system when the switch was tripped at the minimum angle of attack.

This investigation was performed in two parts, the first in the AFIT tunnel and the second in the VKI tunnel. In order to accomodate the larger span of the VKI tunnel, the second part used the same airfoil with extensions. Because of the larger size and the desire for a wider range of pitching motions, a different drive was chosen for the second part of the study. The system chosen. It consisted of a servo motor, an amplifier, a control interface card, and a portable computer. With this system, theoretically, almost any pitching motion could be programmed to the shaft from the computer. Details on the equipment is provided in the Facilities and Instrumentation section.

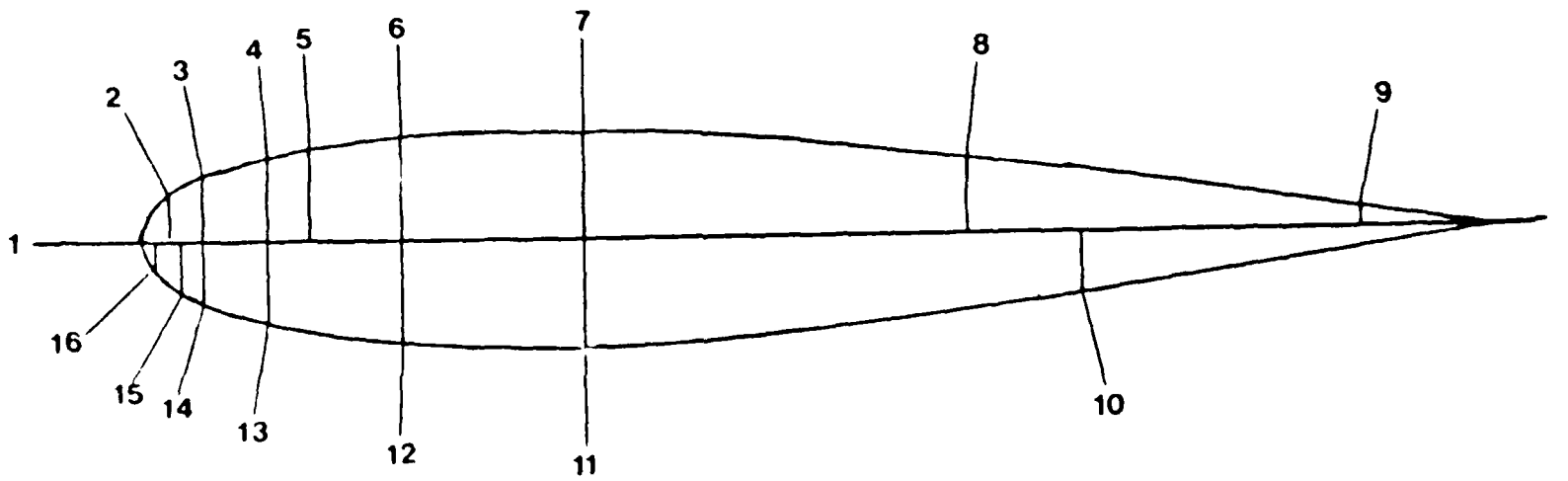

x/c (1) = 0.000	x/c (5) = 0.131	x/c (9) = 0.902	x/c(13) = 0.098
x/c (2) = 0.025	x/c (6) = 0.197	x/c(10) = 0.697	x/c(14) = 0.049
x/c (3) = 0.049	x/c (7) = 0.328	x/c(11) = 0.328	x/c(15) = 0.033
x/c (4) = 0.098	x/c (8) = 0.615	x/c(12) = 0.197	x/c(16) = 0.016

Figure 2. Upper and Lower Surface Pressure Transducer Locations

III. Facilities and Instrumentation

The experimental phase of this work was completed in two different facilities. Descriptions of the equipment used at each facility is provided in this section.

Wind Tunnels

At Wright Patterson AFB, Ohio , the AFIT Smoke Tunnel was used. The Smoke Tunnel is located in building 640 in Area B. The test section of the tunnel is 59 inches long, 39.5 inches high and 2.75 inches deep. The tunnel is capable of test section velocities up to 45 feet/second (13.72 meters/second). The Smoke Tunnel's capabilities are further described by Sisson (Ref 21) and Baldner (Ref 19). Since this experiment did not involve flow visualization, the smoke rake was removed to improve flow quality.

At the von Karman Institute, a modified version of the L-2A low speed wind tunnel was used. The test section of this tunnel was 2 meters long, with a cross section 1 meter high and .28 meters deep. The modified tunnel is capable of test section velocities up to 12 meters/second (39.4 feet/second). Further information on this tunnel and its modification are provided in Appendix C.

Velocity Measurement

Test section static and total pressures were measured using a hemispherical head pitot-static probe in conjunction with a Meriam A-937 water micromanometer. The probe hole was located 31 inches from the point where the test section begins so that the tip of the probe was directly under the leading edge when the airfoil was at zero angle of attack. The position of the probe was determined to be important for the accurate measurement of pressure differences at the model location. The pressure differences were used to determine tunnel velocity during data collection and to calculate pressure coefficients during data reduction.

At the VKI the tunnel was wider so the pitot probe was located at a more conventional position one chord length ahead of the leading edge. The probe was mounted at quarter of the tunel height and positioned along the centerline. Due to the small pressure differences being measured a pressure transducer was used in place of the micromanometer.

Airfoil

The NACA 0015 airfoil used in this experiment had a 12.2 inch chord. In the form used at AFIT, it consisted of a hollow mahogany shell, 2.63 inches deep, closed on both sides by aluminum endplates. The plates were sealed with silicone rubber adhesive. For the work at VKI, blocks were

put on either side of the airfoil to extend its span to 11 inches (about .28 meters). At AFIT the one endplate was rigidly attached to a 14 inch tubular aluminum shaft with an outside diameter of .75 inches. At VKI a 14 inch aluminum shaft with an outside diameter of 1.125 inches and an inner diameter of 1 inch was fixed to one of the blocks. Both shafts had a slot at the midpoint to admit ambient air to the interior of the airfoil so that the transducer reference ports were referenced to ambient (room) pressure. The shell had transducer ports drilled in it at locations shown in Figure 2.

Pressure Transducers

The transducers used in this experiment were ENDEVCO 8506-2 and 8507-2 miniature piezo-resistive pressure transducers. The only difference between the two types is that the 8506 has a threaded mount. Both types of transducers had a range of plus or minus two psig and required an excitation voltage of 10.00 volts DC. Excitation voltage was provided by a Hewlett Packard 6205B Dual DC Power Supply. Resonance frequency response for both transducers was 45,000 Hertz. The rated frequency response was 20% of the resonant frequency or 9000 Hertz, thus the transducer response frequency far exceeded the dynamic requirements of the experiment.

The transducers were flush mounted in the ports according to specifications provided by ENDEVCO (Ref 21). General Electric RTV Silicone Rubber Adhesive Sealant was used as the bonding agent. After completing electrical connections the transducers were calibrated as outlined in Appendix A.

Drive Mechanism

For the work done at AFIT, the airfoil was rotated by a TRW Globe Model 5A2298-4, 12 Volt DC,constant speed planetary gearmotor with a 525:1 reduction ratio. The pitch rate was controlled by varying the voltage supplied to the motor. The voltage was provided through a control circuit designed and built by Jay Anderson, an AFIT technician. The circuit incorporated two relays which were wired to the microswitches. Hitting a switch caused the voltage to switch polarity and the motor to change direction. A variable delay was also built into the system. The circuit required three power supplies: one for the pitch up, one for the pitch down and one to power the relays.

The microswitches were triggered by a flexible spring steel arm which was attached to the shaft of the airfoil. The microswitches were mounted in circular tracks with the

shaft passing through the center. With this set up the switches could be adjusted to set the minimum and maximum angles of attack. Flexible arms were also placed on the microswitches. Flexibility was required to to keep from damaging the microswitches.

At the VKI a more versatile drive system was used. The motor for this system was an ER&G Torque Systems PM Field DC Servo Motor Model MT352B-136DF. The motor was controlled through an A721 Series Pulse Width Modulated DC Amplifier. The amplifier interfaced with a Tandy 100 portable computer through a MINI MC^2 Controller Card. The system also included a digital display for monitoring shaft position. Using the MINI.BAS program provided for the Tandy 100, the shaft could be programmed to do a number of periodic motions. Rotation rates, accelerations, decelerations and overshoots could also be controlled.

Data Acquisition System

The microcomputer system consisted of a Heath Model H-29 monitor and keyboard, a Panasonic KX-P1091 Dot Matrix Printer and a TecMar Computer Chassis. The TecMar box contained two Shugart eight inch floppy disk drives and an S100 bus equipped with an SD Systems SBU 100 Single Board

Computer, an SD System Expandoram II Board, and an MD2022 Tarbell Disk Controller Board. To perform the digital data gathering, two Dual Systems Control Corporation AIM 12 Analog imput module boards were added.

The AIM 12 is a high speed, multiplexed analog-to digital data acquisition module compatible with the standard S-100 bus. The analog-to-digital conversion subsystem on the board can be operated in one of two modes: the unipolar mode which requires an input from 0 to 10 volts or the bipolar mode which accepts input voltages from -5 to +5 volts. The AIM 12 also contains a preconditioning subsystem which amplifies the input signal. The system can provide gains from 1 to 100. Single ended amplifier operation allows 32 separate analog inputs to the multiplexer while the differential mode allows only 16 inputs. Differential operation takes advantage of the high common mode rejection of the amplifier.

As mentioned before, two of the AIM 12 boards were used for data collection. The first was for the pressure transducers. These transducers had a full scale output of 300 mV for 2 psi. Under the conditions of the experiment the maximum output from a transducer was on the order of 1/10 of this range. This obviated the use of the maximum gain setting in the preconditioning subsystem. With a maximum gain of 100 the board is saturated with a 50 mV

signal. Differential mode operation at this gain setting provides 114 dB common mode rejection. The board was operated in the bipolar mode even though the pressure transducers always sensed a negative pressure difference.

The second board took readings from the a 10 turn potentiometer. The total voltage across the potentiometer was set to 10 volts so that the second AIM 12 card could have a gain of 1 and operate in the unipolar mode. Noise was not a problem with the large signal so single ended operation was used.

IV. Experimental Procedure

Transducer Calibration

For the first several days the transducers were calibrated daily. This procedure, which was time consuming, is outlined in Appendix A. The sensitivities, however, varied only two or three millivolts per psi on values on the order of 150 mV/psi. There were some exceptions where the sensitivities varied by 10 mV/psi for one day then returned to values close to previous days. This variance could indicate a faulty precedure or incorrect calculation. Therefore the averages of the first several days sensitivities without the exceptions were used to reduce the data.

Data Collection

This section outlines the standard procedure for taking data during this investigation. The procedure at AFIT and VKI were nearly identical with only slight differences which are mentioned as they arise. First all electrical equipment, including power supplies, multimeters, and the computer, were allowed to warm up for at least 3 hours before any data was taken. This was to allow any large electrical transients to die out.

To begin the data runs, the room temperature and pressure were recorded and the tunnel was started and adjusted to provide a test section velocity of about 30 feet per second. At AFIT using the voltmeter attached to the position indicator as a monitor, the microswitches were positioned in the track to provide the specified minimum and maximum angles of attack. To do this the model was pitched up to its maximum angle of attack. The position was noted and if corrections were required, the airfoil was returned to a lower angle of attack and the microswitch was repositioned.The same procedure was used to set the minimum angle of attack. At the VKI the position indicator was connected to an ultraviolet oscilloscope which provided a hard copy of the motion. Any adjustments in that case were to the servo loop parameters of the controller. In both cases the procedure was accomplished with the tunnel in operation to provide the motions which would be seen during a run. The model was then adjusted to zero angle of attack and the tunnel was shut down.

The rest of the procedure was initiated by executing the TESTRUN program (Appendix F). The program provided a series of requests and commands to aid in the data taking process. The following is a summary of the data taking

sequence. The first series of inputs requested by the program were the date, the time, the room temperature and the room pressure. The inputs were echoed to the operator for verification. Failure to verify resulted in a repeated prompt for data. Next the program read the zero input values from the 16 pressure transducers. The tunnel was not actually shut down (the tunnel was running to set the motions) until just prior to these readings in order to avoid the problems discussed in Appendix B. The program paused before taking the readings. At that time the tunnel was shut down and the pressure difference between the tunnel and the room was allowed to adjust to zero. Then the program is signalled to take the readings. After verification of these readings the operator was prompted to turn on the tunnel.

The next inputs required at AFIT were two manometer readings and two voltage readings. The first manometer reading was for the difference in pressure between the static pressure in the tunnel and the pressure in the room. This was measured by connecting the static side of the pitot-static probe to one side of the micromanometer and venting the other side to the room. The second manometer reading was for the difference between the static and dynamic pressures in

the tunnel. This was obtained by connecting the total side of the pitot static probe to the empty side of the micromanometer. At the VKI the procedure was slightly different. There was a static port separate from the pitot-static probe. The static to room value was read from a Bets manometer and the pitot-static probe was connected to a pressure transducer.

The voltage readings were taken from the voltmeter connected to the position indicator (potentiometer). The first voltage reading corresponded to a 90 degree angle of attack for the airfoil and the second reading to a zero angle of attack. These readings were taken by disconnecting the shaft from the motor and manually turning the airfoil to the correct angle of attack. Two pieces of tape on the test section window marked the zero and ninety degree positions.

Again all inputs were echoed to the screen for verification. Upon verification all inputs entered thus far were stored on a disk.

The next part of the program performed the data collection. The program first requested the number of samples to be collected. The capacity of the computer's local memory was filled wth about 3600 samples. This number

provided 200 passes of the transducers, the position indicator, and the clock. Then the program prompted for a signal to begin data collection. At that time the airfoil was set in motion. If the model was moving freely and the position voltmeter indicated satisfactory motion, data acquisition was initiated. The airfoil was allowed to make at least four cycles to check for irregularities prior to acquisition initiation..

After the data was taken the program would indicate the number of samples actually taken. It then offered the option of saving the data on disk or repeating the run. This was repeated four more times to provide five runs with the same pitching motion.

After five satisfactory runs were completed, static lift coefficient data was generated. The program again prompted for the number of samples to be taken. Then it waited for the signal to begin acquisition. Upon the signal the program gathered and reduced the data to provide coefficients of pressure and the normal force. The pressure coefficients for the upper surface were displayed first and after a line feed, the lower surface coefficients and the normal force were displayed. This allowed the operator, at least qualitatively, to check the results from the runs. The coefficient of normal force was recorded along

with the position voltmeter reading. This process was repeated three times for each angle of attack on the curve. The positions were set by hand using the voltmeter as a guide. Positions from 0 to 22 degrees were used to provide adequate data for a lift versus angle of attack curve. After sufficient data points were collected TESTRUN was terminated and the equipment was shut down.

V. Data Reduction and Discussion

Data reduction for this project was a three step process. The first step was to convert the digital counts to force coefficients. Since the data runs were not initiated at the same point in the cycle, the second step was to aline the data sets. Finally, the data were averaged over five runs to provide the results which are presented in Appendix E.

The first step was accomplished by using the program DOS4A. This program read data from six files, RAWDATA0 through RAWDATA5. RAWDATA0 contained the voltage readings for the zero and ninety degree angles of attack and the zero pressure readings for each pressure transducer. The other files contained data from the test runs. Each file has 200 sets of 18 data points. The data consist of readings for the clock, the angle of attack indicator, and 16 pressure transducers. Each transducer reading was converted to a pressure by the method discussed in the Theory and Approach section. Using the pitot-static pressure along with the pressure difference between the tunnel and the room, which were also on RAWDATA0 the pressures were converted to coefficients of pressure. Transducer 15 did not operate properly so the coefficient of pressure for that location was determined by interpolation between the coefficients of pressure for transducer locations 16 and 14. The angle

of attack was determined by assuming a linear change in voltage readings between successive readings (i.e. linear interpolation). The digital readings from the position indicator voltages were measured via the analog to digital (A/D) card and converted to angle of attack via a calibration coefficient. Since the voltages changes linearly, the calibration was made by using the zero and ninety degree readings as calibration points.

The data from the clock, position indicator, and pressure transducers were collected consecutively. In order to find the force coefficient by integrating the pressure coefficients, the data had to be adjusted to the same time. To do this it was assumed that for the short time required for one data pass (about .005 seconds) the data varied linearly. The pressures and angle of attack were adjusted to the clock reading. With the data adjusted for time, the coefficient of normal force,the coefficient of chordwise force and the coefficient of moment about the leading edge were computed by the method discussed in the Theory and Approach section. Moments due to the pressure in the chordwise direction were assumed negligible due to their short moment arms. The coefficient of moment about the leading edge was converted to a coefficient of moment about the quarter chord by subtracting one quarter of the normal force coefficient. The coefficients of normal and chordwise force were converted to lift and drag coefficients through the

sine and cosine of the angle of attack. Finally, the clock readings, angle of attack and coefficients of lift, drag and moment were stored in file REDUDATA.

The second step was to aline the data from different runs by using REGRAF. REGRAF asks for a time shift for each of five data sets and then adds the time shift to the clock value for each data pass and creates twenty new files to store the data for graphing. There are five files for each of the coefficients and the angle of attack versus time. The time shifts were determined by choosing an angle and determining the coresponding time from REDUDATA. This time was the time shift for each run.

The third step was to average the data from five runs using AVERAG. AVERAG asks for two times which represent the start and end of a cycle. AVERAG steps through the cycle averaging the data from the runs which had data at each time step. Since the runs were not started at the same point in the cycle some did not have values at all points in the cycle. The averaged data was stored in files for graphing. The results are given in Appendix E. The data from the averaged angle of attack versus time file was used to determine the pitch rates up and down. The averaged coefficient of lift data was time averaged over a cycle to provide a value of lift that could be maintained. These results are listed in Tables I and II.

The experimental work for this study was carried out in two stages. The first stage was completed at AFIT and the second stage was accomplished at the VKI. The first part was a continuation of work reported by Jumper, et. al. (Ref 1). Both the work for this study and Reference 1 were completed in the smoke tunnel at AFIT which is only 2.75 inches wide. It was of interest to see if the results would be affected by a change in the span. For that reason some of the work reported in Reference 1 was repeated in the tunnel at VKI, which had a span of eleven inches.

First a static curve was constructed both at AFIT and VKI. The one constructed at AFIT matched the one reported in Reference 1 (Fig 3). The maximum coefficient of lift was between .8 and .9 and it occured at about 14 degrees angle of attack. The second curve, from VKI, showed a more drastic loss of lift after 16 degrees even though the maximum value occured at 14 degrees. The second curve has a maximum coefficient of lift of approximately 1.0 (Fig 3). NACA Report 586 (Ref 26), which shows the effects of Reynolds number on the lift curve for NACA airfoils, predicts a maximum coefficient of lift of .89 for a Reynolds number of 166,000 and a maximum coefficient of lift of .98 for a Reynolds number of 331,000. The Reynolds number for the current work was about 180,000. The NACA report also predicts the loss of lift after stall is more gradual with

lower Reynolds number. The curves in the NACA report do not indicate a decrease as gradual as that shown in the curve from AFIT. The NACA report also indicates the stall should occur between 12 and 14 degrees. Both the VKI and AFIT curves indicate a maximum lift at 14 degrees.

The second part of the work reported in Reference 1 to be repeated at the VKI was the constant pitch rate motions from 0 to 90 degrees angle of attack. The effect of the pitch rate on the coefficient of lift was demonstrated in Reference 1 by plotting the C_L versus angle of attack for four pitch rates on the same graph. The important features of the shape of this graph have already been discussed in the Theory and Approach section. The interesting point about the graphs is that no matter how much the pitch rate changes, the lift curves follow approximately the same path up to dynamic stall. The pitch rates affect the point at which the curves leave the path.

In the similar work completed at the VKI, the pitch rates were 32,45,75 and 100 degrees per second. In Reference 1 the data was much cleaner than the results from the VKI so that all the data from five runs at each pitch rate was published. The result from VKI (Fig 4) is the average of five runs at each pitch rate. The results show the same general phenomenon as was shown in Reference 1. The knee is not as obvious but the increase in slope appears to be

present. The difference is that the increase in slope occurred at a greater angle of attack but the dynamic stall occurred at a slightly lower angle of attack when compared to Reference 1 for the same nondimensional pitch rate. For example, for a nondimensional pitch rate of .0224 in Figure 4, the dynamic stall angle is 26 degrees. In Reference 1, Figure 7, for a nondimensional pitch rate of .0228 the dynamic stall angle is 28 degrees, a difference of two degrees. The static stall angle from the curves made at AFIT and VKI (Fig 3) indicate approximately the same static stall angle. So the change in angle of attack from static to dynamic stall was slightly less at the VKI. Again comparing curves of similar nondimensional pitch rates, the maximum coefficient of lift was greater in the current work than in Reference 1. An example can be taken from the pitch rate just discussed. The maximum C_L at VKI was 2.2 while the result in Reference 1 shows a maximum C_L of 1.8. The ratio of the two numbers is 1.22. This is approximately the ratio of maximum static C_L's from VKI and AFIT (1.18).

Figures 5 ad 6 show the effect of the pitch rate on the drag and moment curves. Both curves show a "peak" (negative peak in the case of the moment) corresponding to the lift peaks on lift curve (Fig 4). The moment curve probably indicates the passage of the leading edge shed vortex. The large negative spike in the curve probably indicates the

passage of the vortex over the trailing edge of the airfoil. In Figure 6 no such spikes occur until after a 20 degree angle of attack. After 20 degrees the curves all show a general negative trend with spikes corresponding to dynamic stall on the lift curve.

The airfoil model spanned the width of the test section at both AFIT and VKI. Since the AFIT tunnel was only 2.75 inches wide some question could be raised about wall effects on the dynamic stall process. The results of these tests seem to indicate that the results from AFIT as well as VKI can be extended to larger models. Since the percentage of increase in dynamic lift is approximately the percentage of increase in static lift from AFIT to VKI the explanation could be in the experimental setup.

The remaining part of the discussion will deal with work performed at both the VKI and AFIT. The work involved pitching the airfoil up and down with constant but different rates. The intent was to excite the separation of the leading edge vortex to provide the excess lift, then to pitch the airfoil back down to allow the flow to reattach. Evidence that this might be possible was given in McAllister, et. al., (Ref 2) where the airfoil was pitched through a sinusoidal pitching motion, $14 \pm 6 \sin(\omega t)$ degrees. The results indicated that the coefficient of lift continued to increase while the angle of attack was decreas-

ing. Based on the results from Reference 1, the leading edge vortex is shed nearly coincident with quarter chord separation and this occurred approximately three to five degrees prior to dynamic stall depending on $\dot{\alpha}_{ND}$. Since part of the project was to see how much lift could be maintained the minimum angle of attack was varied from zero to twelve degrees. Angles of attack greater than 12 degrees would be close to or above the static stall angle. Pitch rates below fifty degrees per second did not demonstrate the increase in lift according to Reference 1 and thus were not used.

Table I shows the resulting pitching motions at AFIT. The angle of attack profiles along with those for the coefficients of lift, drag, and moment are given in Appendix E. The results show the difficulty in setting the maximum angle of attack (see discussion in Appendix D). Also it was hoped that the airfoil could be pitched down much more rapidly than it was pitched up. However this was not possible with the motor used at AFIT.

The first four runs from AFIT (Runs A to D) were motions with a minimum angle of attack of zero and various maximum angles of attack. None of the runs indicated any additional lift after the upward motion stopped. The third motion (Run C) showed an interesting result where the airfoil pitched above the static stall angle but did not appear to excite the formation of leading edge shed vortex.

This is inferred by the levelness of the moment curve. The lift curve seems to indicate that the flow reattached somewhere between 6 and 12 degrees angle of attack on the way down. The indication of reattachment was judged to be a slight rise in the moment above the starting value (a judgement which may have other interpretations).

The next four runs (Runs E through H) were from six degrees up. Again the first run shows a profile where coefficient of moment was fairly constant. Again the airfoil was pitched to only 20 degrees angle of attack. The profiles for the second and third runs (F and G) indicate a leveling of the coefficient of lift curve as the angle of attack decreases. This possibly could be interpretted as indicating reattachment; however, unlike runs A and D, corresponding to this levelling is a levelling of the moment curve and a then continued decline. This might indicate the separation of a second vortex. As with the first four runs there was no increased lift after the upward motion ceased. The averaged coefficient of lift in the table for runs E through H show a value comparable to the maximum static coefficient of lift.

The final four runs reported from AFIT (I through L) had minimum angles of atack of 12 degrees. In Run I the flow seems to have remained attached throughout the motion. This is indicated by the fact that the C_L curve mimics the

angle of attack profile and the coefficient of moment curve is constant. In the other three runs in this group (J through L) the C_L curve drops below the initial value of C_L while the airfoil is pitching down and regains the initial value only when the downward motion ceases.

The difference between Run I and Runs J through L was that the last three went to slightly higher angles of attack with higher pitch rates. The effect of the pitch rate as seen in Figure 4 appears to be to allow the airfoil to pitch to a higher angle of attack before stalling. Based on Figure 4 all these runs (I through L) would reach the maximum angle of attack for their motion before dynamic stall. However, as soon as the upward motion ceased, dynamic stall appears to occur on Runs J through L. Since these three runs were taken to higher values of angle of attack they obtain higher maximum coefficients of lift. The fact that after stall the C_L drops quickly to a value below the C_L value for the minimum angle of attack causes the average lift for these runs to be less than the average lift for Run I. Therefore Run I appears to be the best profile for maintaining extra lift from the angle of attack profiles run at AFIT.

The remainder of the figures in Appendix E and the results in Table II were from work completed at the VKI. The runs at VKI were more controlled for their minimum and maximum angles of attack. Also the pitch motion down was

more rapid. However constant pitch rates and delays were more difficult to obtain.

The first nine runs at the VKI were at low pitch rates. The work from AFIT indicated that the pitch rate did not have to induce vortex separation to provide the higher average lift. The runs were in two sets of four, the four consisted of runs from 0, 5, and 10 degrees up to 20 degrees and one motion from 0 to 25 degrees. The final run of the first nine was to see if the faster pitch down would affect the average coefficient of lift at higher pitch rates. The runs up to 25 degrees indicate that the dynamic stall occurs before the maximum angle of attack is reached. The indication was a drop in the lift curve while the angle of attack is still increasing. The rest of the runs showed the same pattern as was seen at AFIT for low pitch rates to low angles of attack. The coefficient of lift followed the angle-of-attack curve. The motion which provided the best average lift had a pitch rate of about 50 degrees per second with a maximum angle of attack of 20 degrees and a minimum angle of attack of 10 degrees. This is almost the same profile as the one that provided the best average C_L at AFIT. The difference was a more rapid pitch down for the motion at VKI. The ratio for the average C_L's for similar runs at AFIT and VKI was 1.21, again close to the value of the ratio of the maximum static C_L's. For the last run the

airfoil was pitched up to 24 degrees. The maximum lift for this run was only slightly higher than for the previous eight runs (AA through HH). The average C_L for the run was higher than the value for other runs over a similar range.

The last nine runs were made at higher pitch rates up to 129 degrees per second. Four of the runs were made with maximum angles of attack of twenty degrees to investigate the effect of pitch rate vortex shedding. The other five were made with maximum angles of attack between 25 and 30 degrees. Above 30 degrees, dynamic stall would occur before the maximum angle of attack was reached, so no runs were made to higher angles. The four runs to 20 degrees suggested that the maximum lift was not affected by the pitch rate. Comparing Runs JJ,KK,MM to Runs AA and EE the curves show that the C_L reaches a maximum slightly above 1.4 no matter how fast the airfoil is pitched. The graphs indicate no major negative moment spikes which would indicate flow separation. This would be consistent with Figure 6 since no moment spikes are indicated until after 20 degrees angle of attack. Exciting vortex shedding without pitching to higher angles of attack does not appear possible with these pitch rates.

When the maximum angle was increased, the maximum coefficient of lift increased to over 2.0, with one case (Run RR) going to 2.5. However, the drag increased more than

proportionally and the coefficent of lift at zero degrees angle of attack was well below zero providing average coefficients of lift less than those at lower pitch rates-(Runs AA through HH). For pitching motions above 20 degrees angle of attack the maximum C_L is affected by the pitch rates; an example is Runs QQ and RR. In Run RR the airfoil was pitched up at a rate of 102 degrees per second while in Run QQ it was pitched at 129 degrees per second. Both pitched up to approximately the same angle of attack yet the maximum C_L for QQ was about 2.3 while for RR it was 2.5. The higher C_L could indicate that the strength of the shed vortex is a function of the pitch rate.

From the results of this investigation it appears that the best angle of attack profile for maintaining the excess lift from pitching-motion effects is to pitch the airfoil to an angle just below separation and then pitch back down to an angle below the static stall angle of attack. It does not appear to matter how fast the airfoil pitches, at least for the range of pitch rates in this study. Using this method, however, would limit the amount of extra lift that can be expected. The limit according to this study was 1.4 times the maximum static lift coefficient (based on the peak C_L for the motions).

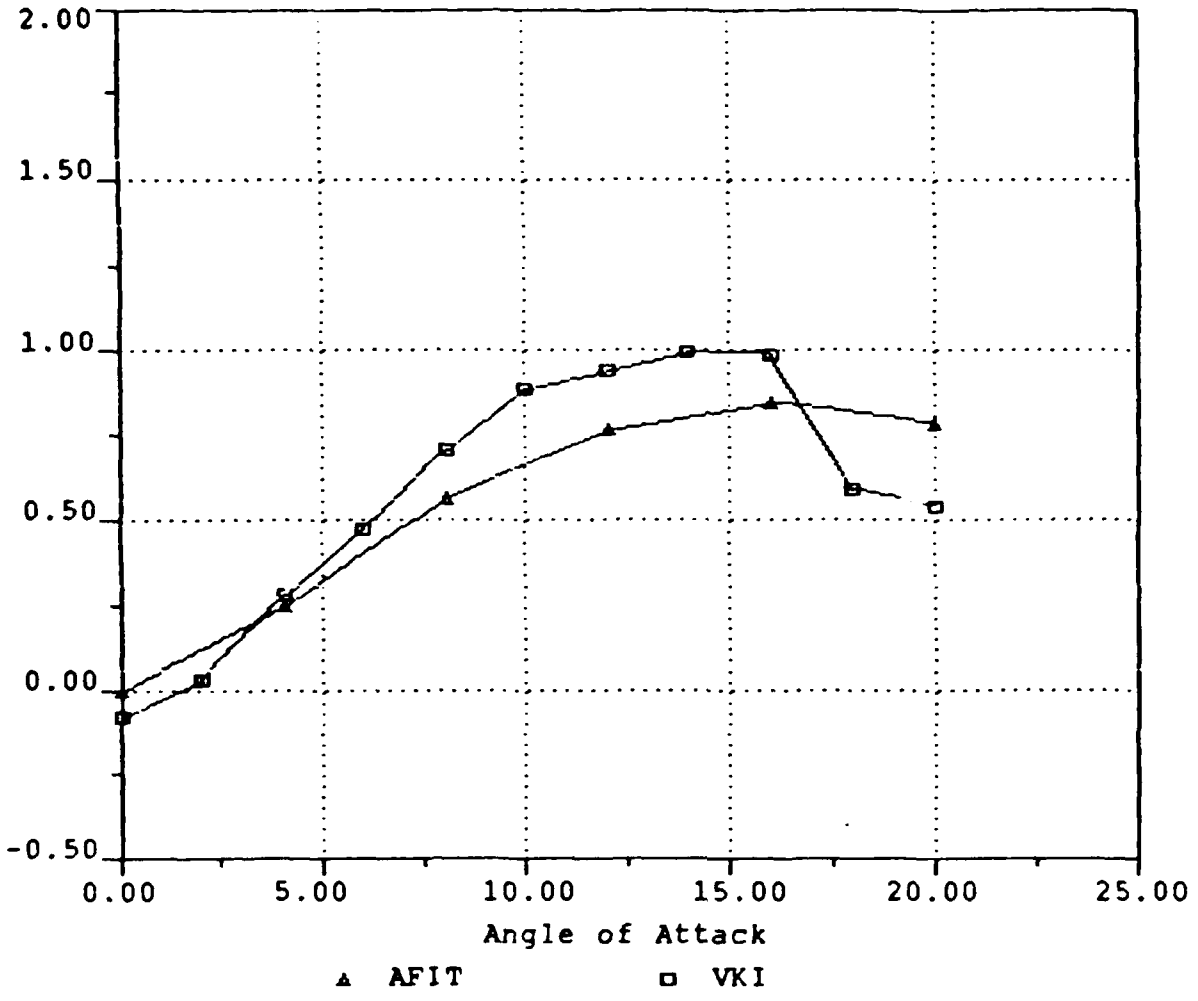

Figure 3. Effect of Tunnel Size on Lift Curve

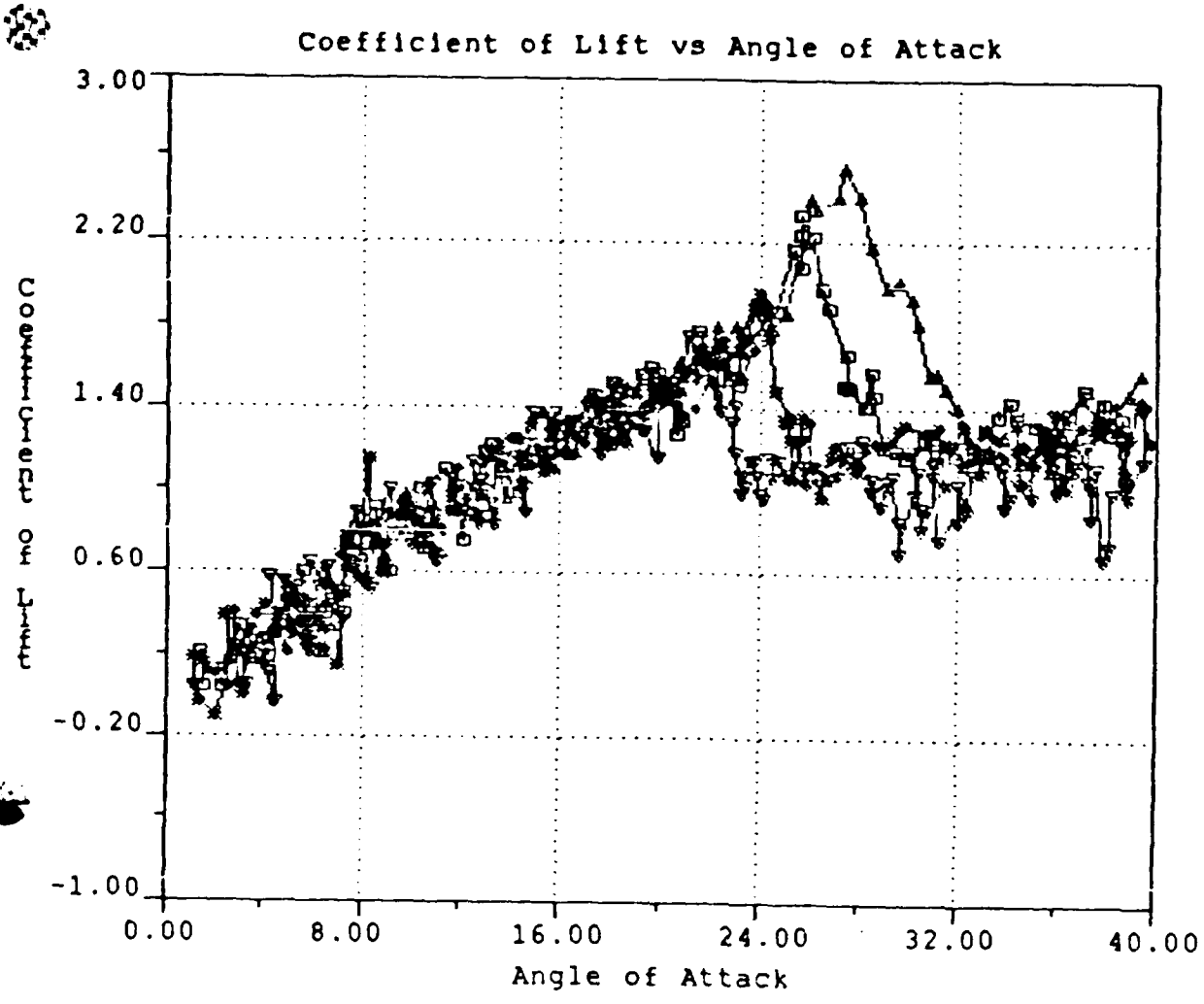

Figure 4. Effect of Pitch Rate on the Lift Curve
$\dot{\alpha}_{ND}$ = 0.0097,0.0134,0.0224,0.0297

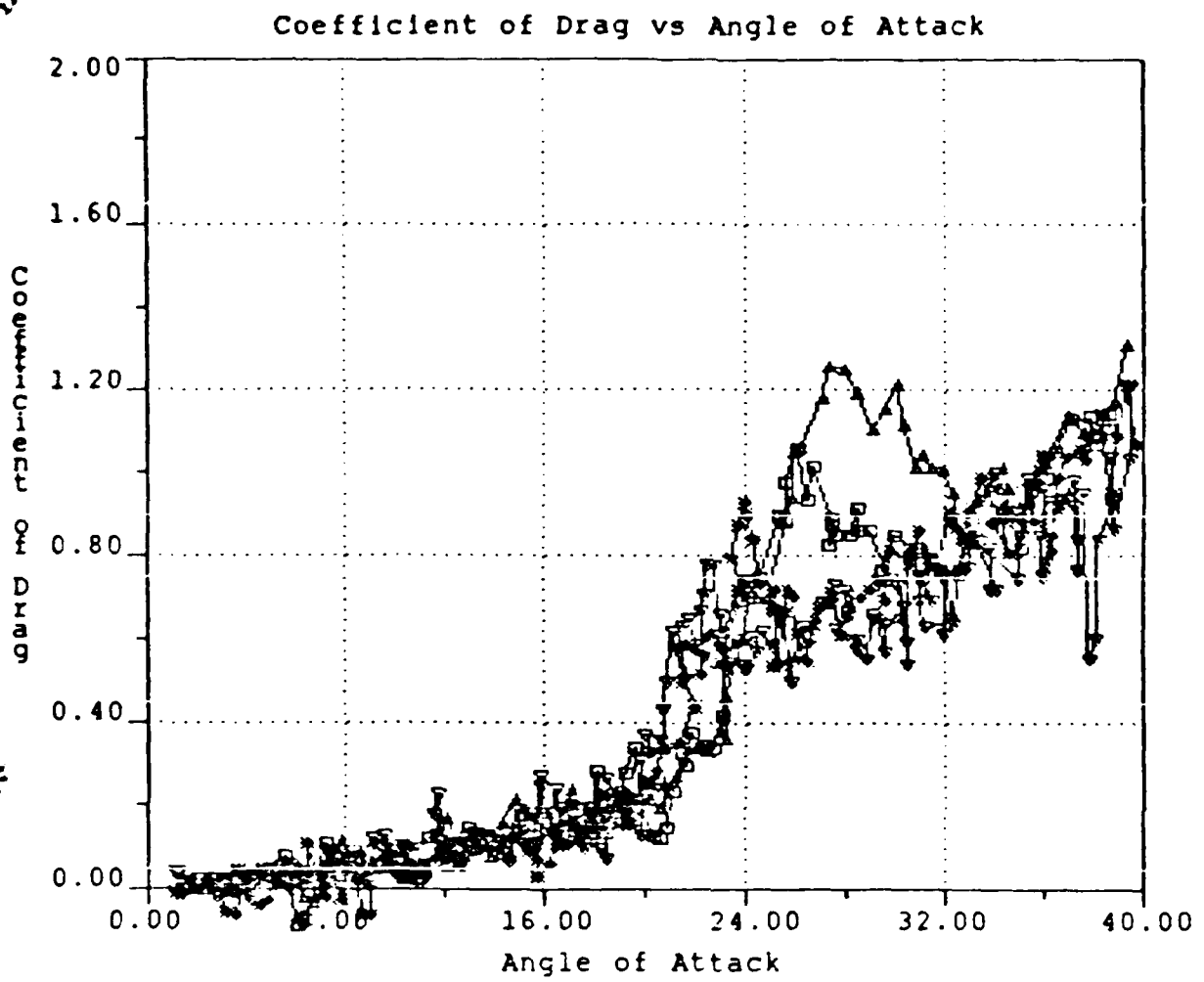

Figure 5. Effect of Pitch Rate on the Drag Curve
q_{ND} = 0.0097,0.0134,0.0224,0.0297

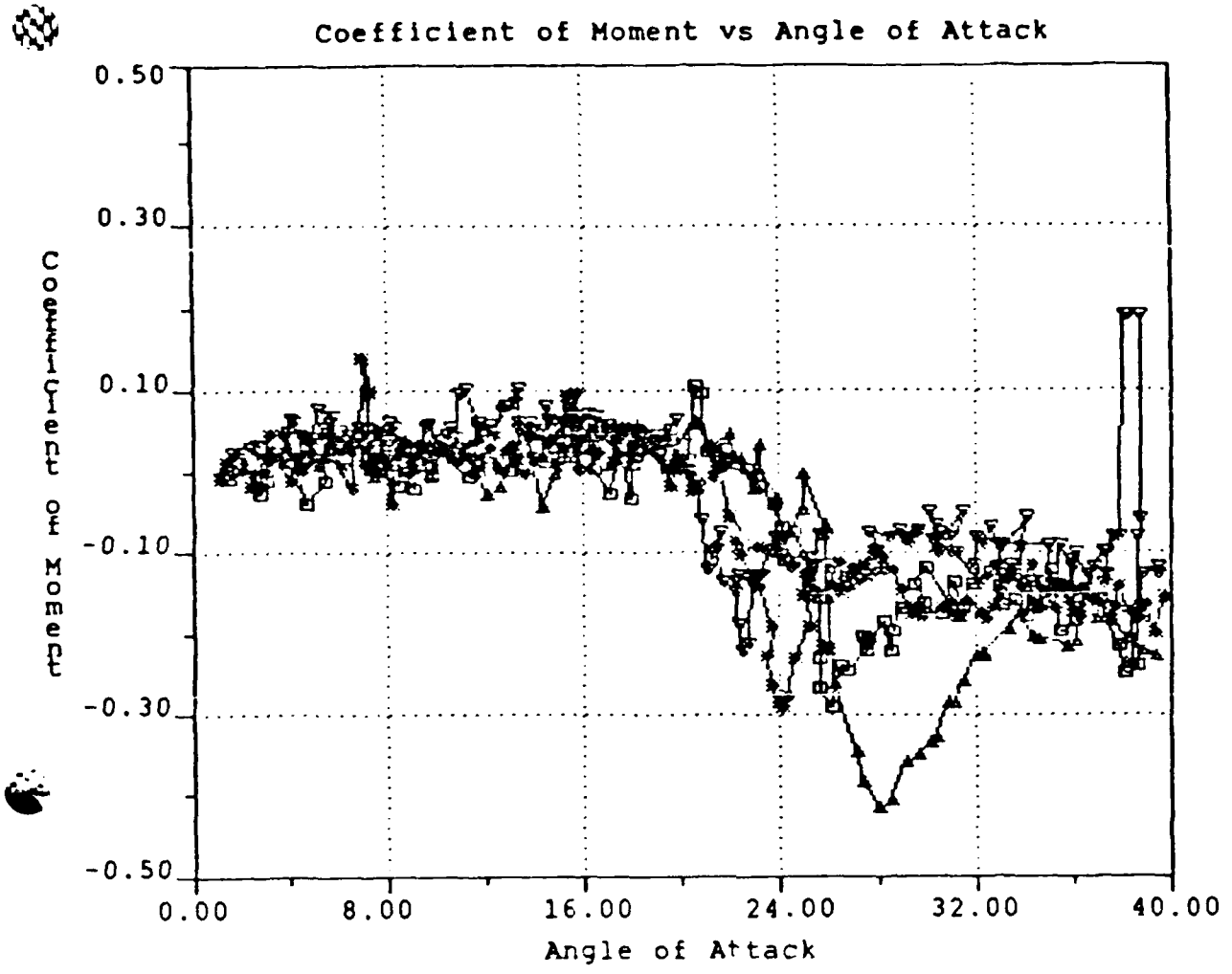

Figure 6. Effect of Pitch Rate on the Moment Curve
$\dot{\theta}_{ND}$ = 0.0097,0.0134,0.0224,0.0297

Table I

Resulting Motions and Average Lift
for Runs at AFIT

Run	$\dot{\alpha}_{up}$	$\dot{\alpha}_{ND}$	$\dot{\alpha}_{down}$	$\dot{\alpha}_{ND}$	α Range (deg)	Average C_L
A	65.81	.0195	93.25	.0276	1-25	.684
B	81.16	.0240	106.11	.0313	0-26	.723
C	89.21	.0264	94.20	.0279	2-22	.515
D	91.07	.0269	109.95	.0325	0-26	.505
E	55.84	.0165	86.57	.0256	6-22	.693
F	73.21	.0217	91.12	.0269	6-26	.830
G	81.42	.0241	93.43	.0276	6-26	.832
H	84.93	.0251	77.64	.0230	6-25	.586
I	49.53	.0146	69.53	.0206	12-22	.918
J	63.33	.0187	82.49	.0244	13-25	.855
K	69.89	.0207	86.59	.0256	12-27	.859
L	72.76	.0215	87.97	.0260	11-27	.834

Table II

Resulting Motions and Average Lift
for Runs at VKI

Run	$\dot{\alpha}_{up}$	$\dot{\alpha}_{ND}$	$\dot{\alpha}_{down}$	$\dot{\alpha}_{ND}$	α Range (deg)	Average C_L
AA	35.06	.0104	161.85	.0479	2-19	.797
BB	37.17	.0110	220.44	.0652	2-26	.807
CC	36.71	.0109	124.34	.0368	5-20	1.043
DD	40.16	.0119	70.45	.0208	11-20	1.108
EE	41.50	.0123	176.81	.0523	-1-21	.793
FF	46.71	.0138	242.95	.0718	-1-28	.814
GG	43.22	.0128	129.61	.0383	5-21	.981
HH	48.05	.0142	84.43	.0250	11-20	1.114
II	86.57	.0256	252.74	.0747	0-24	.868
JJ	65.81	.0195	174.08	.0515	2-21	.789
KK	66.05	.0195	177.06	.0524	0-19	.757
LL	63.91	.0189	196.66	.0582	4-25	.700
MM	110.53	.0327	245.06	.0725	2-21	.833
NN	105.57	.0312	237.88	.0703	0-26	.640
OO	108.85	.0322	269.82	.0798	1-27	.761
PP	108.05	.0320	224.19	.0663	3-21	.879
QQ	102.63	.0304	286.11	.0846	4-28	.942
RR	129.75	.0384	313.67	.0928	0-27	.826

VI. Conclusions

The first objective of this project was to determine an angle of attack versus time profile which could maintain a coefficient of lift greater than the maximum static coefficient of lift. It has been demonstrated (Tables 1 and 2) that for several different angle of attack profiles an average coefficient of lift equal to or greater than the maximum static lift seems to be maintained by pitching back and forth through the static stall angle using constant pitch rate motions. The best case was a motion with a nondimensional pitch rate up of .0145 from 10 to 20 degrees with a rapid pitch down to 10 degrees. This profile provides a sustained 10% increase over the static maximum coefficient of lift. It should be added however that better performance might be possible.

Attempts to excite the vortex shedding without continuing the upward motion of the airfoil does not appear to be possible over the range of nondimensional pitch rates used in this study. The attempts were made by pitching the airfoil to an angle of attack just below where the vortex sheds and then pitching back down. It may be important to note that up to this point, about 20 degrees angle of attack, the pitch rate seems to have little effect on the C_L versus angle of attack curve. Above this point the pitch

rate seems to affect when the vortices separate and their strengths.

Although there appeared to be a slight difference in the static and dynamic lift curves between the AFIT and VKI experiments, the essential features of the dynamic stall events remain the same. Further the slight differences in the AFIT and VKI results may not be due totally to aspect ratio, although, the aspect ratio was the single largest difference in the two experimental set ups. It should be noted that this means experimental-set-up aspect ratio since in both cases the airfoil spanned the tunnel thereby, ideally, both simulated infinite aspect ratios. Even if the differences are attributed to the experimental-set-up aspect ratio, it is clear that the differences are slight, which indicates that the results from studies in the AFIT tunnel are essentially extendable to larger aspect ratios.

Recommendations

This study showed that for the pitch up snap back profiles the best way to maintain the extra lift is with lower pitch rates. Other studies could be conducted to find the effect of a fast pitch up and slow pitch down. This might take advantage of higher lift values while not dropping back through a zero coefficient of lift.

Some flow visualization should be done to determine what happens to the vortex after the airfoil stops pitching up. Also it would be interesting to know if a second vortex actually does separate at the places where it was suspected.

Finally this study provides data for periodic motions with constant pitch rates but does not compare them to results from other profiles, such as sinusoidal. Sinusoidal data is available. Other profiles have not been explored.

Bibliography

1. Jumper, E. J.; Schreck, S. J.; and Dimmick, R. L. "Lift Curve Characteristics for an Airfoil Pitching at a Constant Rate," AIAA-86-0117

2. McAllister, K. W.; Carr L. W.; and McCroskey, W. J. "Dynamic Stall Experiments on the NACA 0012 Airfoil," NASA Technical Paper 1100

3. Schreck, S. J. "Continued Experimental Investigation of Dynamic Stall," Master's Thesis AFIT/GAE/AA/83D-21

4. Carta, F. O. "Unsteady Normal Force on an Airfoil in a Periodically Stalled Inlet," J of Aircraft, September-October 1967,pp 416-421

5. Herbst, W. B. "Future Fighter Technologies," J of Aircraft, Volume 17,No 8,August 1980 pp 561-566

6. McCroskey, W. J. "The Phenomenon of Dynamic Stall," VKI Lecture Series 1981-4

7. Francis, M. S. and Keesee J. E. "Aerodynamic Stall Performance with Large Amplitude Motions," AIAA Journal, Volume 22, Mo 11, November 1985 pp 1653-1659

8. Dimmick, R. L."Pitch Location Effectson Dynamic Stall," Master's Thesis AFIT/GAE/AA/85D-4

9. Liiva, J. "Unsteady Aerodynamics and Stall Effects on Helicopter Rotor Blade Sections," J of Aircraft, Volume 6,No 1,1969, pp46-51

10. Chow, C. W. and Chiu C. S. "Unsteady Loading on Airfoil Due to Vortices Released Intermittently from Its Surface," J. of Aircraft, Volume 23,No 10, pp 750-755

11. Ham, N. D. "Aerodynamic Loading on a Two Dimensional Airfoil During Dynamic Stall," AIAA Journal, Volume 6, No 10, October 1968, pp 1927-1934

12. Milne Thomson, L. M. Theoretical Hydrodynamics, MacMillian ad Co., London, England 1938

13. Carta, F. O. "Effect of Unsteady Pressure Gradient Production on Dynamic Stall Delay," J of Aircraft,Volume 8,No 10,October 1971, pp 839-841

14. Johnson, W. and Ham, N. D. "On the Mechanism of Dynamic Stall," Journal of the American Helicopter Society, Volume 17,No4,October 1972, pp 36-45

15. Ward, J. W. "The Behavior and Effects of Laminar Separation Bubbles on Aerofoils in Incompressible Flow," J of the Royal Aeronautical Society ,Volume 67,No 636, December 1963, pp 783-798

16. Martin, J. M.;Empey, R. W.;McCroskey, W. J.; and Caradonna, F. X. "Experimental Analysis of Dynamic Stall on an Oscillating Airfoil," J of the American Helicopter Society, Volume 19,No 1, January 1974 pp 26-32

17. Herbst, W. B. "Dynamics of Air Combat," J of Aircraft, Volume 20,No 7, July 1983, pp 594-599

18. Daley, D. C. "Experimental Investigation of Dynamic Stall," Master's Thesis, AFIT/GAE/AA/82D-6

19. Baldner, J. L. "Completion of the Development of the AFIT Smoke Tunnel," Master's Thesis, AFIT/GAE-2

20. Kramer, Von M., "Die Zunahme des Maximalauftriebes von Tragflugeln bei plotzlicher Anstellwinkel-vergro Berung (Boenefekt)," Zeitschrift fur Flugteknik und Motor-luftschiffahrt, 7, 14 April 1932, pp 185-189

21. Sisson, F. E. II "Completion of the AFIT Smoke Tunnel," Master's Thesis, AFIT/GAE-12

22. ENDEVCO Corporation, Series 8507 Miniature Piezo-resistive Pressure Transducers, San Juan, California, ENDEVCO Corp.

23. Walker, J. M.;Helin, H. E.;and Strickland, J. H. "An Experimental Investigation of an Airfoil Undergoing Large Amplitude Pitching Motions," AIAA Journal Volume 23,No 8,August 1985 pp 1141-1142

24. Jumper, E. J.;Hitchcock, J. E.;Lawrence, T. S.; and Docken, R. G. "Investigation of Dynamic Stall Using a Modified Momentum Integral Method," AIAA-87-0431

25. Allaire, A. J. S., "Investigation of Potential Viscous Flow Effects Contributing to Dynamic Stall," Master's Thesis, AFIT/GAE/AA/84S-1

26. Jacobs, E. N. and Sherman, A. "Airfoil Section Characteristics as Affected by Variations in the Reynolds Number," NACA Report 586,1937

Appendix A

Transducer Calibration

The sensitivity calculation for the transducers was a simple job but required two people. One person held the pressure on the transducer and the second took the readings. The pressure was provided through three pieces of Tygon tubing which were connected in a T-shape. One tube was connected to a manometer, the second to a low pressure source and the third was left open. At AFIT, the low pressure source was a hand operated vacuum pump. At the VKI the source was the researcher. The tubes had an inner diameter of .375 inches. The open end was held manually against the airfoil and over the transducer. No vacuum grease was used to improve the seal for fear of contaminating the transducers. With a pressure being applied, readings were taken through the program CALIB. This program asks for the appropriate transducer number, then takes 100 readings from that transducer and returns an average. The readings were provided in digital counts.

The sensitivities were determined by taking readings at four different pressures between zero and two inches of water along with the zero pressure readings. The readings were converted to millivolt changes by subtracting the zero pressure reading and multiplying by 50 mV per 2048 digital

counts. The manometer reading was reduced to pounds per square inch by the factor 27.68 inches of water per psi. The sensitivities were the ratio of two numbers. The sensitivities ranged from 111 to 227 mV/psi. The upper values were beyond the range specified by the manufacturer, however they showed good linearity over the pressure range. The sensitivities are listed in Table III.

At first the transducers were calibrated daily, however, most of them varied only two percent from one day to the next. If the transducer varied more than two percent the sensitivities returned to their former values the next day. This may indicate an error in the calibration procedure. After that the calibration was only performed when transducers were removed and replaced. Again the sensitivities only varied two percent.

Table III

Transducer Sensitivities

Transducer Number	Sensitivity (mV/psi)
1	197.0
2	170.3
3	173.0
4	227.5
5	178.0
6	179.0
7	189.0
8	211.3
9	171.5
10	111.5
11	116.2
12	130.2
13	135.5
14	147.0
15	*
16	219.0

* Transducer malfunctioned during the tests so this transducer was not used

Appendix B

Sources of Error

This section was prompted by the inability of the researcher to produce an adequate pressure profile at a zero degree angle of attack. Profiles at higher angle of attack appeared reasonable. However at zero angle of attack the profile did not show a smooth transition from low pressure near the leading edge to a higher pressure at the trailing edge. Rather the pressure was up and down along the upper surface. A second point was that the leading edge transducer (which should provide a coefficient of pressure, C_p, of 1.0 for a zero angle of attack) always returns a C_p lessthan 1.0.

The method of calculating the C_p's has been discussed in the Theory and Approach section. Equation 7 will be used to investigate the effect of errors in pressure measurements on the C_p values. For ease of writing the terms in Equation 7 were renamed. Renaming Δp_{tran} as p_1, $p_{amb}-p_\infty$ as p2 and p_o-p_∞ as p_3, the equation becomes

$$C_p=(p_1+p_2)/p_3 \qquad (8)$$

To study dependence the differential was take

$$dC_p = dp_1/p_3 + dp_2/p_3 + C_p*dp_3/dp_3 \qquad (9)$$

For this experiment p_1 and p_2 were on the order of .1 psi while p_3 was on the order of .01 psi. From the equation it could be deduced that a 10% change in p_2 or p_1 would cause a change in C_p of 1.0. It can also be seen that the change in C_p is proportional to the change in p_3.

An example of the magnitude of the error is a reading of 0.5 for the leading edge transducer. p_3, which was being measured through a pitot tube using a pressure transducer, varied only about 2%. This wouldn't be nearly large enough to cause a .5 error. p_2, which was being measured with a Bets manometer, varied only 1%. This would be enough for an error of .1, but the C_p was calculated from the average of 100 readings so the fluctuation errors should average out.

The numerator of the remaining term in Equation 9 can be written as

$$dp_1=(50/2048)\{d(counts)/sens - d(sens)*counts/sens^2\}$$

where 'counts' is the change in digital output from the A to D board and 'sens' is the transducer sensitivity. In this equation the counts are on the order of 500 and the sens is on the order of 150. To find out what kind of error could be found in the transducer readings 100 samples were taken from

the upper nine transducers. A mean and variance was calculated for each and is shown is Table IV. These transducers seem to be responding to the turbulence in the tunnel which was between 1 and 2 percent (see Appendix C). The results for the first five transducers are plotted in Figure 7. The figure shows all the readings fell within $\pm$6% of the mean value. Plugging a 6% error into the equations along with the approximate values indicates that a 6% change in 'counts' could cause the C_p to be 0.7. Again this error should average out.

Another possibility is zero drift with a temperature change on the transducer. To check for drift a reading was taken of the leading edge transducer after the tunnel had been idle for about an hour. A reading was actually an average of 100 readings. Consecutive readings indicated that the output from the transducer varied less than 2 digital counts. After some calibration tests where the tunnel ran for about 25 minutes the tunnel was shut down. When the Bets manometer indicated that the room and tunnel pressure were identical a another reading was taken which read seven counts less than the original zero pressure value. An error of seven digital counts could change the C_p by .16. This isn't enough to explain an error of .5 but it's in the right direction.

A final possible error is the error in sensitivity. As

discussed in Appendix A, the sensitivity were determined within 2%. From Equation 9 it can be seen that an error in p_1 would be proportional to an error in the sensitivity. To test the sensitivity the tunnel was run up through four different speeds consecutively and then back down through the same speeds. The speeds were indicated by measurements from the pitot probe. The pressure readings along with an expected value of pressure from the leading edge transducer are given in Table V. The expected value is found by assuming a C_p of 1.0 at the leading edge.

A sensitivity was found by changing the digital count change to millivolts through the 2048 to 50 conversion from the A to D board. This number was divided by the expected pressure the provide a sensitivity. Table VI gives the results. The count change was determined by two methods. The first used the original zero pressure values. The second assumes a negative seven count zero drift.

From the results show that the sensitivity decreases with increasing. This would be the case if the transducer behaved linearly but the zero was shifted. This behavior is more evident in the first case than the second. It could be assumed that while the tunnel was settling after the run the transducer was warming up so that the drift is actually higher seven counts. If the actual drift was 14 counts Table VII gives the results.

Table VII shows a more linear result and the value is closer to the sensitivity calculated in Appendix A. (the values of sensitivity give in Appendix A were for the set up at AFIT. The transducers were rearranged at VKI so that transducer 14 from Table 3 is at the leading edge). The first value in the table could be explained by the fact that the tunnel had not run long enough or fast enough to provide the drift. A zero drift of 14 counts along with some error in the sensitivity could cause the .5 error.

A shift of 14 counts would be equivalent to a shift of .34 mV. According to the ENDEVCO catalog, maximum zero shift over the compensated temperature range is 3% of the full scale output. The full scale output is 300 mV, so the maximum zero drift would be 9 mV. The compensated range is zero to 200 degrees Fahrenheit with a reference temperature of 75 degrees. Therefore a shift of .34 mV could be explaned by a few degrees of cooling. Since the transducer gets warm during operation, the wind blowing on it could cause this cooling.

If this an accurate description of what is happening to the transducer the effect should be most prominent at the leading edge. Secondly as the pressure differences climb the effect would be less noticable because the error percentage would decrease. This could explain the good pressure profiles at higher angles of attack. To test the theory the

airfoil was held at zero angle of attack for 10 minutes in the wind. Then the tunnel was shut down. The zero pressure readings before and after the run are listed in Table VIII. These results show that aft the third transducer there is little effect on the zero readings.

As a result of these tests the procedure for taking the zero pressure readings was changed. Since the tunnel has to be running to set the motions, that time is used to "cool" the transducers. Then the transducers are read as soon as the manometer indicates consistent pressures inside and outside the tunnel. The scatter in the data during dynamic runs can be explained fluctuations in tunnel pressures with tubulence. This demonstrates the need for averaging the data.

Table IV

Averaged Readings from Transducers
(Results from 100 Readings)

Transducer	Mean Count	Variance
1	414.3	.020
2	673.3	.018
3	670.8	.016
4	577.2	.018
5	678.9	.018
6	572.4	.021
7	553.8	.018
8	699.5	.015
9	421.7	.020

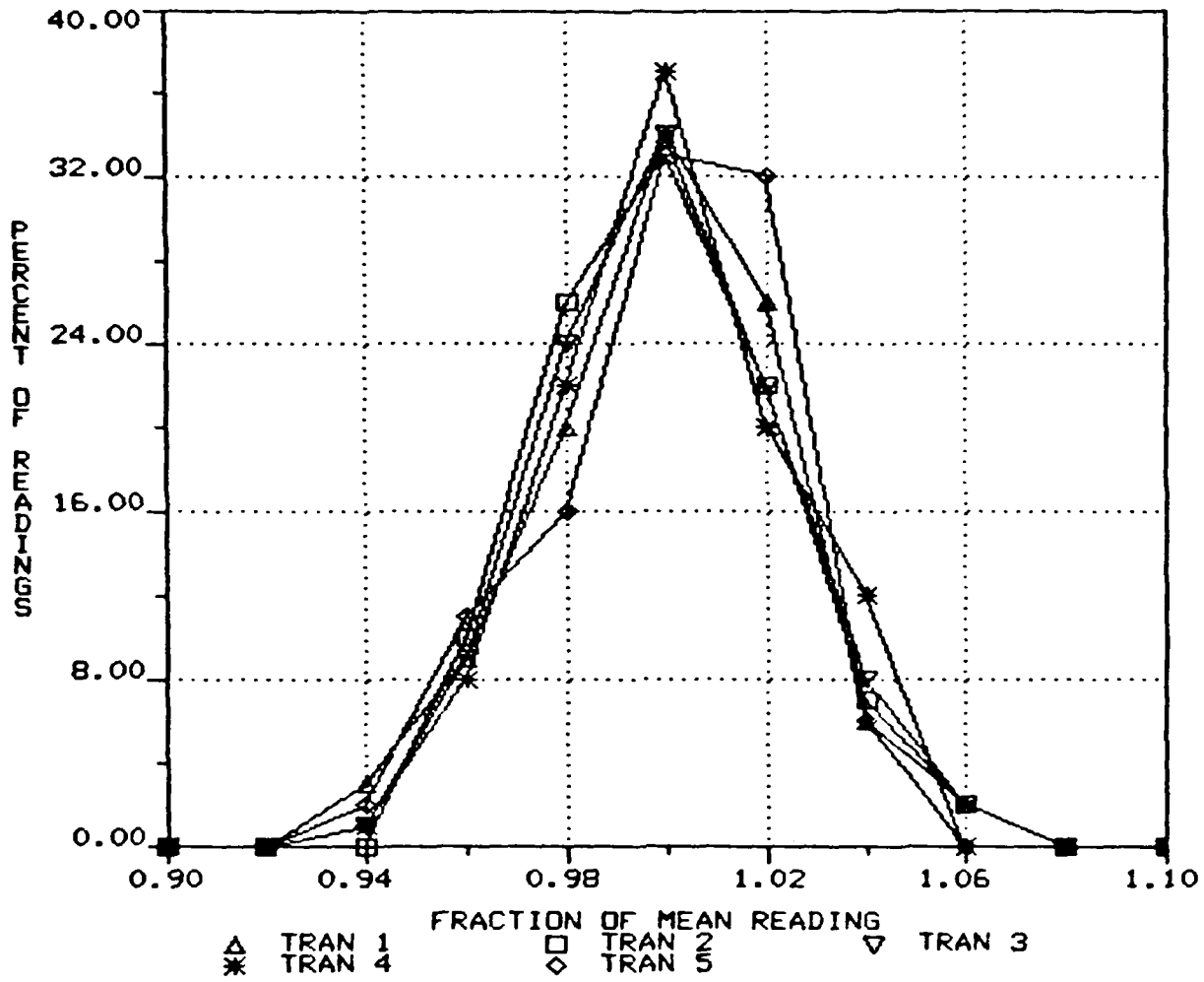

Figure 7. Scatter in Transducer Readings for Pressure Transducers 1 through 5

Table V

Readings from Leading Edge Transducer

Pitot-Static Pressure (in H_2O)	Reading (Digital Counts)	Room-Static Pressure (mm H_2O)	Expected Local Pressure (psi)
0.00	2032.1	0.0	0.00
0.05	1906.6	14.5	0.0188
0.10	1813.9	26.3	0.0338
0.15	1713.6	39.0	0.0501
0.20	1625.3	50.5	0.0646
0.15	1721.6	38.2	0.0489
0.10	1810.0	26.5	0.0341
0.05	1907.9	14.0	0.0181
0.00	2025.4	0.0	0.00

Table VI

Calculated Sensitivity
for Leading Edge Transducer

Pitot-Static Pressure (in H_2O)	Sensitivity Original (mV/psi)	Sensitivity with Drift (mV/psi)
0.05	162.9	154.2
0.10	157.6	152.8
0.15	155.2	151.9
0.20	153.7	151.2
0.15	155.0	151.7
0.10	159.0	154.2
0.05	167.5	158.5

Table VII

Possible Sensitivity
for Leading Edge Transducer

Pitot-Static Pressure (in H_2O)	Sensitivity Proposed (mV/psi)
0.05	144.7
0.10	147.4
0.15	148.3
0.20	148.4
0.15	148.0
0.10	148.9
0.05	148.5

Table VIII

Variation in Transducer Reading with Run Time
for Leading Edge Transducer

Transducer	Original Reading	Readings at t after Shutdown t(min) 0	1	4	9	14
1	2028	2021	2024	2026	2027	2028
2	1994	1974	1984	1988	1993	1994
3	1983	1934	1986	1986	1983	1983
4	1735	1735	1736	1736	1736	1736
5	1901	1900	1901	1902	1902	1902
6	2192	2191	2192	2192	2192	2192
7	1841	1839	1841	1841	1841	1841
8	2169	2161	2167	2169	2170	2171
9	2021	2020	2021	2021	2022	2022

Appendix C

Wind Tunnel Modification

The objective in going to the von Karman Institute was to extend the work at AFIT. To accomplish this, the same airfoil model was used with extension to allow investigation of experimental-set-up aspect ratio effects. For low speed wind tunnel work the VKI has several tunnels, the largest being its L-1 tunnel with a three meter cross section. The next size down is the L-2A which has a 28 centimeter test section. with a 12.2 inch chord (about 31 cm) on the model the L-2A tunnel was too small. The availability of the L-1 precluded its use and sixteen pressure transducers would not fit in a smaller model. Therefore the L-2A wind tunnel was modified.

The original L-2A with its 28 centimeter octagonal test section could provide a test section velocity of 40 meters/second. With a 28 centimeter depth maintained and the height increased to one meter, the existing fan could provide a test section velocity between 10 and 15 meters/second. This is approximately the range of velocities for the tests performed at AFIT. The one meter height would provide a three to one ratio of height to chord length, identical to AFIT's Smoke Tunnel.

Thus a test section two meters long with a cross section one meter high and .28 meters deep was constructed from plywood to connect with the existing fan. To reduce the swirling effects from the fan a 3 meter section of pipe was attached directly upstream. Based on availability, the pipe with diameter nearest that of the fan (66 cm) had a diameter of 63 centimeters. This required a short section of the original diffuser to be cut upstream of the fan to accomodate the mismatch. To transition from the rectangular test section to the circular pipe a steel diffuser section 94 centimeters long was fabricated. This length provided an overall divergence of only 2 degrees, small enough to keep the flow from detaching. At the opening of the test section plastic tubing was used to provide a inlet for the tunnel. The tubing had an outer diameter of 12.5 centimeters and was split in half to provide semicylinders which were mounted to the inlet. A plexiglas window was placed halfway down the side of the tunnel to provide visual access to the model. The window was 50 centimeters wide and extended the height of the tunnel.

With these modifications an attempt was made calibrate the wind tunnel. A pitot probe, mounted on the center line and just upstream of the window, was used to find the velocity. However, the reading varied too much to get an accurate reading. Therefore a hot wire anemometer with some

approximate linearization constants was used to determine the turbulence in the test section. The turbulence level was 9%. Some further modifications were required the turbulence into a reasonable range. First to eliminate any effects from the fan a piece of open-cell polyurethane foam was placed at the junction between the pipe and the new diffuser. The foam was one centimeter thick with 20 pores per inch. When this failed to make a major difference in the turbulence readings, a tuft of yarn was used to search for areas of separated flow. The tuft tests revealed regions of separation in the corners of the inlet. Aluminum honeycomb was placed in the inlet to reduce this separation. The honeycomb was eight centimeters thick with cells approximately 3 millimeters in diameter. This addition reduced the turbulence to about 5%. An additional layer of polyurethane foam in front of the honeycomb reduced the turbulence to about 1.5%.

This level of turbulence is not much more than was encountered at th AFIT Smoke Tunnel and therefore was suitable for continuing the experiment. With these modifications the tunnel can still reach 12 meters/second but the test were run at about 10 meters/second. Table IV shows the turbulence and velocity profiles for the tunnel running at 10 meters/second. These values were measured with a hot wire probe. The probe was calibrated using a rotating

fan anemometer.

Figure 9 shows the access ports to the tunnel. The static port was along the centerline and 54 centimeters ahead of the leading edge. The pitot port is located at one quarter the height and one chord length ahead of the leading edge. The access door is 31 centimeters high and 35 centimeters long and is located aft of the window. The access door was added to provide acces to the airfoil for transducer calibration.

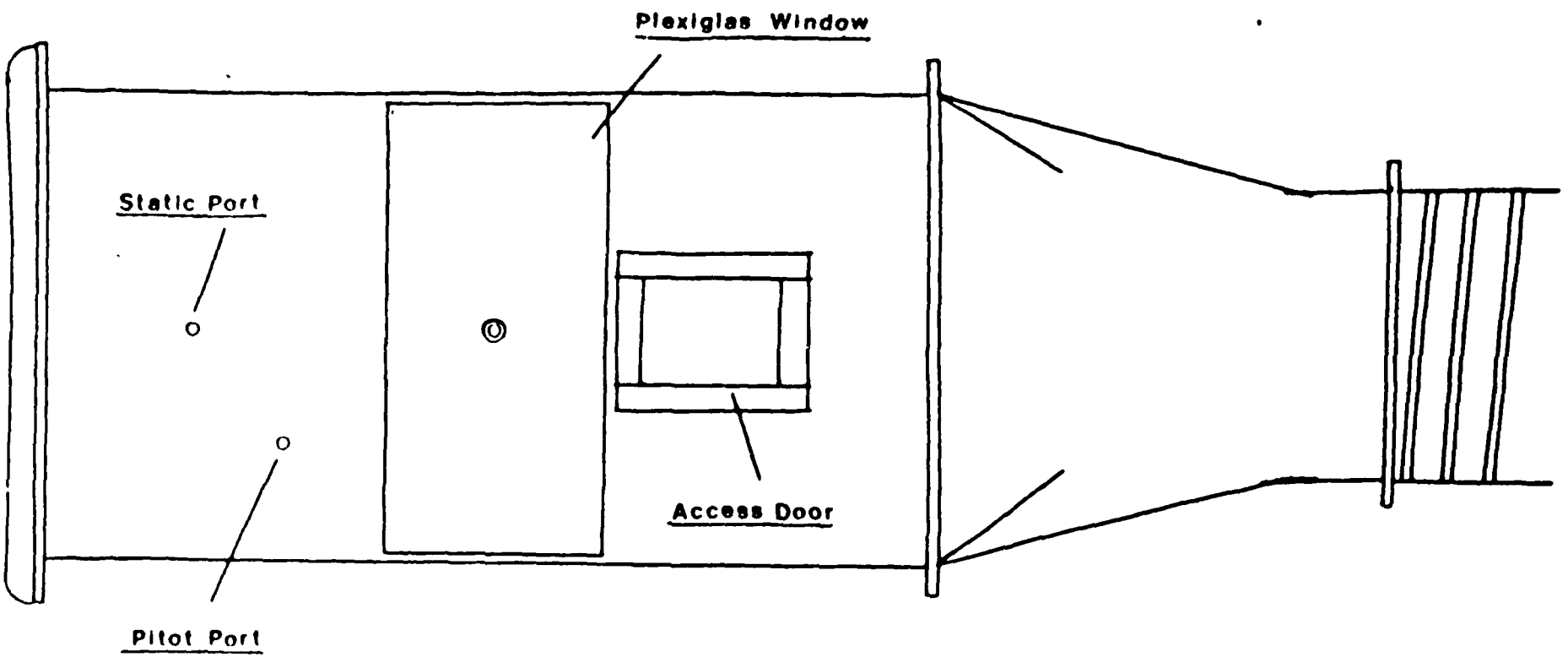

Figure 8. Modified L-2A Wind Tunnel

Table IX

Calibration of Modified Wind Tunnel
for 10 m/s Airspeed

x-position (cm)	Velocity (m/s)	Turbulence
wall	6.9	.119
0.1	7.4	.096
0.2	7.7	.091
0.3	8.0	.085
0.4	8.3	.081
0.5	8.6	.075
0.6	8.9	.070
0.7	9.1	.066
0.8	9.3	.061
0.9	9.4	.057
1.0	9.6	.051
1.1	9.9	.044
1.2	9.9	.040
1.3	10.1	.030
1.4	10.2	.026
1.5	10.3	.021
1.6	10.3	.018
1.7	10.3	.017
2.2	10.2	.012
4.2	10.3	.013
6.2	10.2	.015
8.2	10.2	.015
10.2	10.2	.017
11.2	10.1	.016
12.2	10.0	.016
13.2	10.2	.016
14.2	10.1	.016
15.2	10.2	.016
16.2	10.1	.018
17.2	10.2	.014
18.2	10.1	.017
19.2	10.0	.016
20.2	9.8	.018
21.2	9.9	.018
22.2	9.7	.019
23.2	9.6	.021

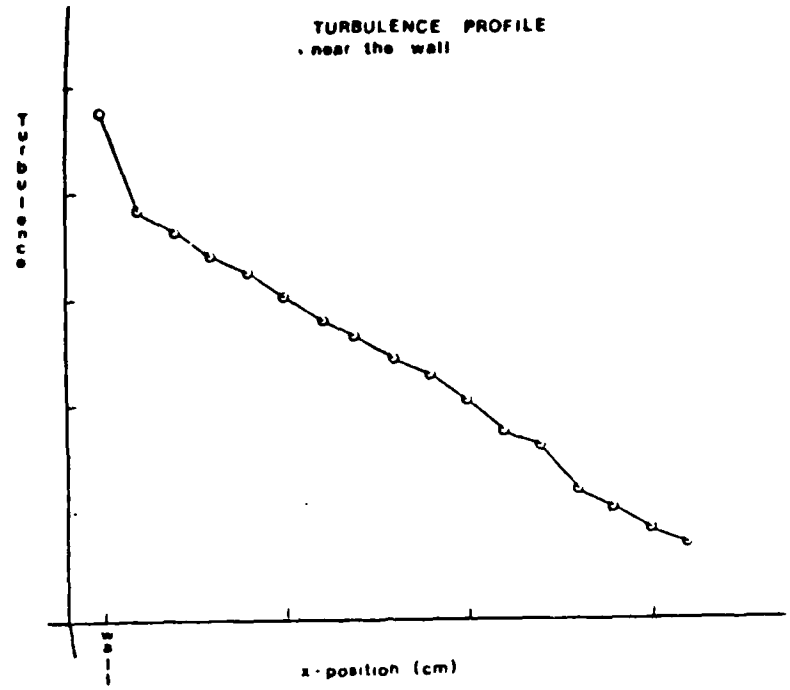

Figure 10. Turbulence Profile Near the Wall for the Modified L-2A

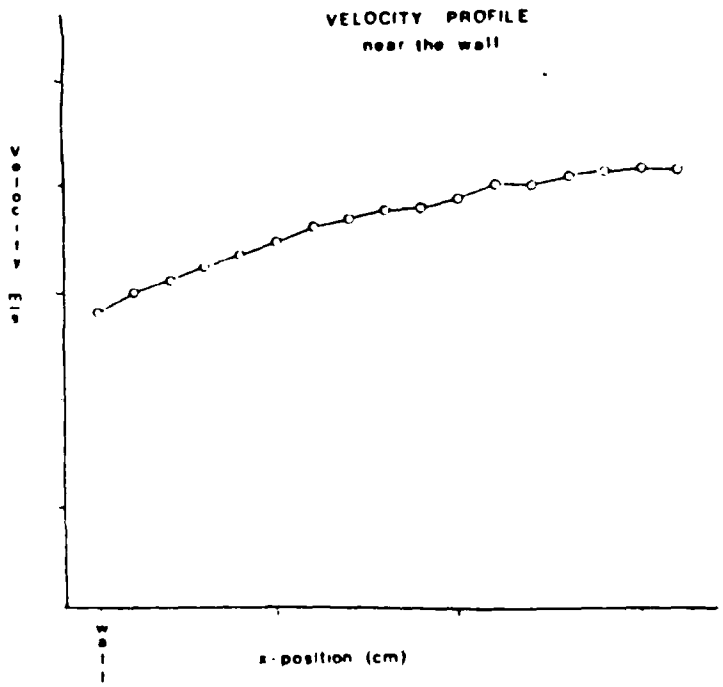

Figure 9. Velocity Profile Near the Wall for the Modified L-2A

Appendix D

The Drive Systems

Providing a periodic motion with constant pitch rates required special drive mechanisms. At AFIT the system was built around the TRW Globe Model 5A2298-4 gearmotor. At the VKI, to provide for a larger model and to allow the option of several different kinds of motion, a more complicated system constructed from a servo motor driven by an amplifier from a portable computer. In this investigation each system had advantages and disadvantages.

The gearmotor used at AFIT had been used in previous work with the same model to provide constant pitch rates in one direction only. To provide the periodic motion a circuit was designed and built by Jay Anderson, an AFIT technician. The circuit required three power supplies: one to supply the pitch up voltage, the second for the pitch down, and the third to power the reed relays that switched the voltage from one source to the other. The relays were triggered by two microswitches that were mounted on a circular track surrounding the airfoil shaft. The switches were positioned on the tracks to provide the maximum and minimum angles of attack. Each microswitch had a flexible arm over the button which would contact another flexible, spring steel arm which was fixed to the airfoil

shaft. Flexible arms were used to reduce the stress on the connections between the arm and the shaft. Failure of the shaft to stop could damage the data lines.

The advantage of this system was its simplicity. The motor provided good constant rate pitch motions with rapid accelerations, which can be seen in Appendix E. The disadvantage came in repeatability. The flexible arms did not contact and bend in the way same every time. The maximum could vary up to two degrees in five runs. The second disadvantage was the ability of the motor to provide the rapid pitch down motion. The motor could provide a pitch down of about 100 degrees per second. This wasn't very rapid compared to 90 degrees per second pitch up. The third disadvantage was the delay at the maximum angle of attack. This could be attributed to slippage in the connections. The connection between the shaft and the arm was made with set screws pressing against the shaft. With rapid acceleration and deceleration it was hard to prevent slippage.

The second system, from VKI, incorporated a servo motor, controlled through a TRS-80 model 100 computer. A basic package provided by the manufacturer allowed the researcher to write programs to set the maximum and minimum angles of atack along with the relative pitch rate of the up and down motions. Outside the program different parameters

of the system's servo control loop could be varied to improve the linearity of the motion. To prevent slippage in this system the shaft of the motor was large enough to have a key way and the connection at the shaft was made by screwing into the shaft, not just against it.

The big advantage of this system was repeatability. A motion, once described could be repeated within a degree consistently. The second advantage was also a disadvantage. That was the flexibility of the system to provide several motions. This made it difficult to provide a constant pitch rate motion. With the preset values for the servo loop the model / control system was unstable. When the position indicator was in place it provided some damping and made the system more stable but adding the wind reduced the stability. To improve the stability the feedrate was set high and the servo loop gain low. The process was then trial and error to find the proper settings for the desired motions. The process was improved with the used of an ultraviolet oscilloscope connected to the position indicator to provide quicker printouts of the motions. This procedure was long and each new pitch rate, maximum or minimum angle of attack required some adjustments to the system.

The second system has the potential to be a better drive system with its flexibility and more power than the first system. However before the system is used again some research should be done to find the equation for the motion with all the variables included so that the trial and error method could be discarded.

Appendix E

Results from Test Runs

AD-A179 512 INVESTIGATION OF PERIODIC PITCHING THROUGH THE STATIC STALL ANGLE OF ATTACK(U) AIR FORCE INST OF TECH WRIGHT-PATTERSON AFB OH SCHOOL OF ENGINEERING 2/2

UNCLASSIFIED E C STEPHEN MAR 87 AFIT/GAE/AA/87M-4 F/G 20/4 NL

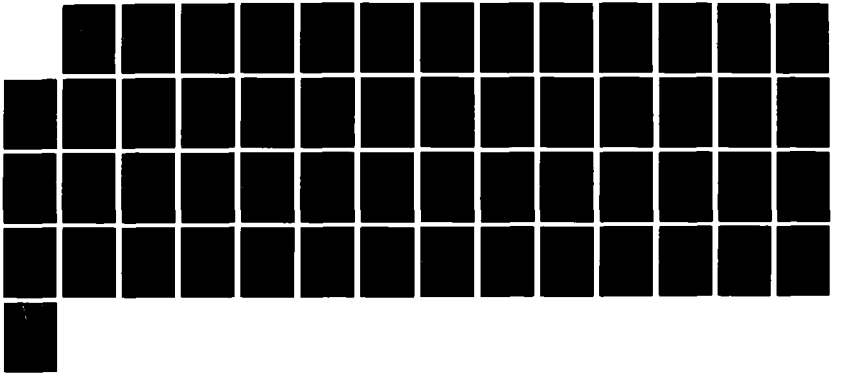

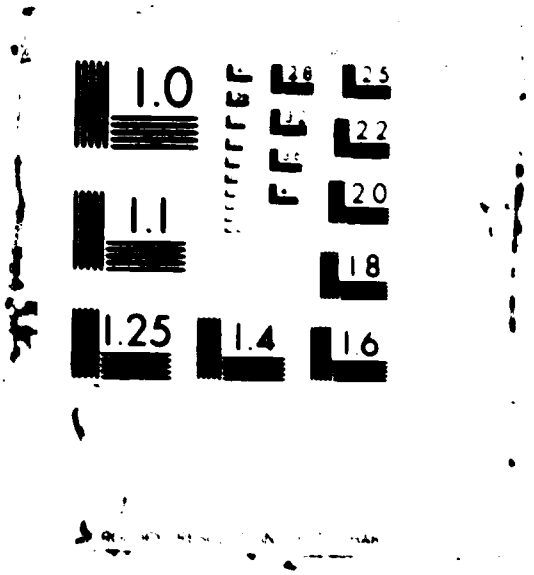
1.0
1.1
1.25
1.4
1.6
2.5
2.2
2.0
1.8

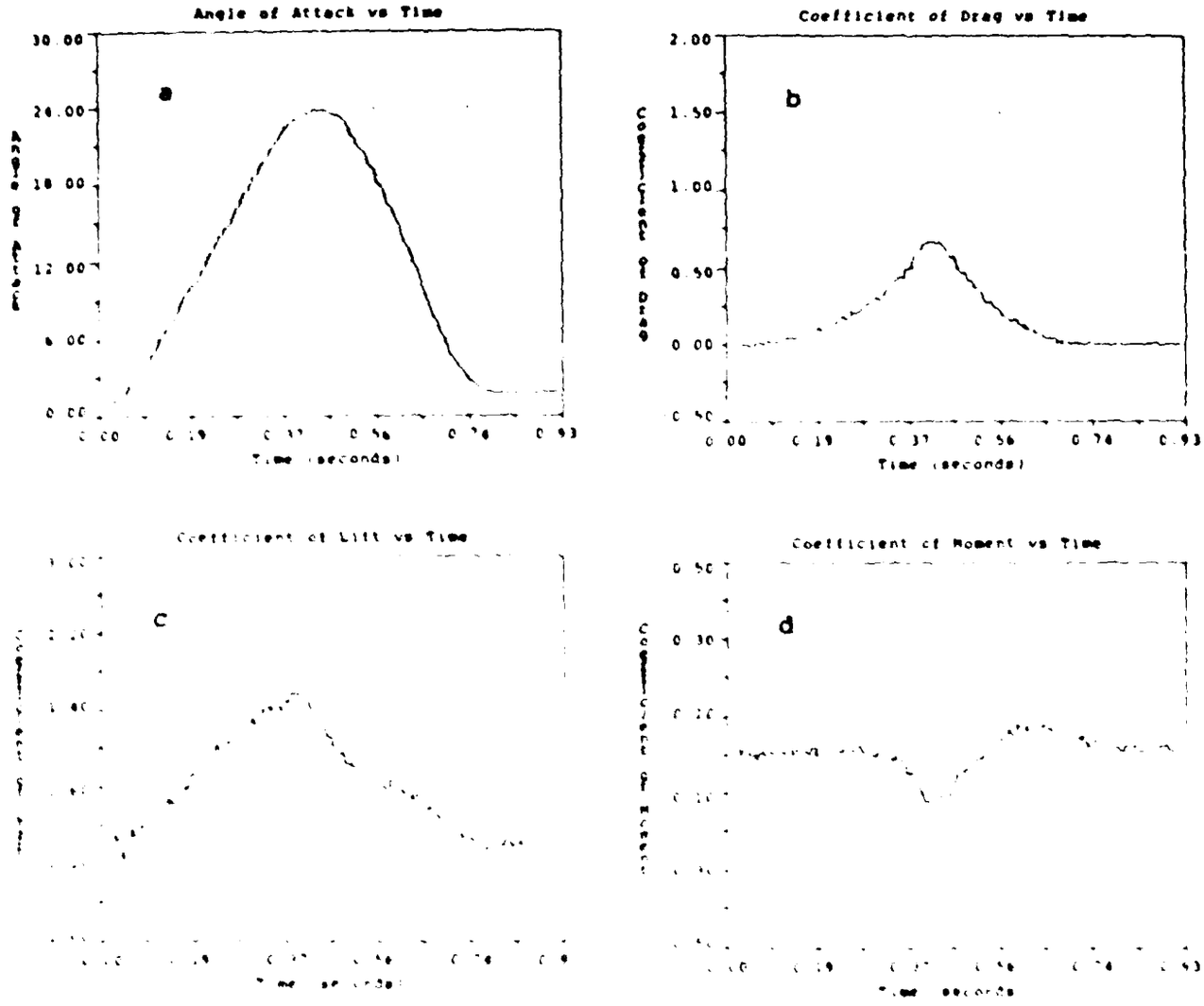

Figure 11. Results from Run A α_{ND} = .0195, α_{SD} = .0276

a) Angle of Attack Profile, b) Effect on C_L

c) Effect on C_D, d) Effect on C_M

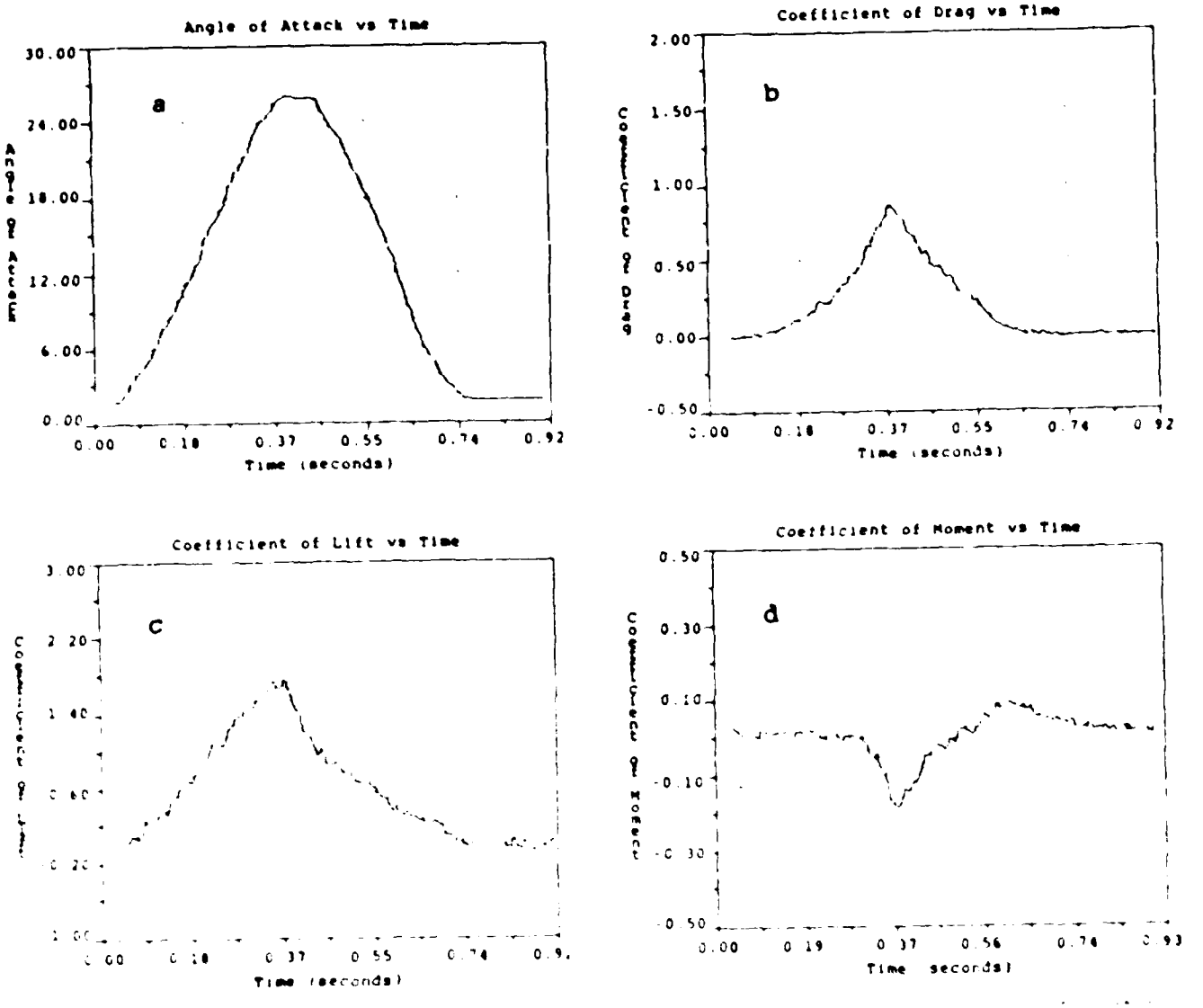

Figure 12. Results from Run B $\alpha_{ND_{up}} = .0240, \alpha_{ND_{down}} = .0$

a) Angle of Attack Profile, b) Effect on C_L

c) Effect on C_D, d) Effect on C_M

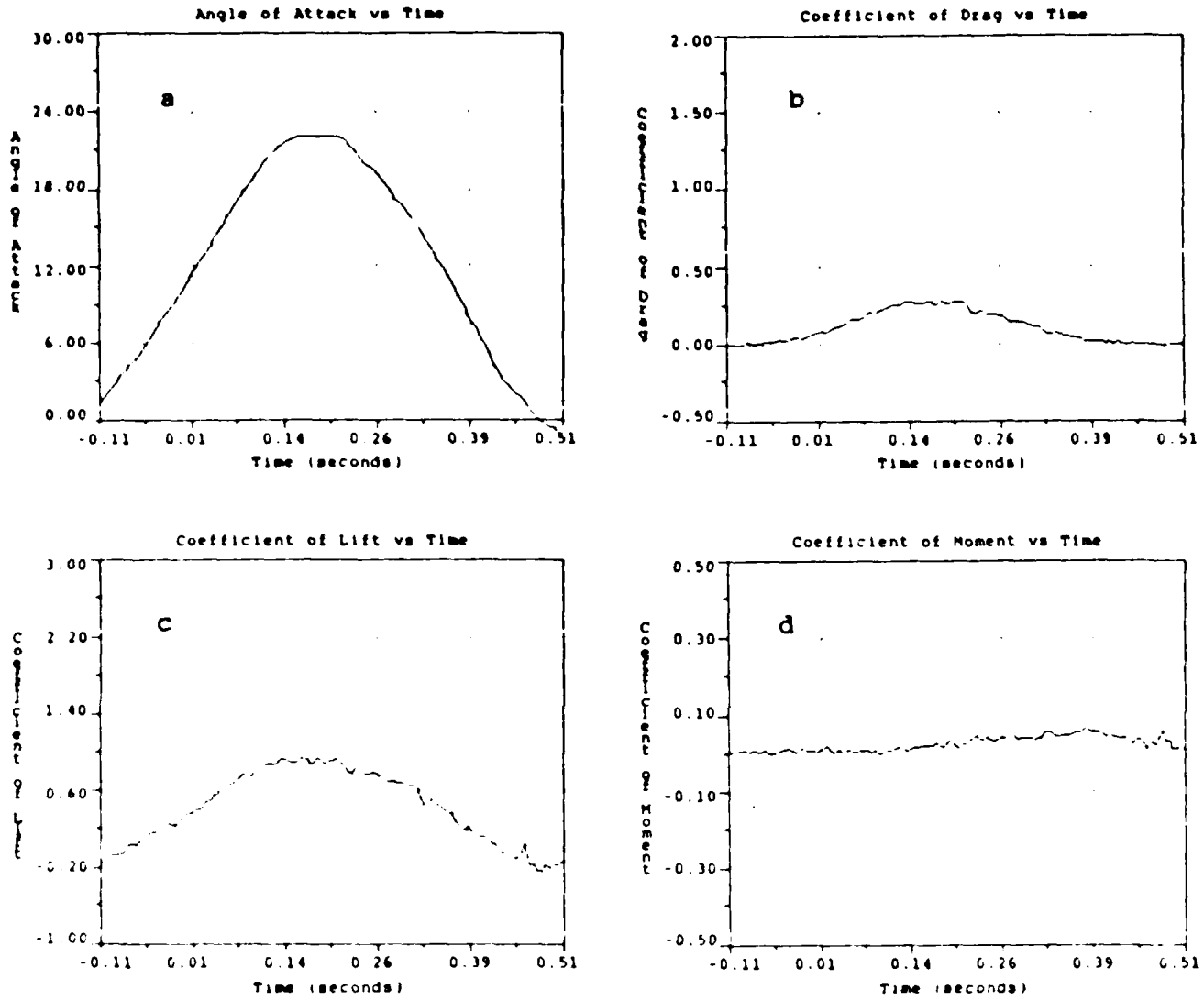

Figure 13. Results from Run C $\dot{\alpha}_{ND_{up}} = .0264, \dot{\alpha}_{ND_{down}} = .0279$
a) Angle of Attack Profile, b) Effect on C_L
c) Effect on C_D, d) Effect on C_M

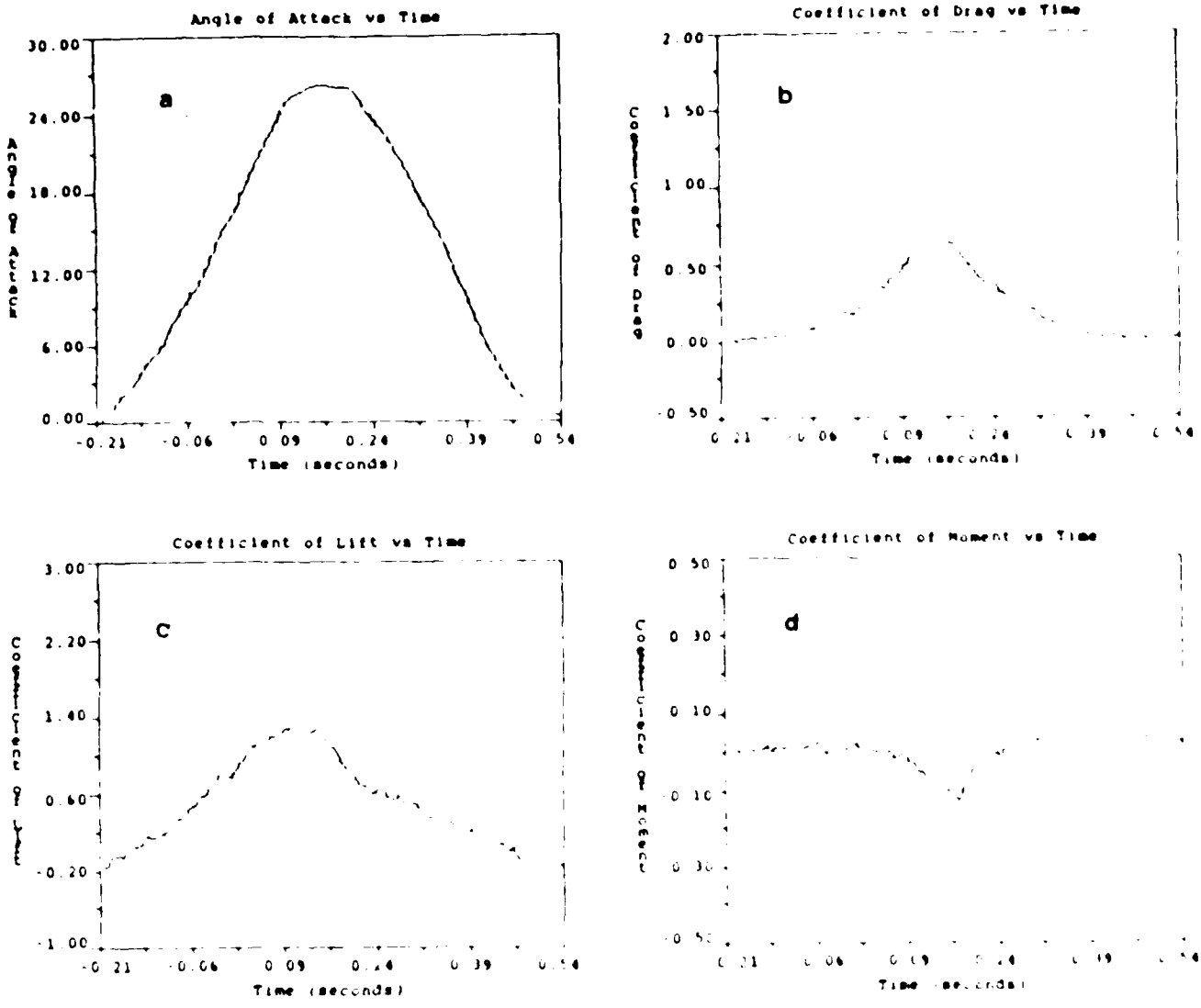

Figure 14. Results from Run 1 $\alpha_{ND_{up}} = .0269$, $\dot{\alpha}_{ND_{down}} = .0325$
a) Angle of Attack Profile, b) Effect on C_L
c) Effect on C_D, d) Effect on C_M

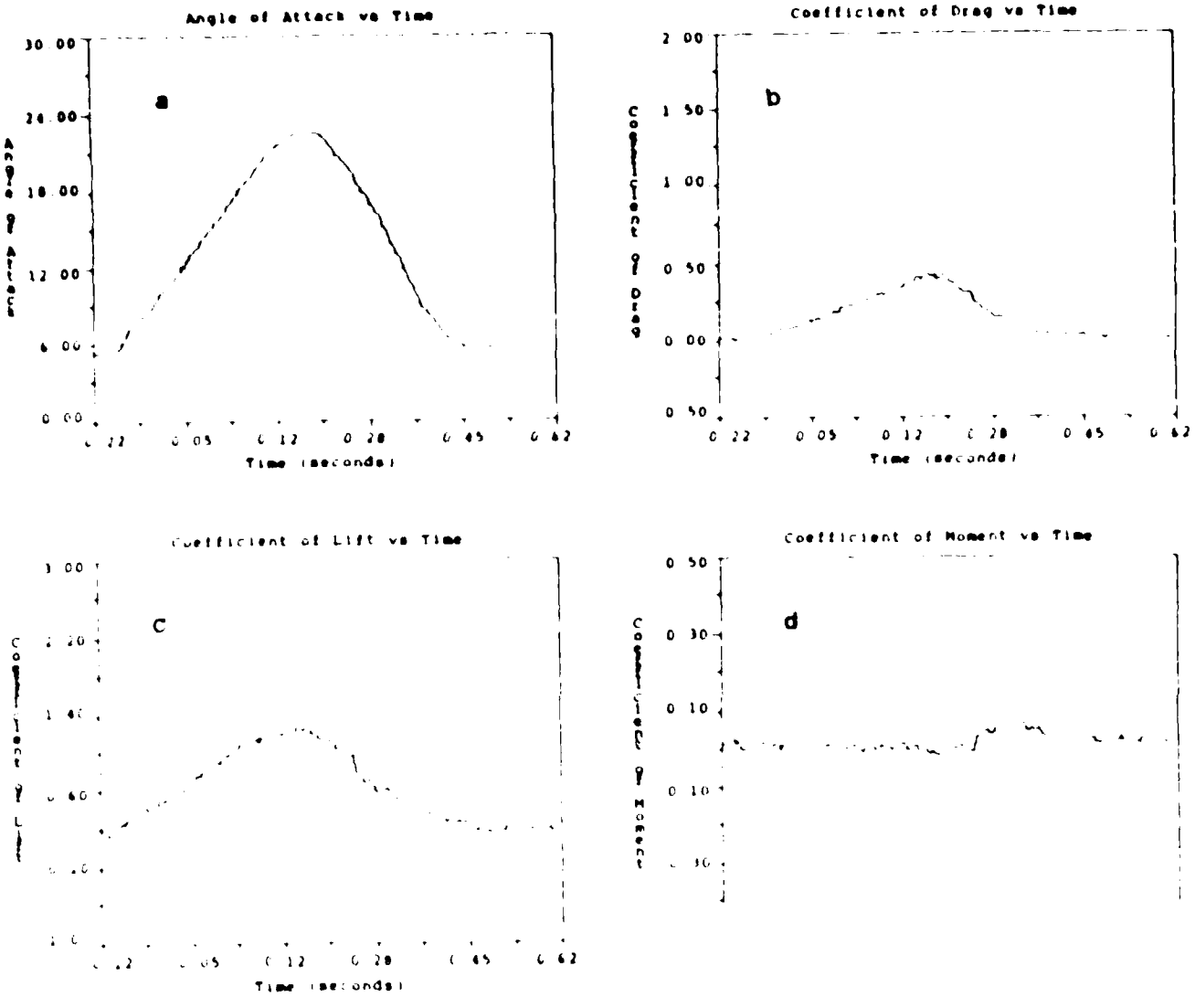

Figure 15. Results from Run E $\dot{\alpha}_{up}$ = .01 , $\dot{\alpha}_{down}$ = .0256

a) Angle of Attack Profile, b) Effect on C_L

c) Effect on C_D, d) Effect on C_M

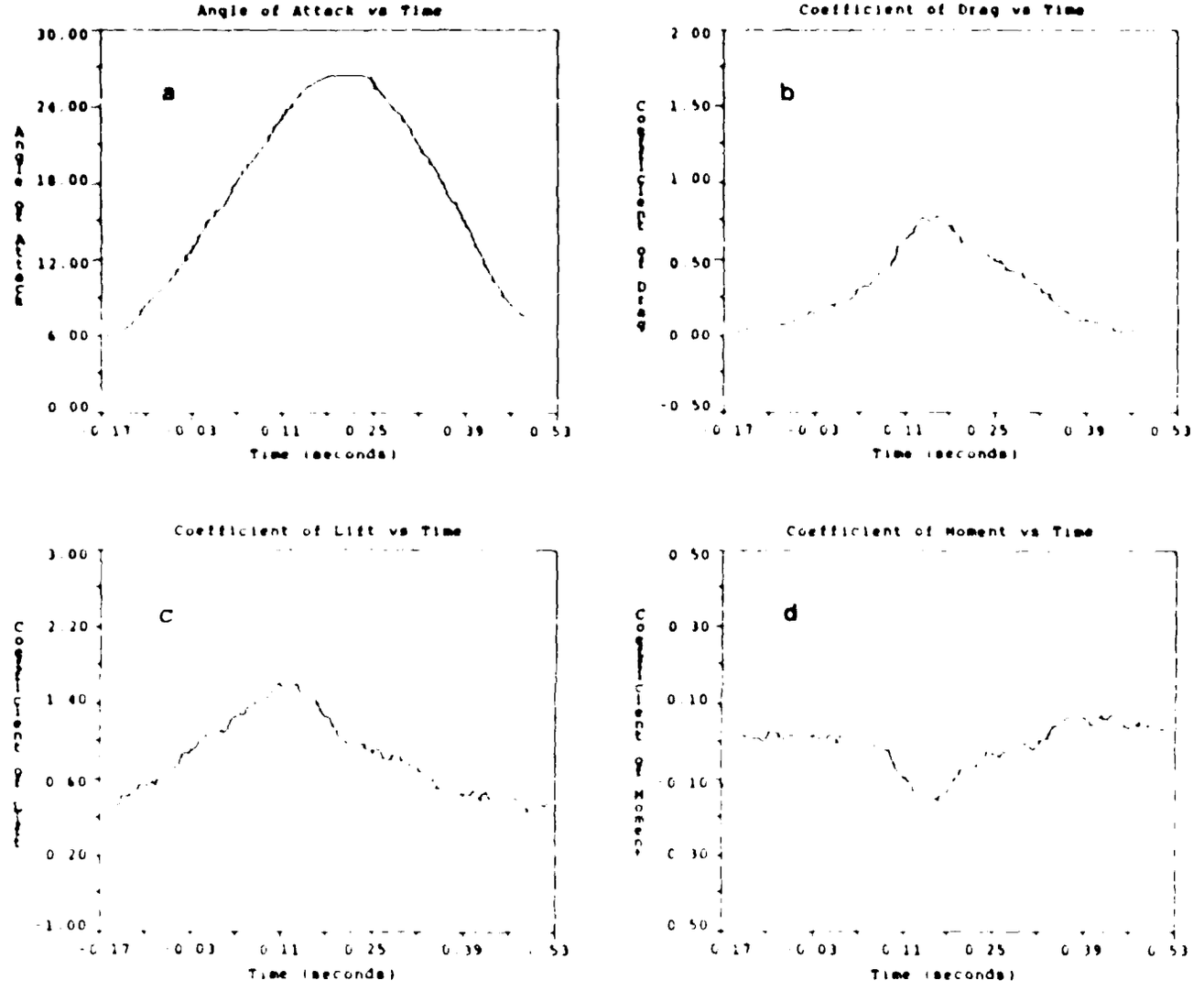

Figure 16. Results from Run F $\dot{\alpha}_{nD_{UP}} = .0217$, $\dot{\alpha}_{nD_{down}} = .0269$

a) Angle of Attack Profile, b) Effect on C_L

c) Effect on C_D, d) Effect on C_M

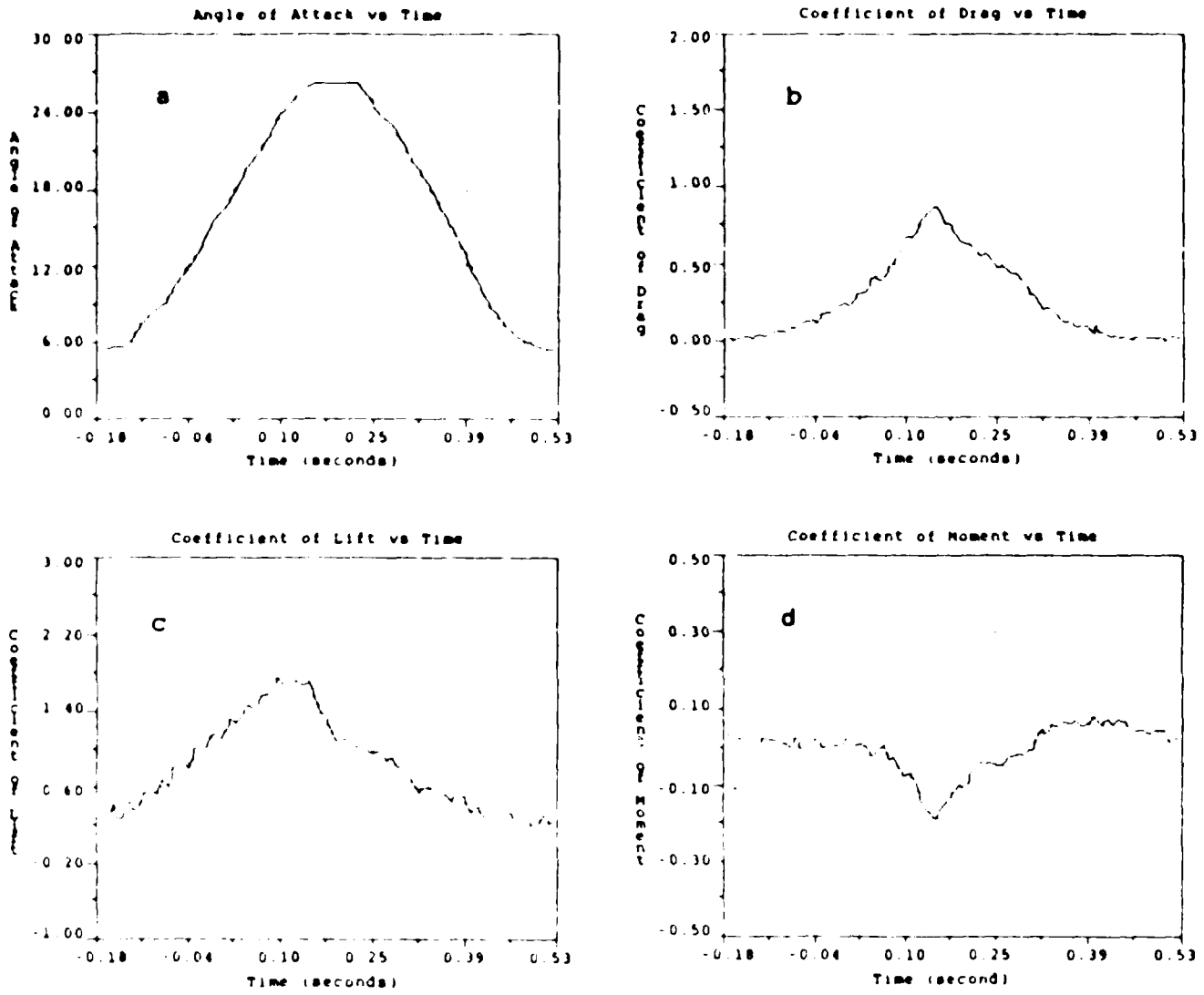

Figure 17. Results from Run 6 $\dot{\alpha}_{NP}$ =.0241, $\dot{\alpha}_{NP}$ =.0276
a) Angle of Attack Profile, b) Effect on C_L
c) Effect on C_D, d) Effect on C_M

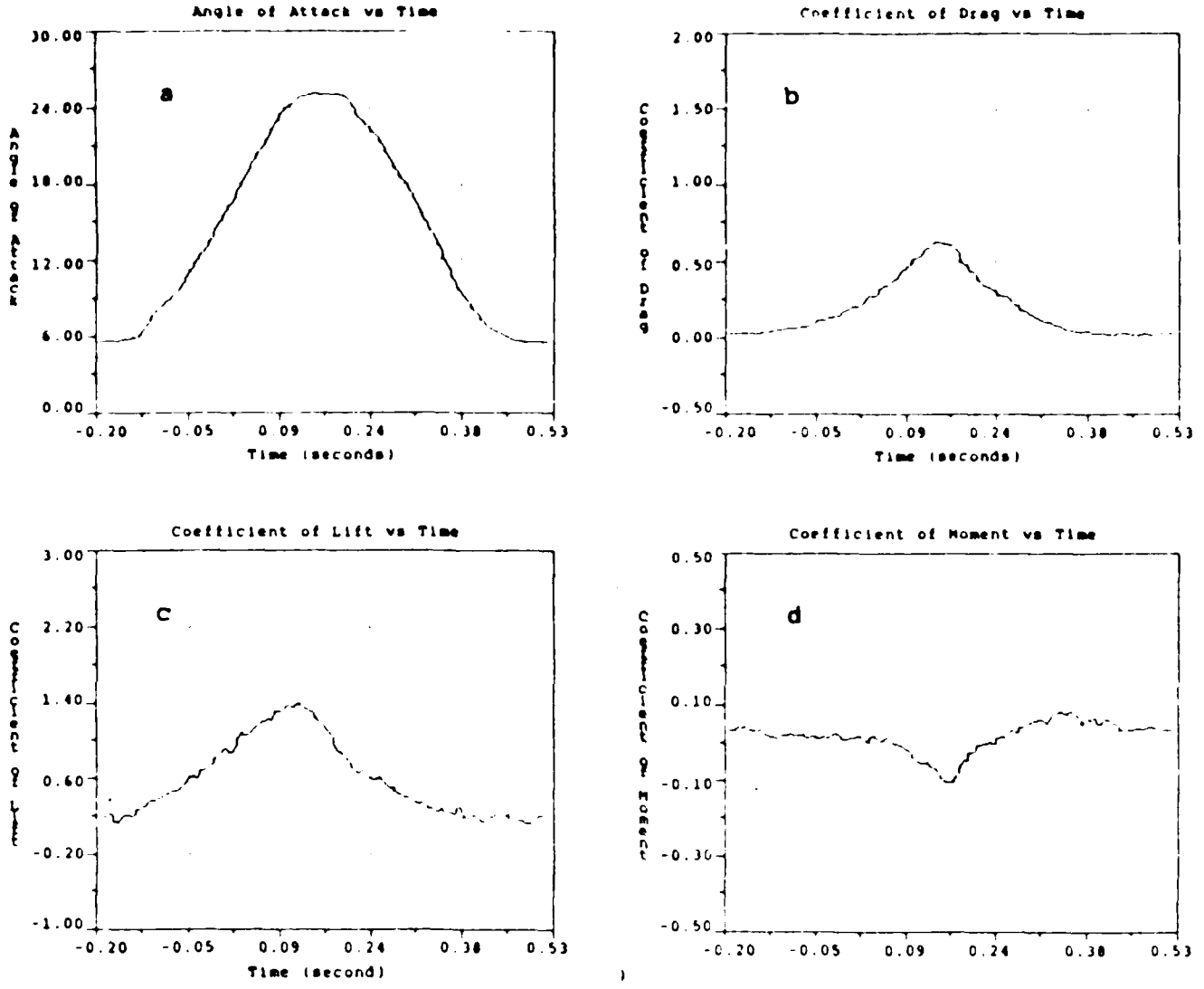

Figure 18. Results from Run H $\dot{\alpha}_{ND_{up}} = .0251$, $\dot{\alpha}_{ND_{down}} = .0230$
a) Angle of Attack Profile, b) Effect on C_L
c) Effect on C_D, d) Effect on C_M

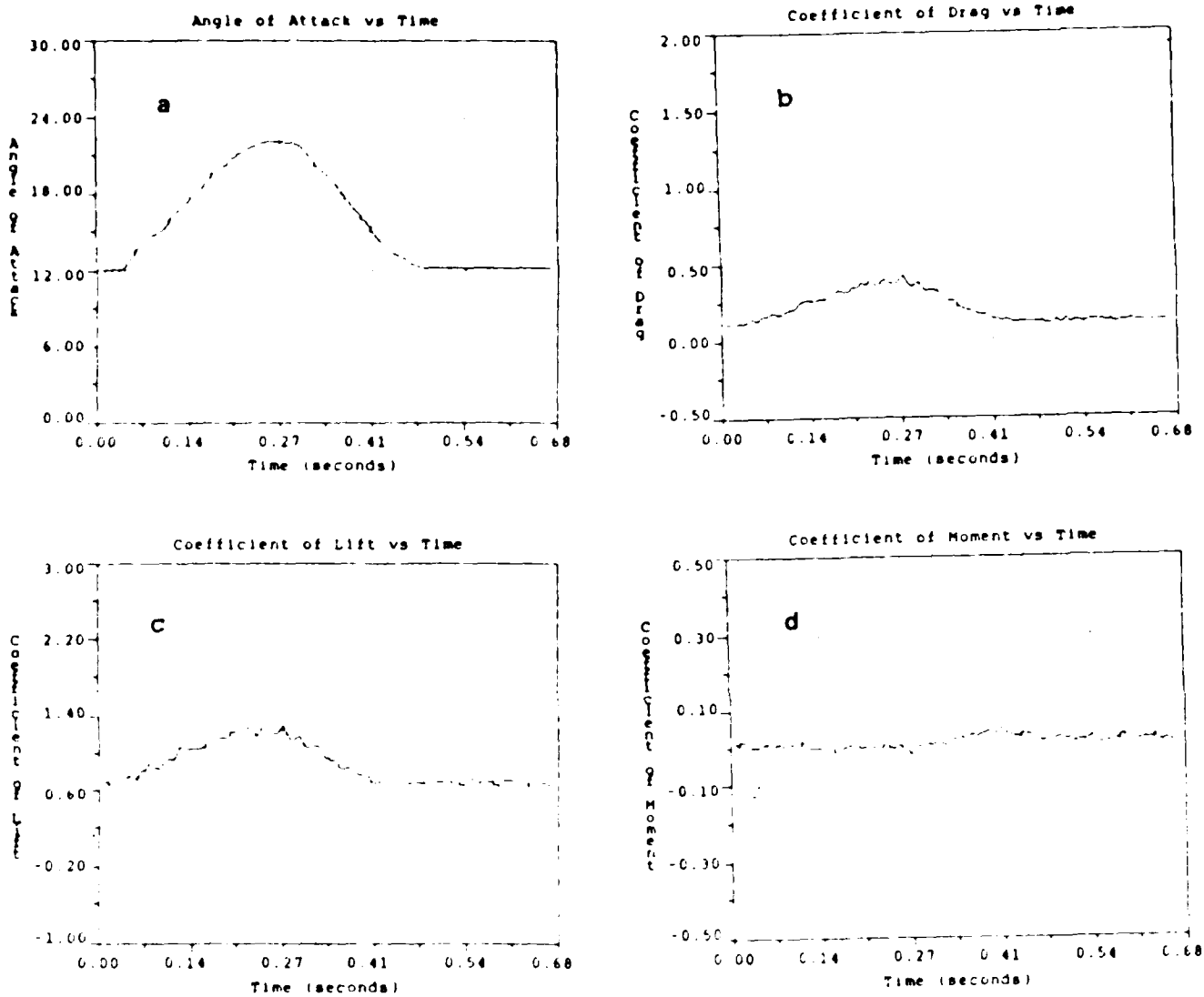

Figure 19. Results from Run 1 $\dot{\alpha}_{ND_{up}}$ =.0146, $\dot{\alpha}_{ND_{down}}$ =.0206
a) Angle of Attack Profile, b) Effect on C_L
c) Effect on C_D, d) Effect on C_M

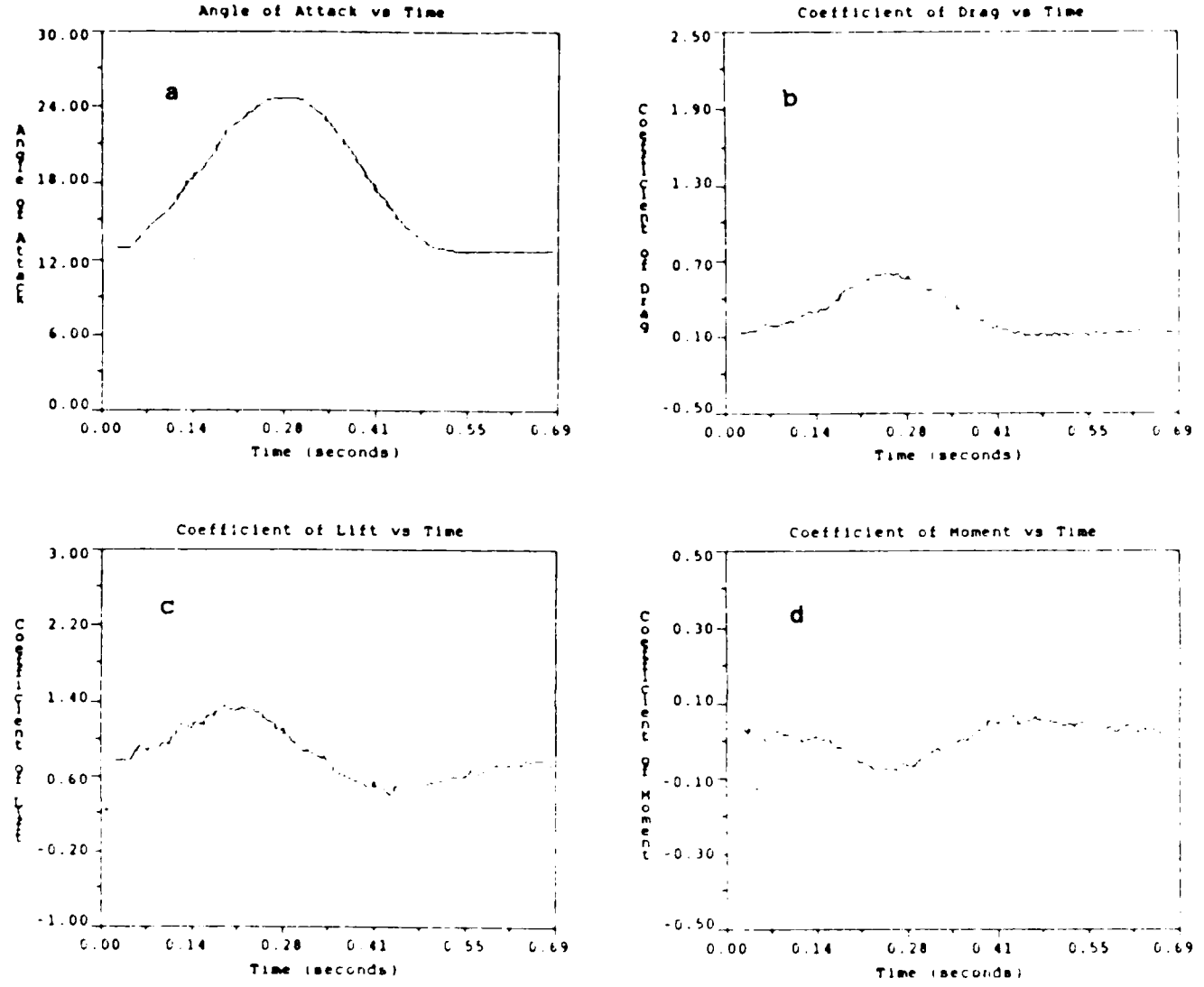

Figure 20. Results from Run J $\dot{\alpha}_{ND_{up}} = .0187$, $\dot{\alpha}_{ND_{down}} = .0244$
a) Angle of Attack Profile, b) Effect on C_L
c) Effect on C_D, d) Effect on C_M

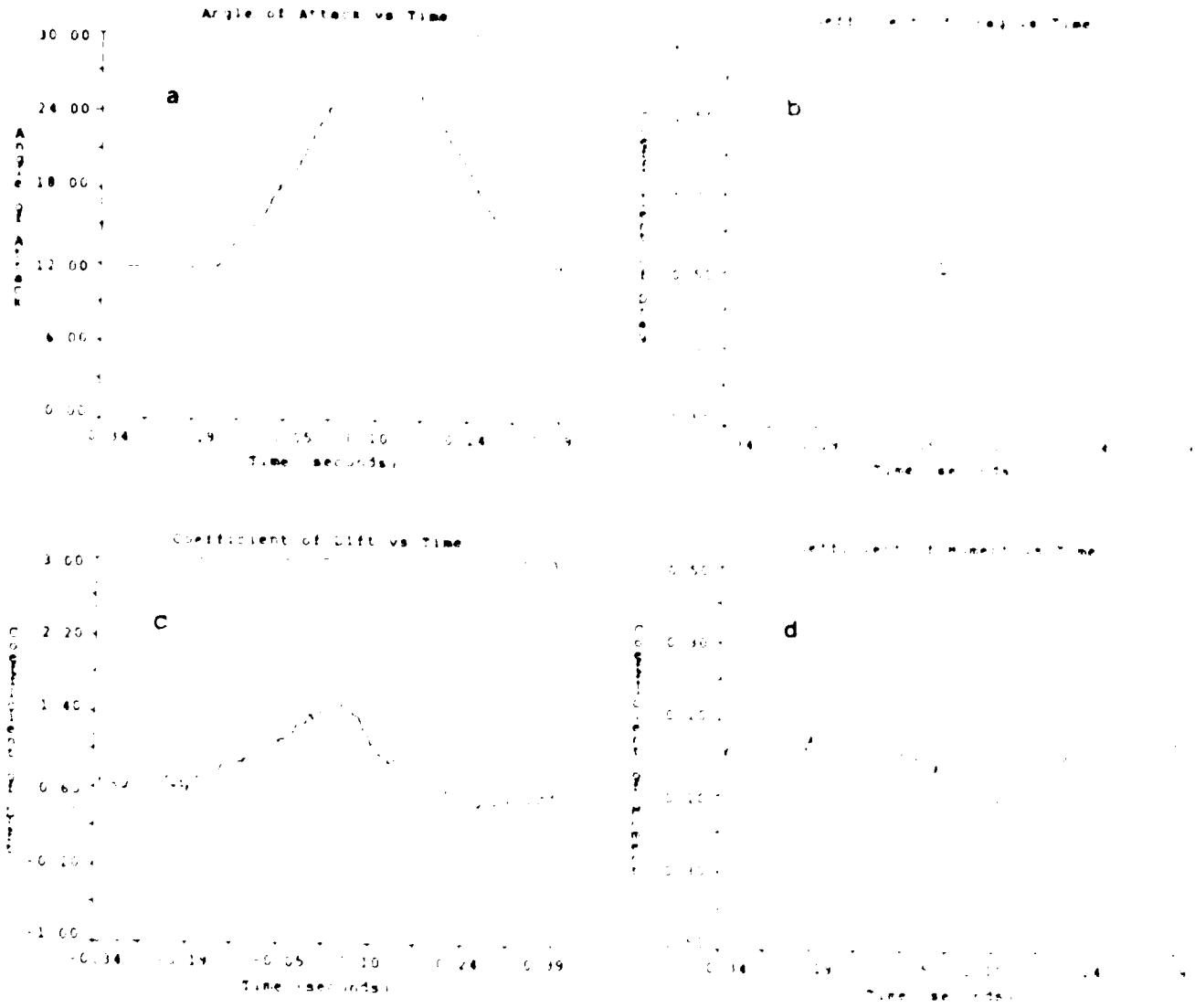

Figure 21. Results from Run K $\dot{\theta}_{UP}$ =.0207, $\dot{\theta}_{DOWN}$ =.0256
a) Angle of Attack Profile, b) Effect on C_L
c) Effect on C_D, d) Effect on C_M

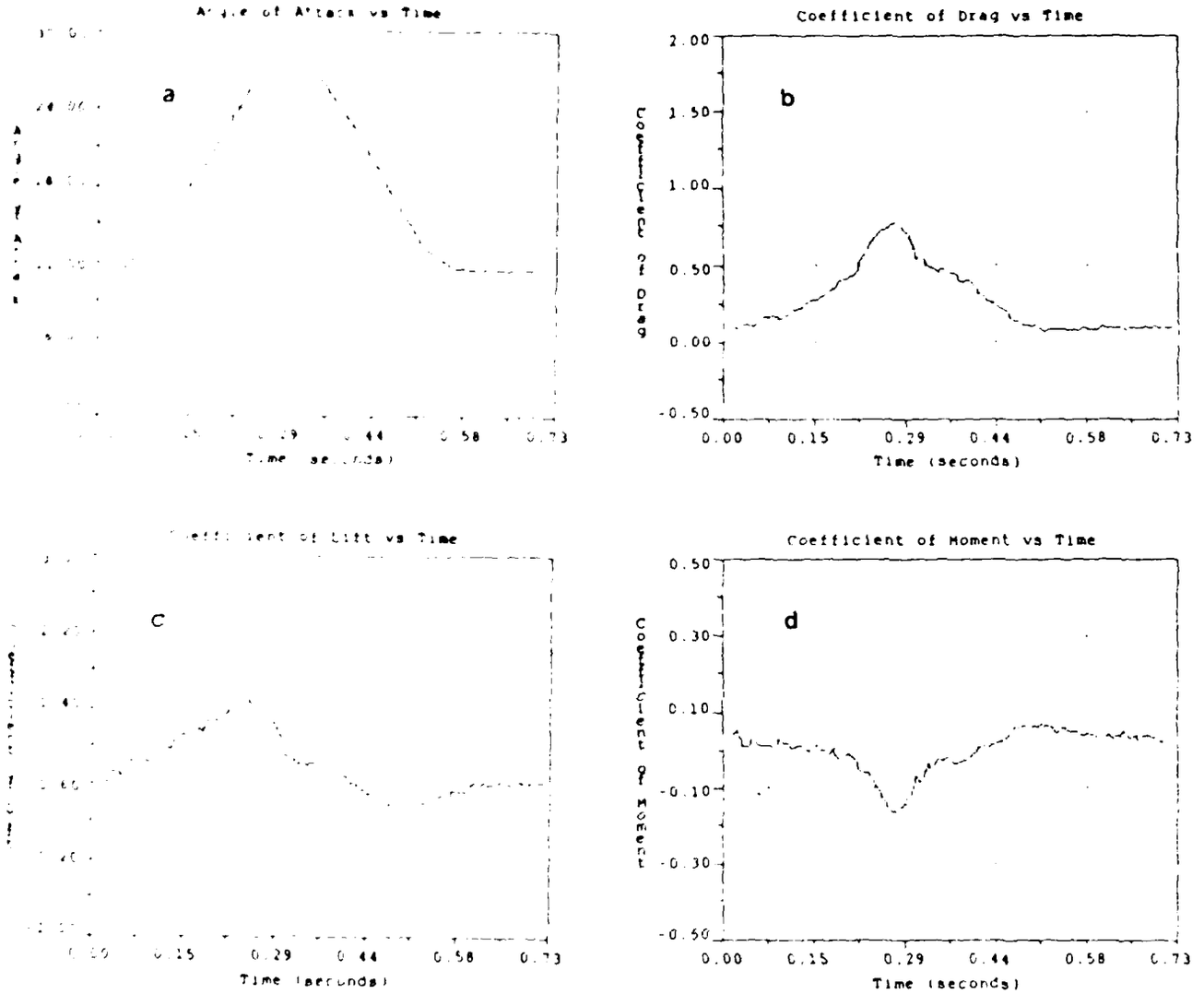

Figure 22. Results from Run L $\dot{\alpha}_{ND_{up}}$ =.0215, $\dot{\alpha}_{ND_{down}}$ =.0260
a) Angle of Attack Profile, b) Effect on C_L
c) Effect on C_D, d) Effect on C_M

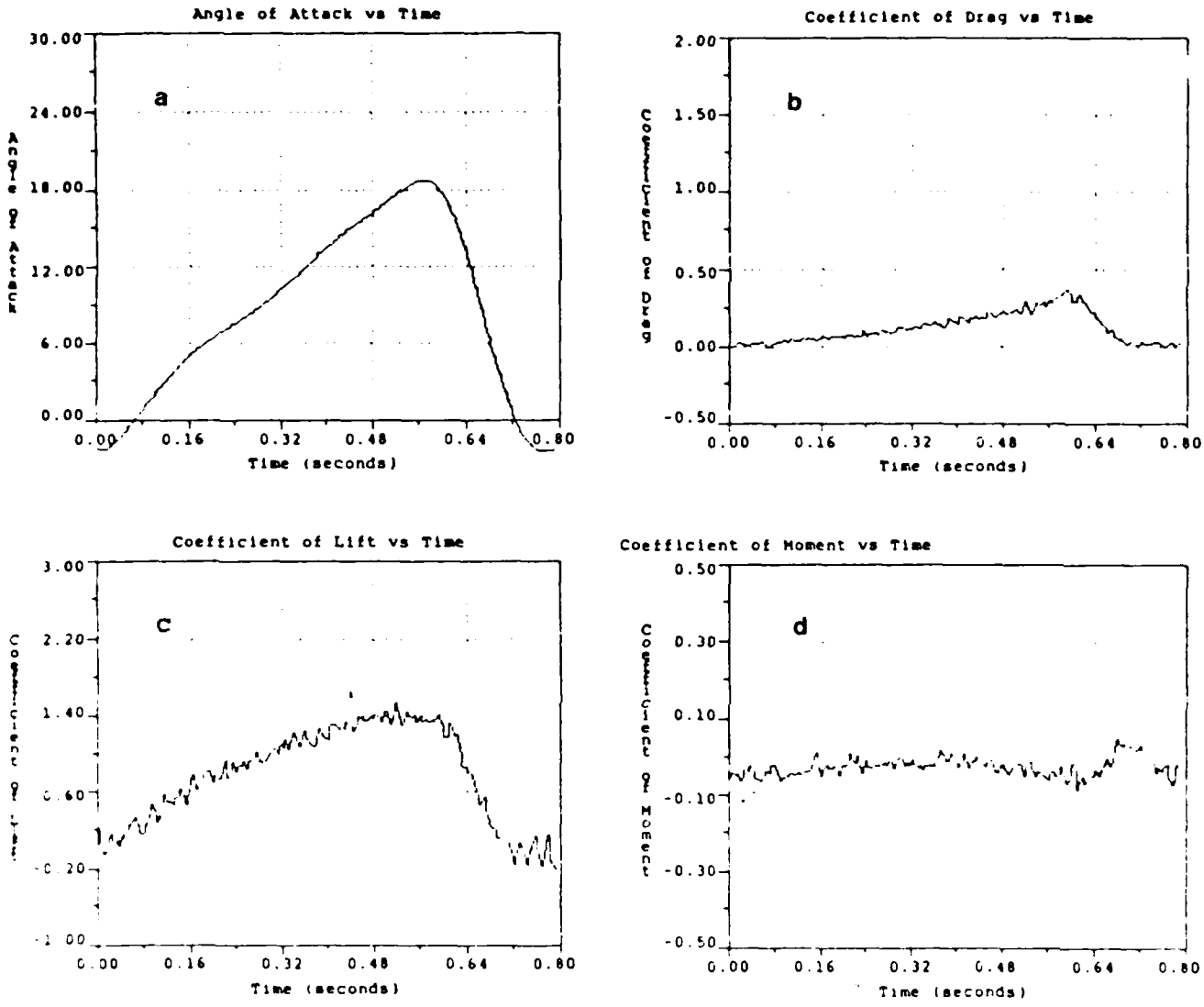

Figure 23. Results from Run AA $\dot{\alpha}_{ND_{up}} = .0104, \dot{\alpha}_{ND_{down}} = .0479$

a) Angle of Attack Profile, b) Effect on C_L

c) Effect on C_D, d) Effect on C_M

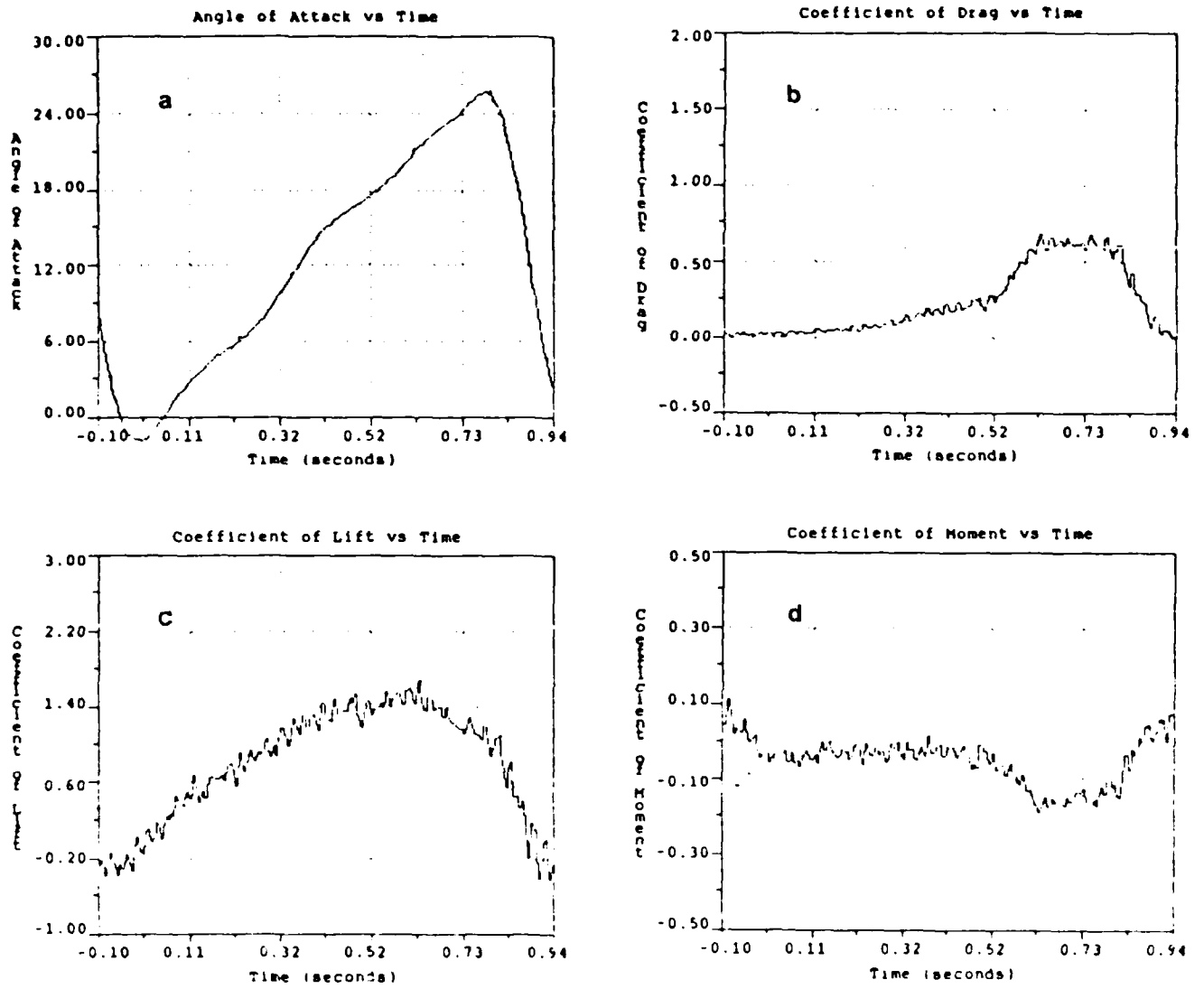

Figure 24. Results from Run BB $\dot{\alpha}_{ND_{up}} = .0110$, $\dot{\alpha}_{ND_{down}} = .0652$
a) Angle of Attack Profile, b) Effect on C_L
c) Effect on C_D, d) Effect on C_M

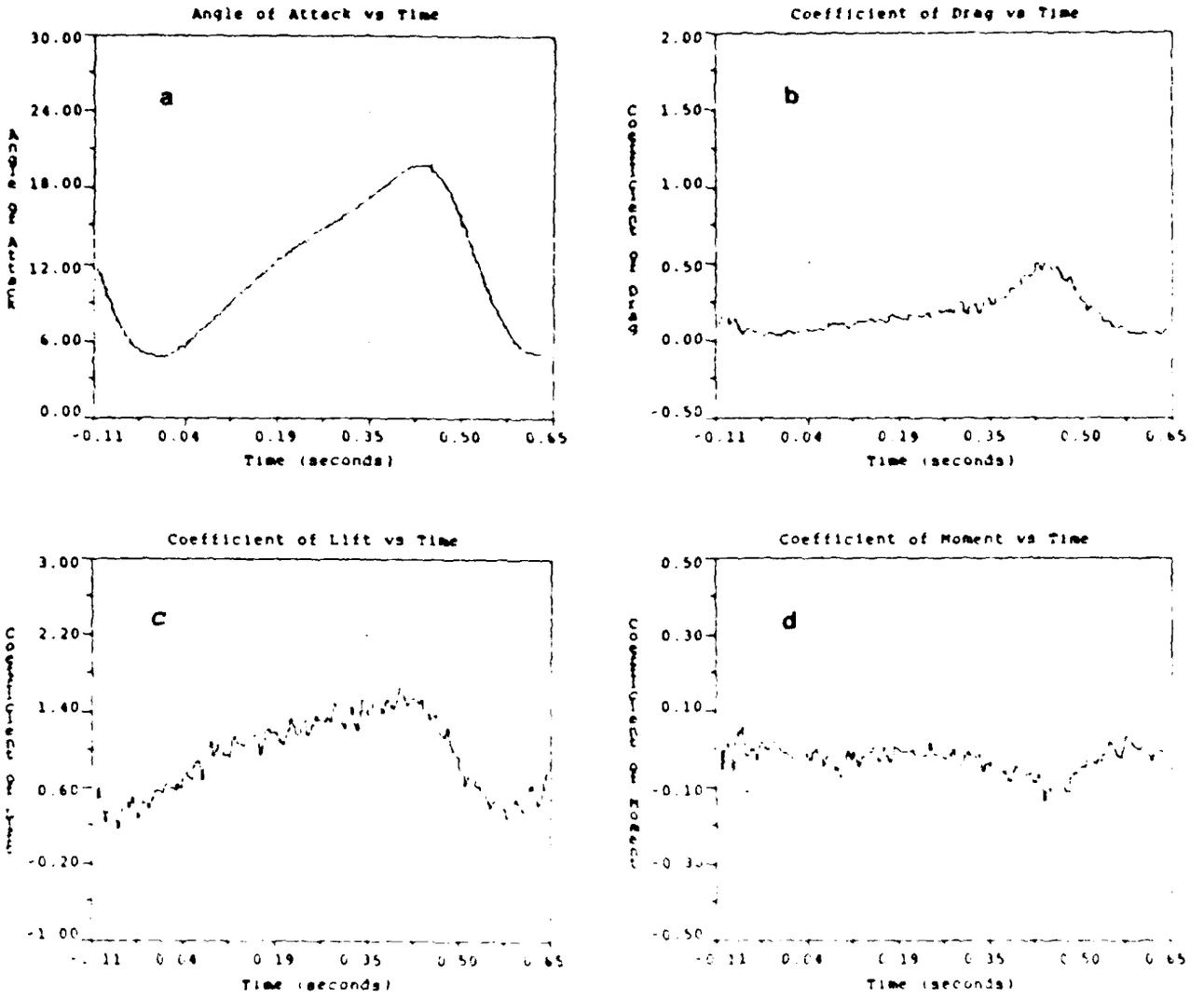

Figure 25. Results from Run CC $\dot{\alpha}_{ND_{up}}$ =.0109, $\dot{\alpha}_{ND_{down}}$ =.0368

a) Angle of Attack Profile, b) Effect on C_L

c) Effect on C_D, d) Effect on C_M

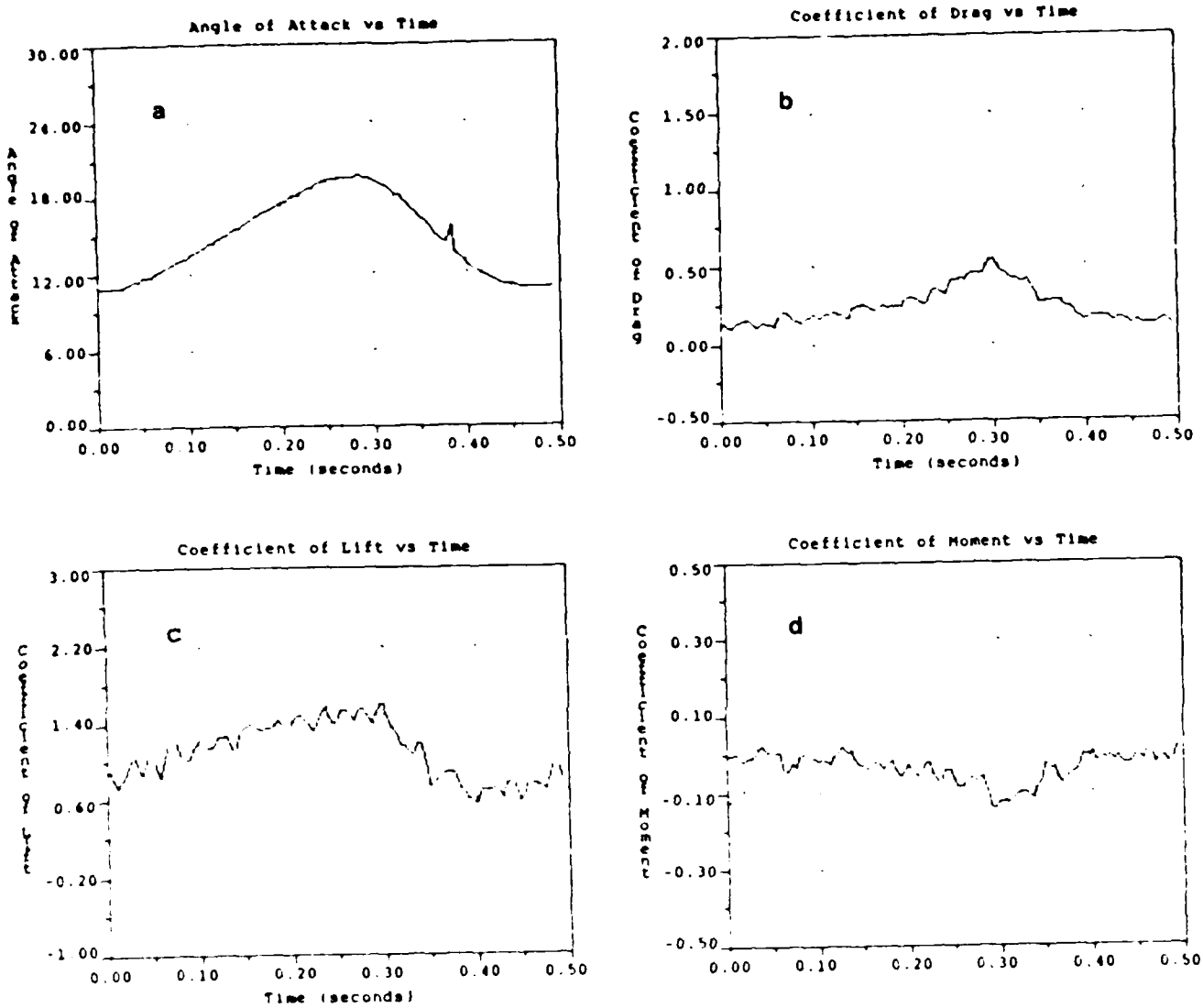

Figure 26. Results from Run DL $\dot{\alpha}_{ND_{up}}$ =.0119, $\dot{\alpha}_{ND_{down}}$ =.0208
a) Angle of Attack Profile, b) Effect on C_L
c) Effect on C_D, d) Effect on C_M

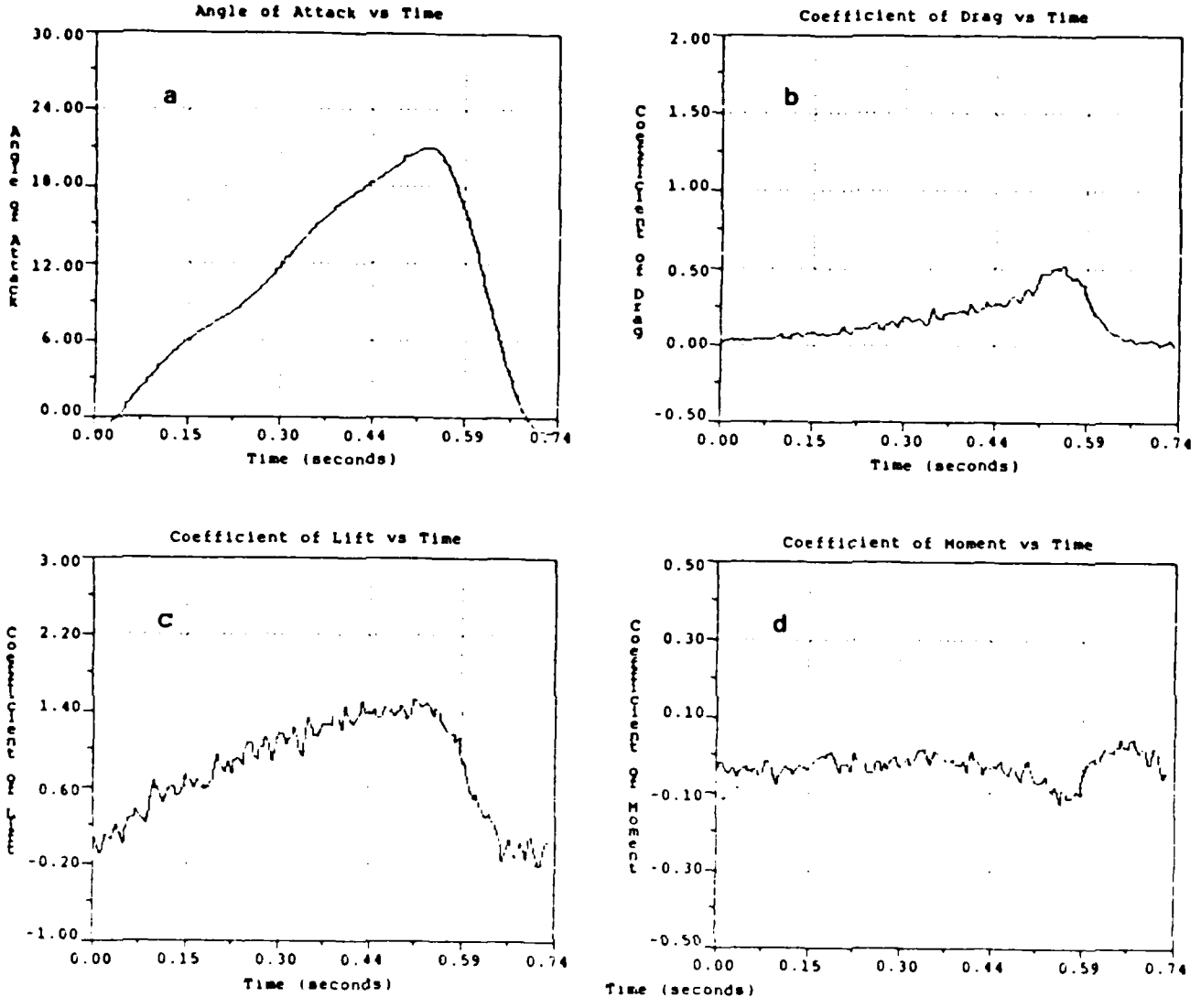

Figure 27. Results from Run EE $\dot{\alpha}_{ND_{up}}$ =.0123, $\dot{\alpha}_{ND_{down}}$ =.0523
a) Angle of Attack Profile, b) Effect on C_L
c) Effect on C_D, d) Effect on C_M

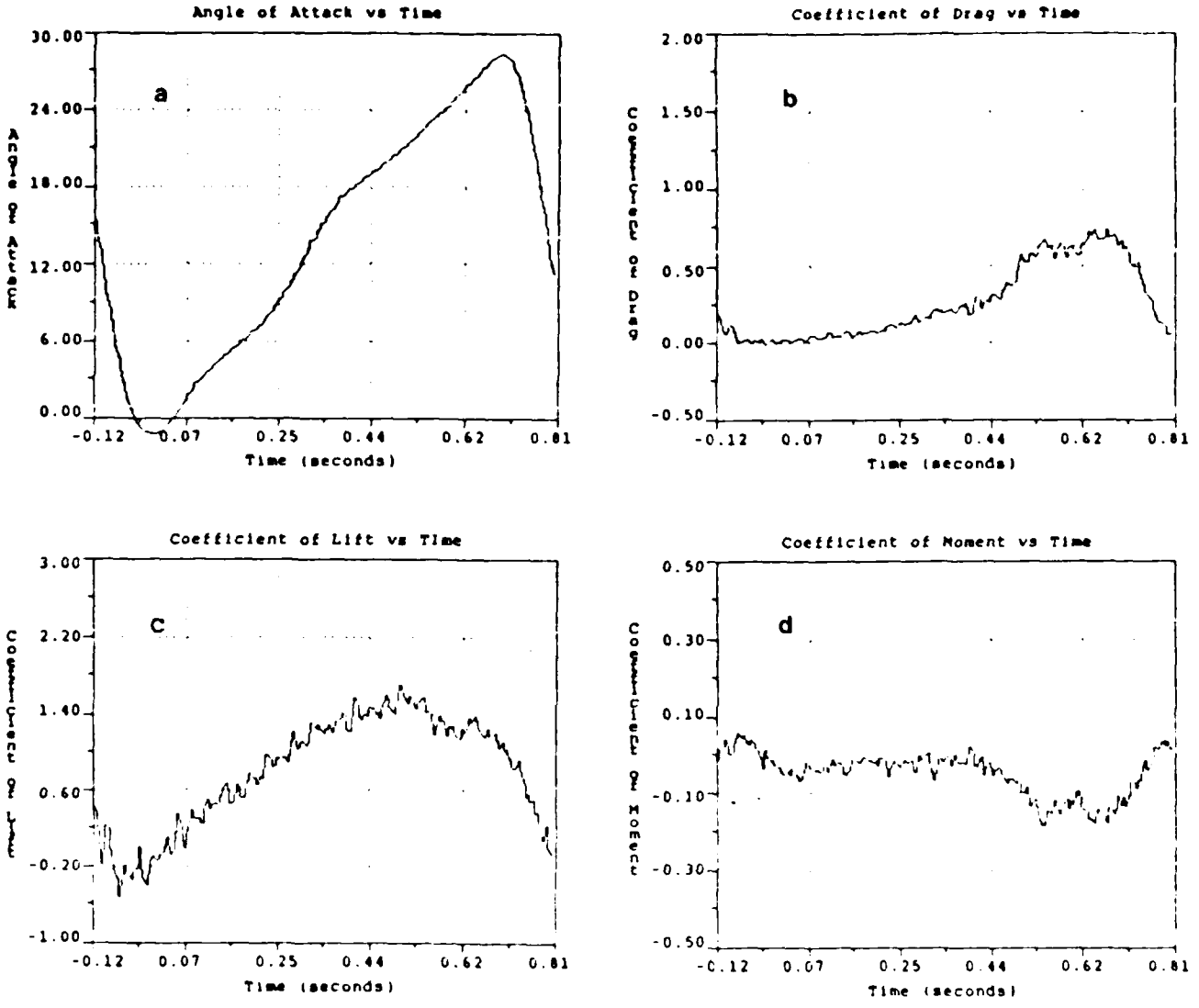

Figure 28. Results from Run FF $\dot{\alpha}_{ND_{up}}$ =.0138, $\dot{\alpha}_{ND_{down}}$ =.0718
a) Angle of Attack Profile, b) Effect on C_L
c) Effect on C_D, d) Effect on C_M

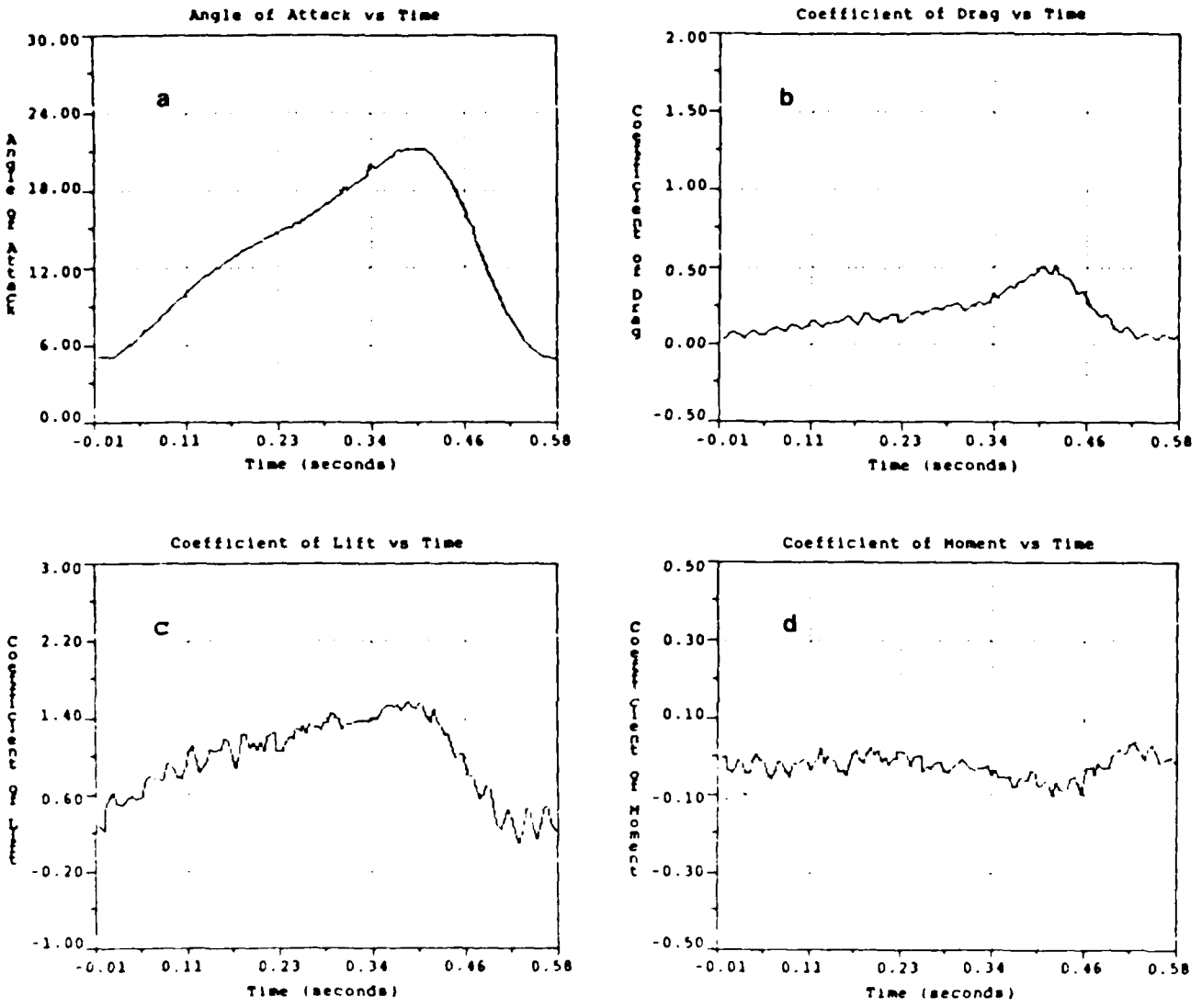

Figure 29. Results from Run GG $\dot{\alpha}_{ND_{up}} = .0128, \dot{\alpha}_{ND_{down}} = .0383$
a) Angle of Attack Profile, b) Effect on C_L
c) Effect on C_D, d) Effect on C_M

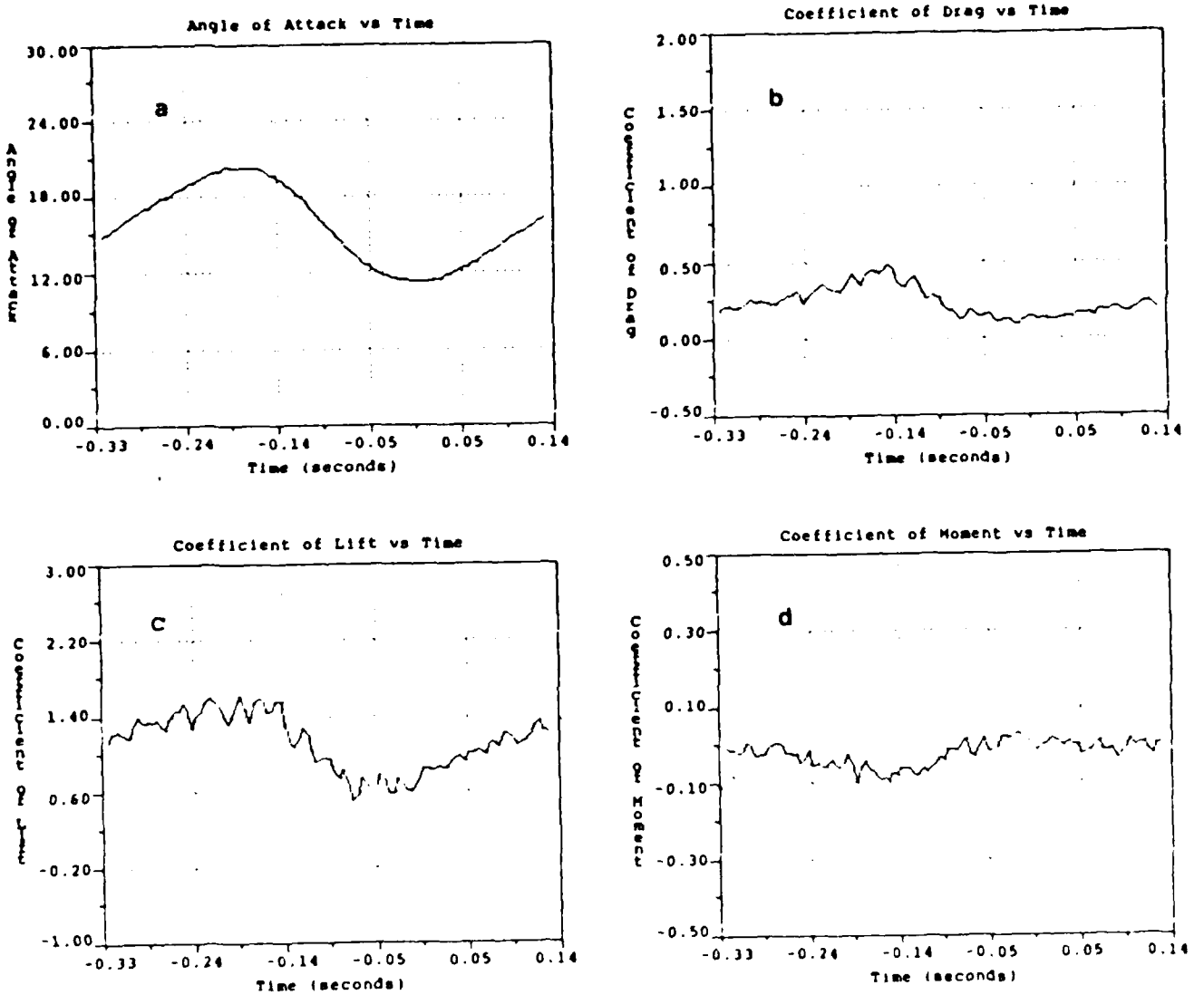

Figure 30. Results from Run HH $\dot{\alpha}_{ND_{up}} = .0142$, $\dot{\alpha}_{ND_{down}} = .0250$
a) Angle of Attack Profile, b) Effect on C_L
c) Effect on C_D, d) Effect on C_M

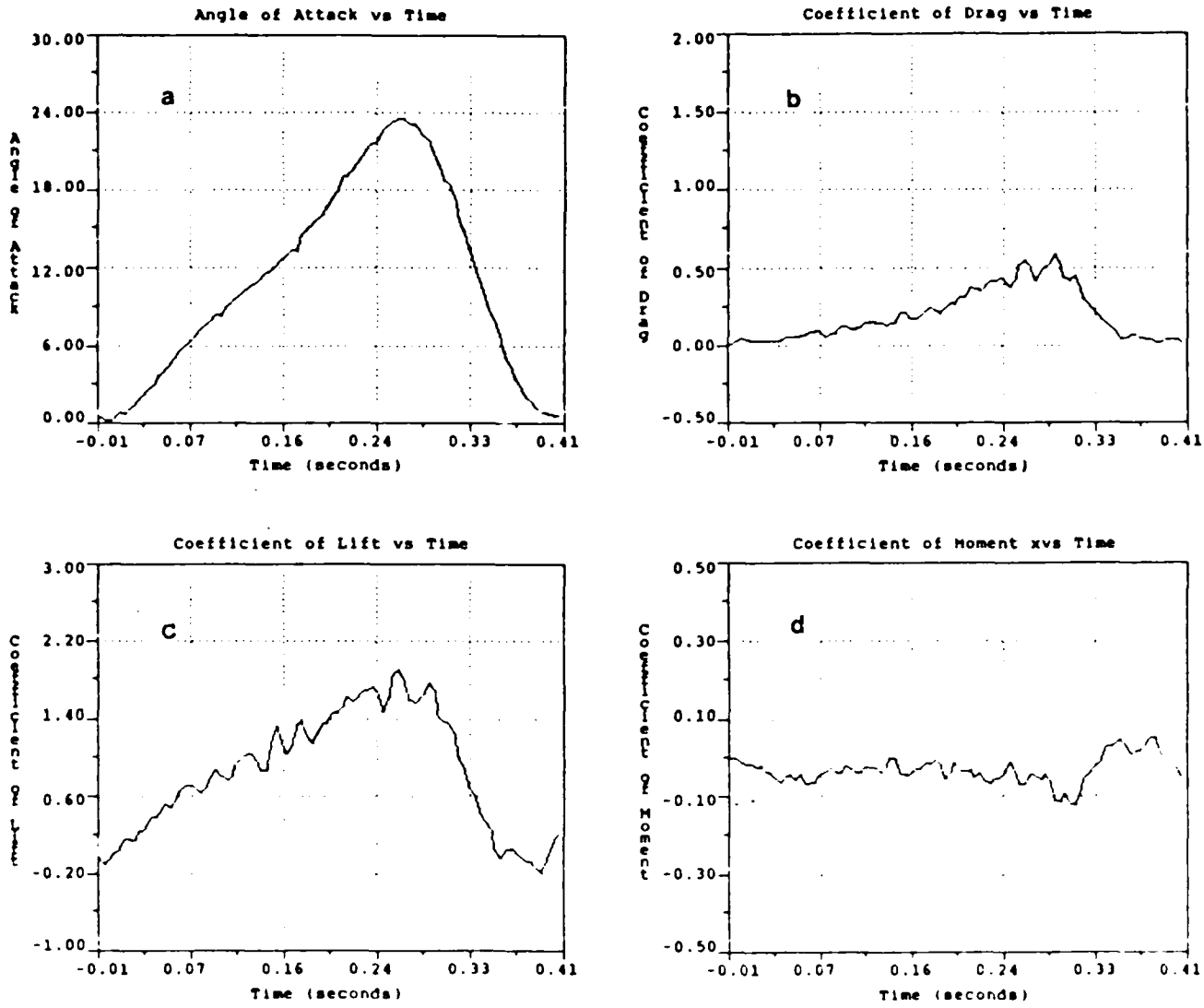

Figure 31. Results from Run II $\dot{\alpha}_{ND_{up}} = .0256$, $\dot{\alpha}_{ND_{down}} = .0747$
a) Angle of Attack Profile, b) Effect on C_L
c) Effect on C_D, d) Effect on C_M

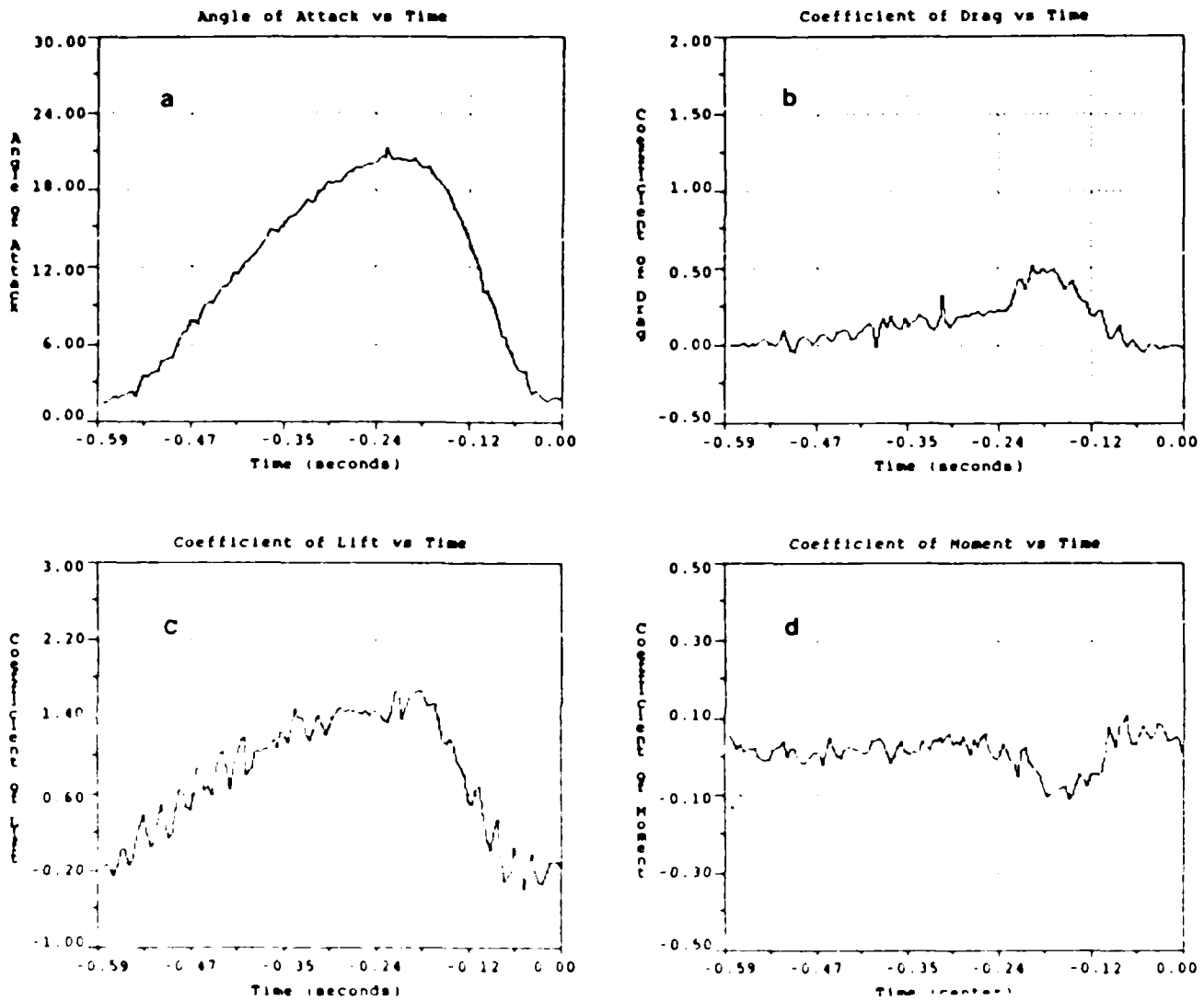

Figure 32. Results from Run JJ $\dot{\alpha}_{ND_{UP}} = .0195$, $\dot{\alpha}_{ND_{DOWN}} = .0515$
a) Angle of Attack Profile, b) Effect on C_L
c) Effect on C_D, d) Effect on C_M

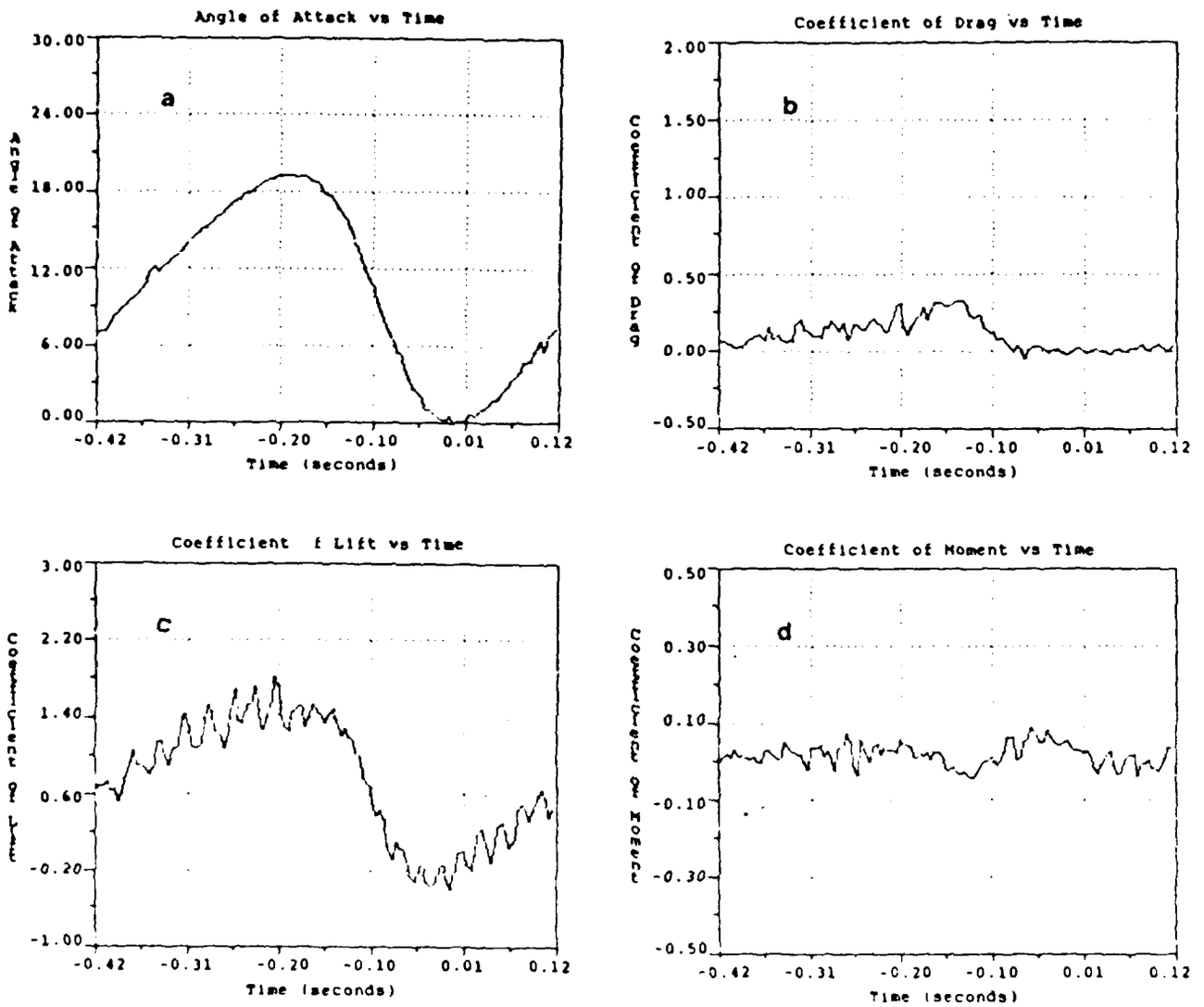

Figure 33. Results from Run KK $\dot{\alpha}_{ND_{up}}$ =.0195, $\dot{\alpha}_{ND_{down}}$ =.0524
a) Angle of Attack Profile, b) Effect on C_L
c) Effect on C_D, d) Effect on C_M

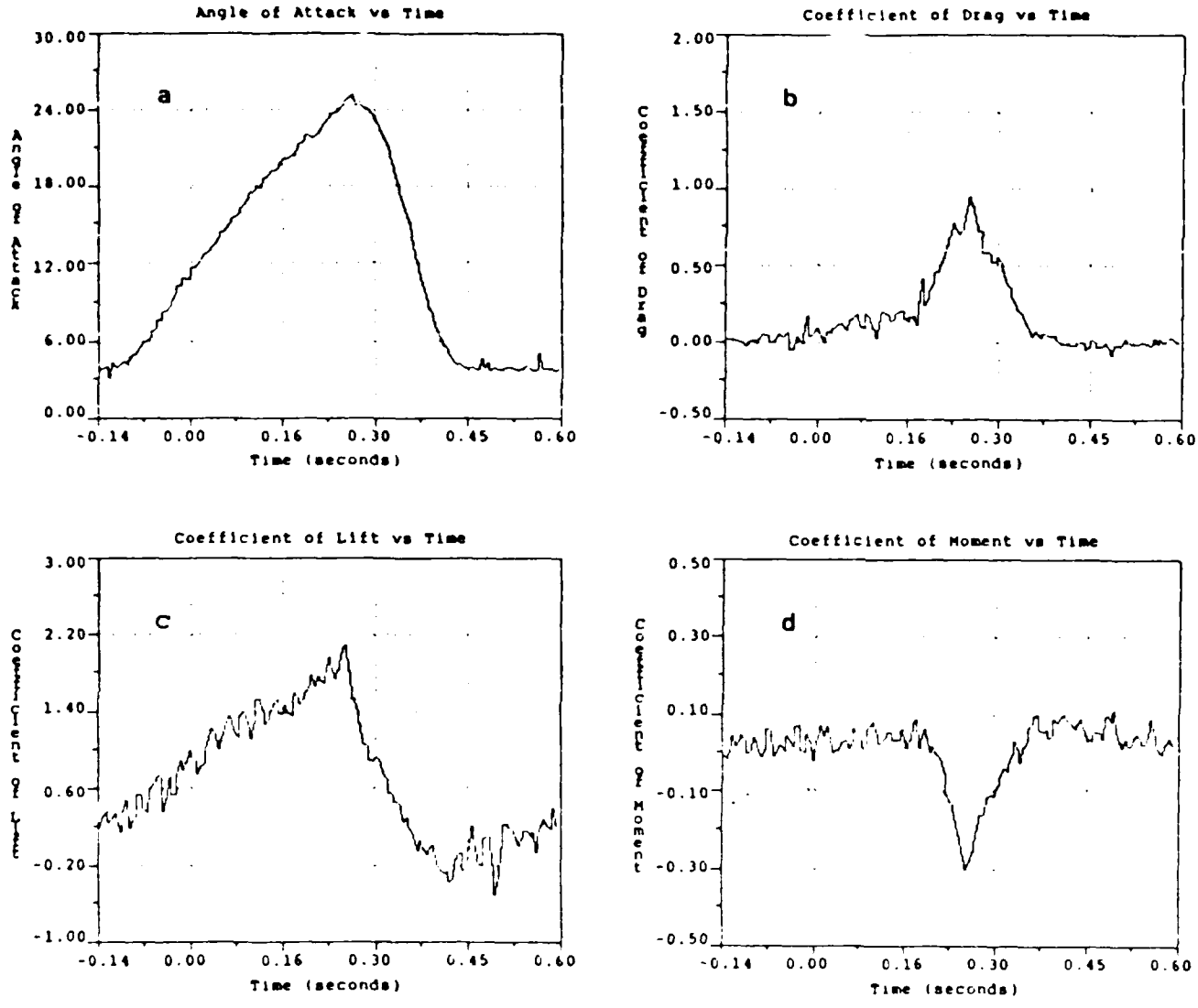

Figure 34. Results from Run LL $\dot{\alpha}_{ND_{up}} = .0189$, $\dot{\alpha}_{ND_{down}} = .0582$
a) Angle of Attack Profile, b) Effect on C_L
c) Effect on C_D, d) Effect on C_M

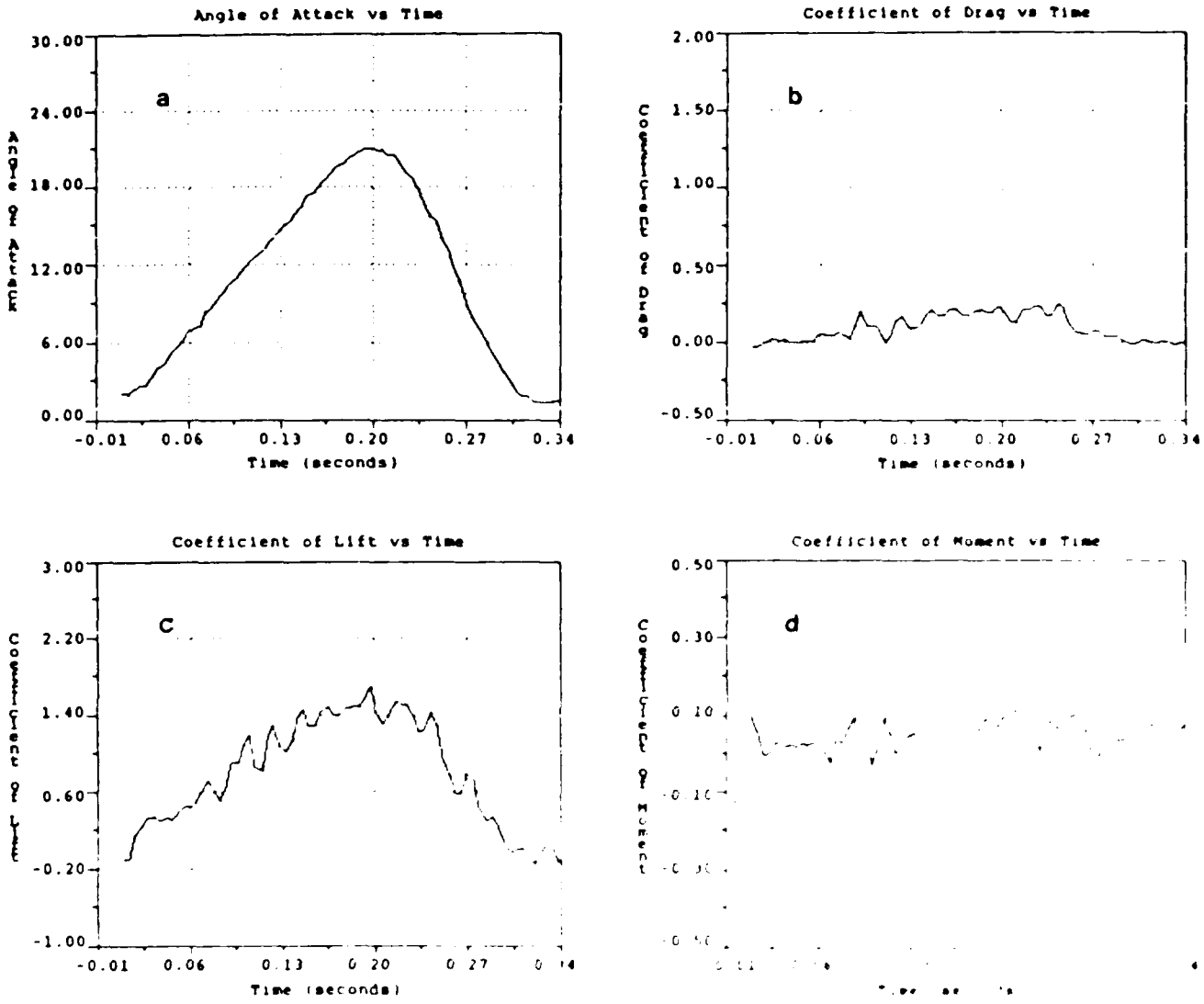

Figure 35. Results from Run MM α_{ND} =.0320, $\dot{\alpha}_{ND}$ =

a) Angle of Attack Pr

c)Effect on C_L,

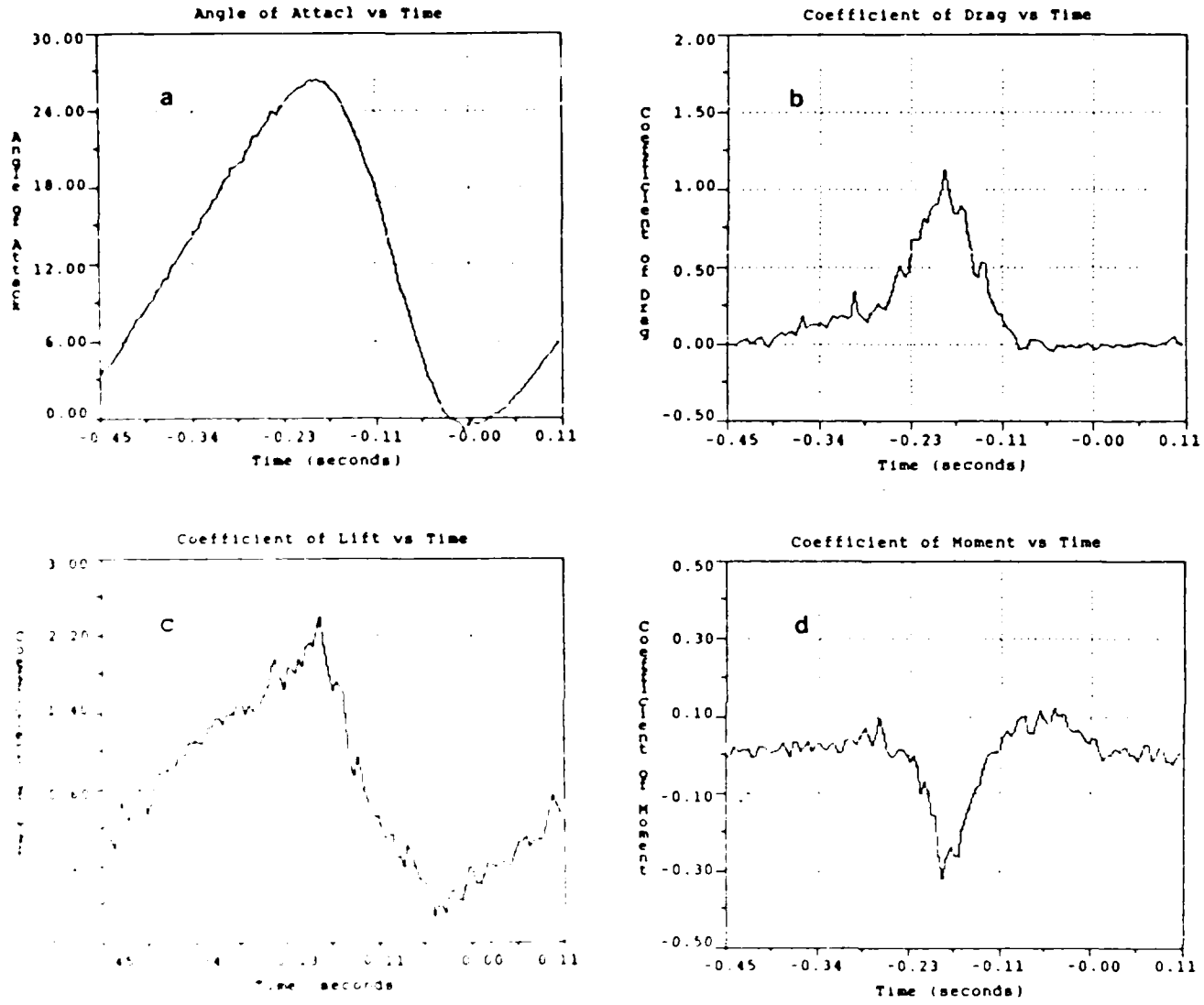

Figure 3: Results from Run NN $\dot{\alpha}_{ND_{up}} = .0312, \dot{\alpha}_{ND_{down}} = .0703$

a) Angle of Attack Profile, b) Effect on C_L
c) Effect on C_D, d) Effect on C_M

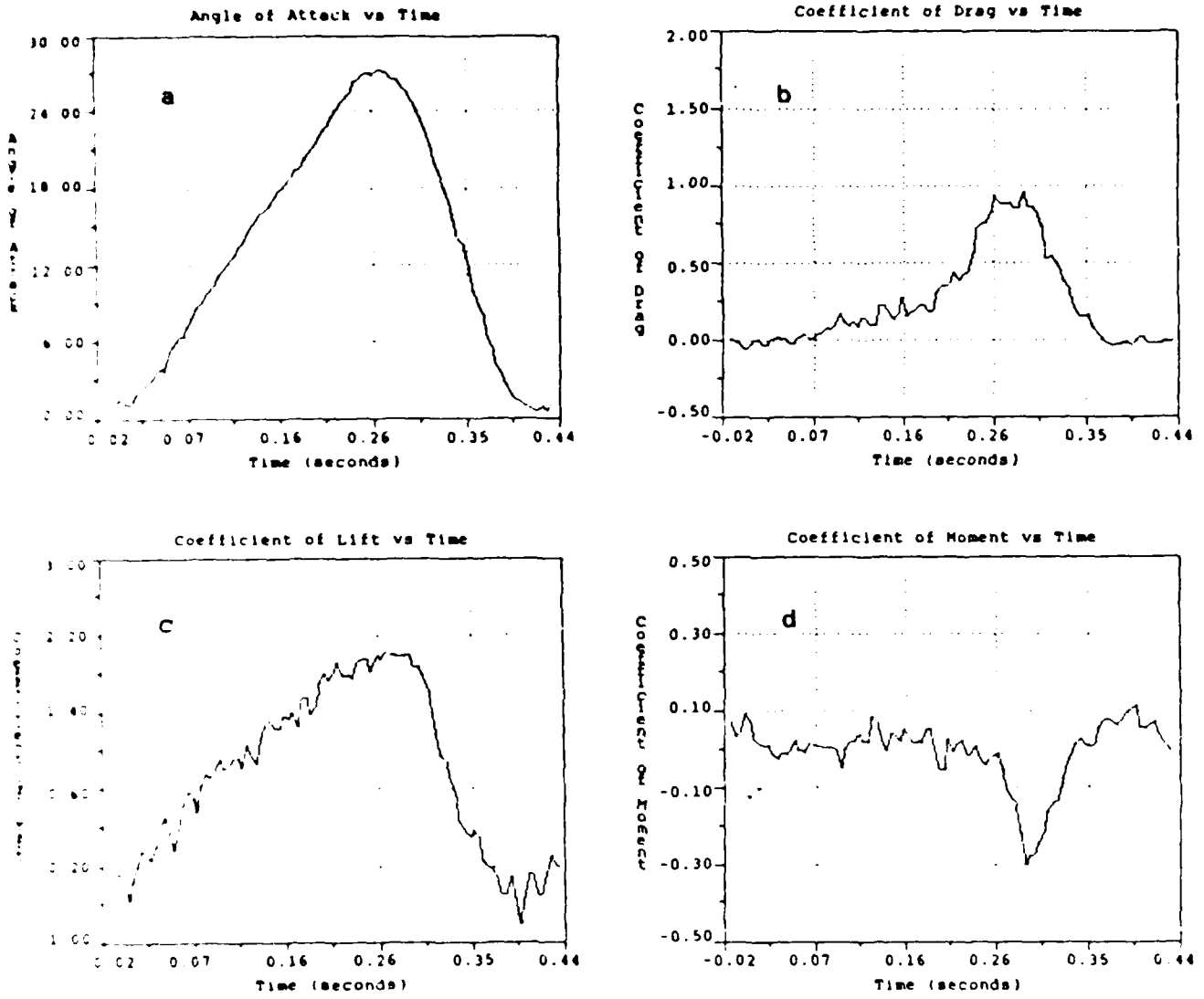

Figure 37. Results from Run 00 $\dot{\alpha}_{ND_{up}}$ =.0322, $\dot{\alpha}_{ND_{down}}$ =.0798
a) Angle of Attack Profile, b) Effect on C_L
c) Effect on C_D, d) Effect on C_M

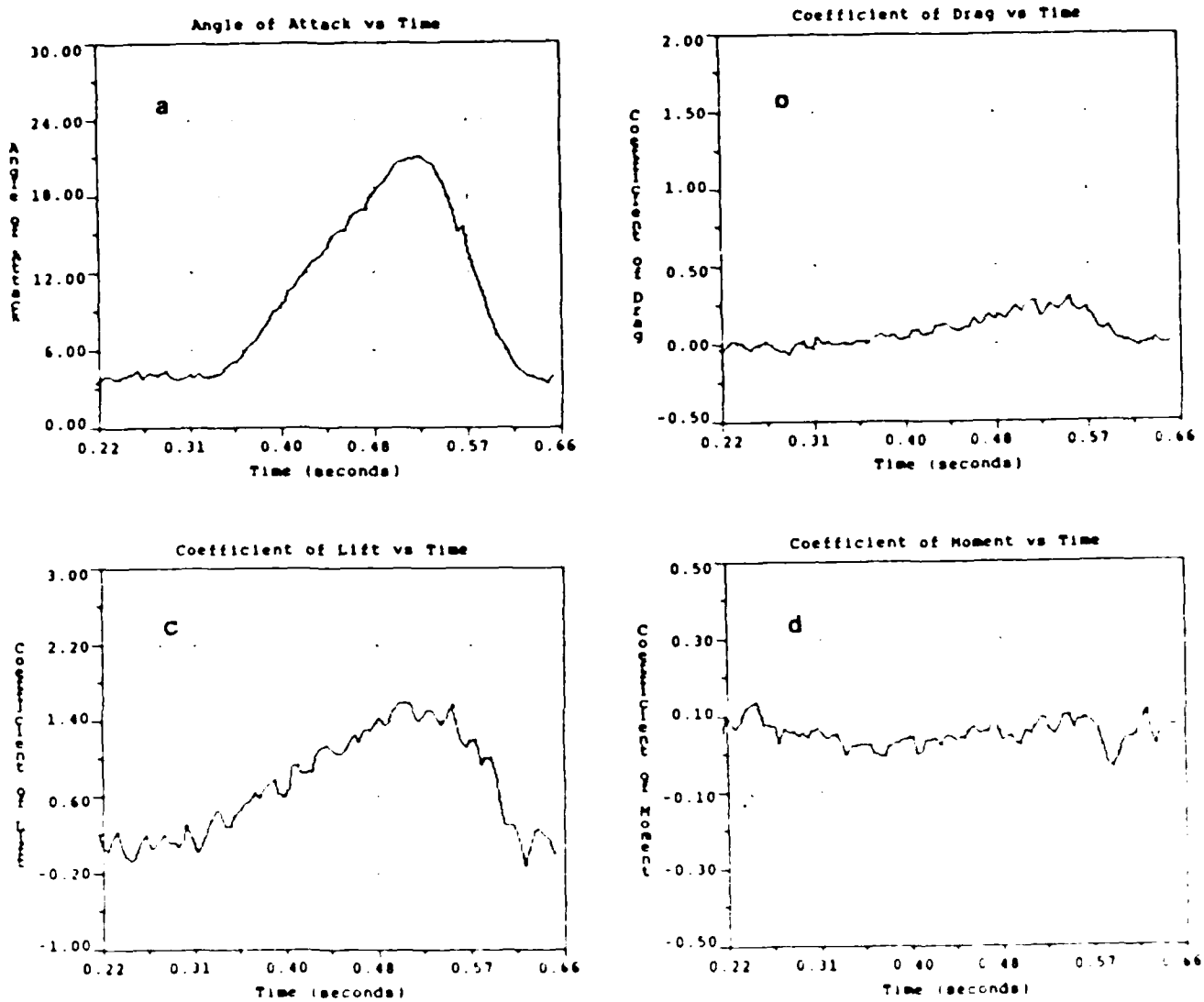

Figure 38. Results from Run PF $\dot{\alpha}_{ND_{up}}$ =.0320, $\dot{\alpha}_{ND_{down}}$ =.0663
a) Angle of Attack Profile, b) Effect on C_L
c) Effect on C_D, d) Effect on C_M

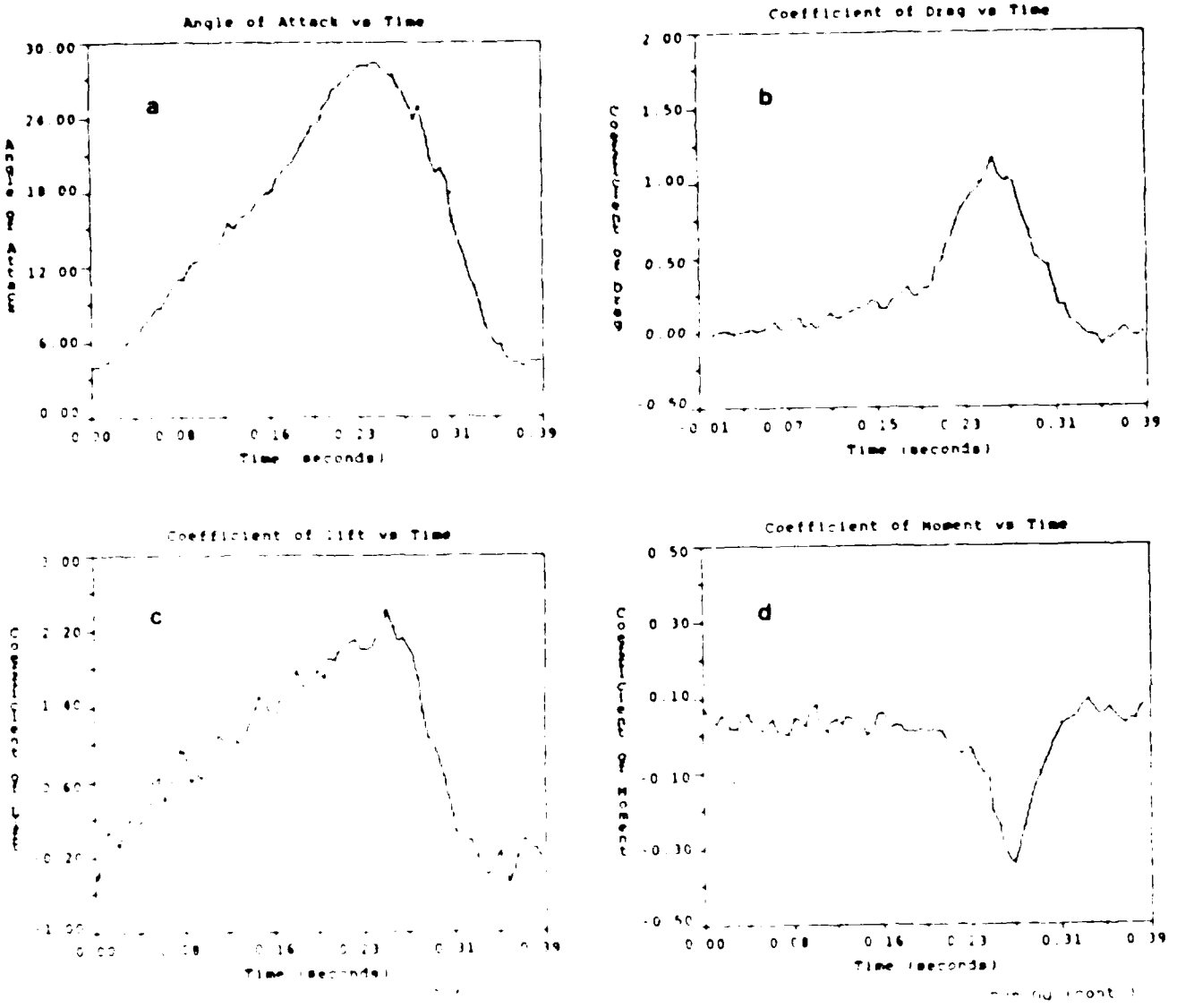

Figure 39. Results from Run 96 $\alpha_{ND_{up}}$ =.0304, $\alpha_{ND_{down}}$ =.0846
a) Angle of Attack Profile, b) Effect on C_L
c) Effect on C_D, d) Effect on C_M

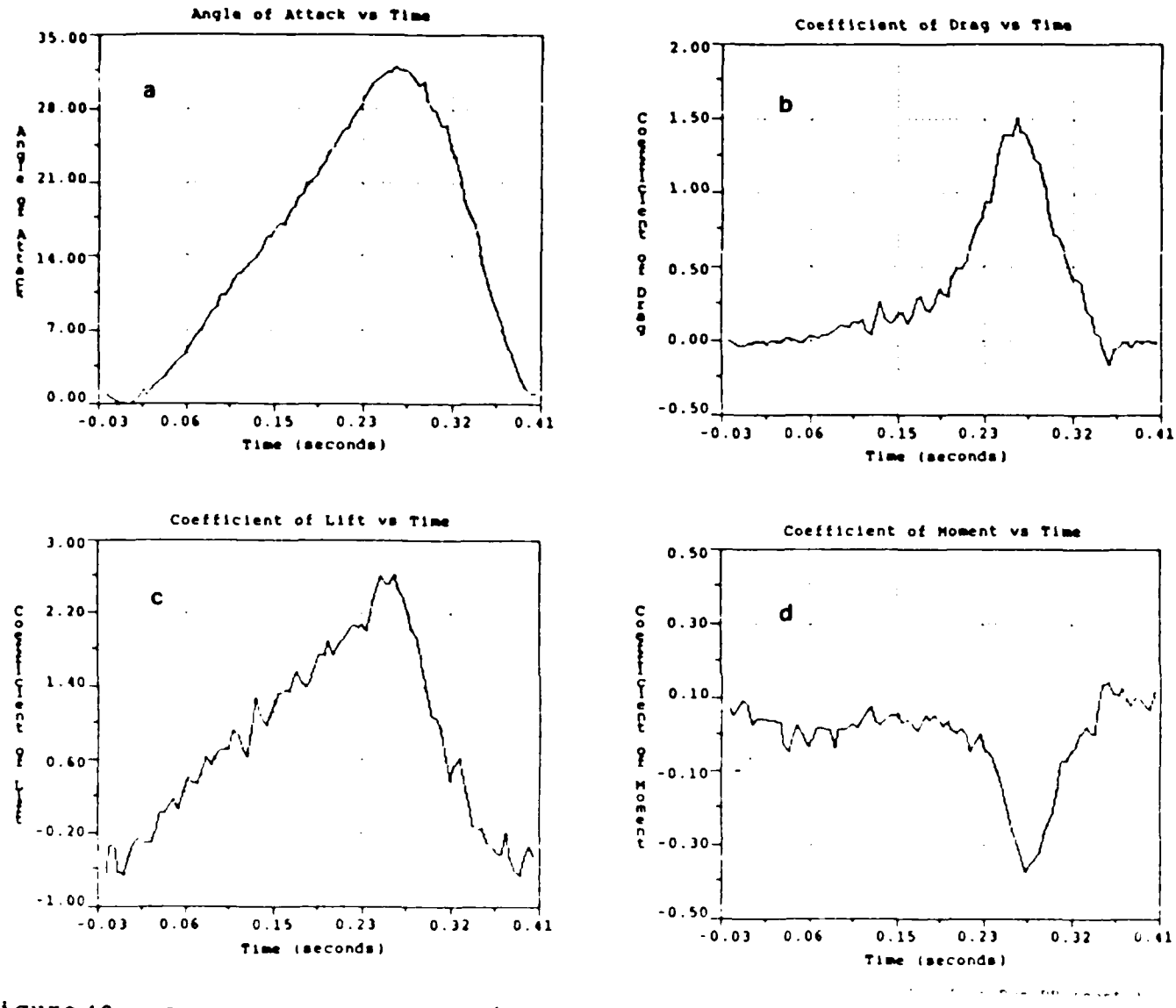

Figure 40. Results from Run RR $\dot{\alpha}_{ND_{up}} = .0384$, $\dot{\alpha}_{ND_{down}} = .0928$
a) Angle of Attack Profile, b) Effect on C_L
c) Effect on C_D, d) Effect on C_M

Appendix F

Software Package

This appendix includes the major programs that were used for data collection and reduction. TESTRUN was used for data collection and DOS4A was used for reduction. The machine language subprograms are included because of their importance for rapid data collection. The PRINTER program is included because it allowed interface between the computer and printer completing unit so that research could go from wind tunnel to final report at one independent station.

```
      TESTRUN
 1:           PROGRAM TESTRUN
 2:   C ----  To gather and store data for further processsing
 3:   C ----  Link:  TESTRUN,STCLK,GETTIM,ADIO,FORLIB/S,TESTRUN/N/E
 4:   C
 5:           IMPLICIT INTEGER (A-Z)
 6:           REAL AVSTAT(16),STATIC(16),BAROM,TEMP,MANOM1,MANOM2,TUNVEL
 7:           REAL MOTVOL,P90,P0,RHO,DTIM,DPOSV,DPOSD,ROTRAT,VPD
 8:           REAL PORTU(10),PORTL(10),SENS(16),CPU(10),CPL(10)
 9:           REAL IDATAT(16),NORMCO,PRESS,STICKY
10:           REAL CP(16),AREAUT,AREALT,LNGTHU,LNGTHL,AREAU,AREAL,INTU,INTL
11:           REAL RKOUNT
12:           INTEGER IDATA(3960),HOUR,CHECK,CHAN,DAY,MONTH,YEAR,XX
13:           INTEGER VALUE,CHEK,NS,N,A,DI,K,J,B,AA,L,C,KOUNT,S,T,U,DD,EE,ZZ
14:           INTEGER DIFANG,INK,RUNS,XXX,YYY,RRR,ZERANG,SNAP,SELECT
15:           INTEGER CHECK,CHEK,CHAN,VALUE,KOUNT,Z,W,S,CCC
16:           INTEGER II,JJ,KK,WW,DD,X,V,Y,TT,ZZZ
17:           INTEGER SDATA(5,18)
18:           REAL CNORM
19:   C
20:   C ---- Load transducer sensitivities (millivolts/psi)
21:           DATA SENS/197.0,170.3,173.0,227.5,178.0,179.0,189.0,
22:          +211.3,171.5,111.5,116.2,130.2,135.5,147.0,150.0,219.0/
23:   C
24:   C ---- Load transducer locations on upper surface (percent chord)
25:           DATA PORTU/0.0,0.0242,0.0484,0.0969,0.129,0.194,0.323,0.605,
26:          +0.888,1.000/
27:   C
28:   C ---- Load transducer locations on lower surface (percent chord)
29:           DATA PORTL/0.0,0.0161,0.0319,0.0484,0.0969,0.194,0.323,
30:          +0.686,1.000/
31:   C
32:   C ----  Initialize count of passes to zero.
33:   C
34:    10     KOUNT=0
35:   C
36:   C ----  Input date, time, barometer, and room temperature
37:   C ----  for experimental records.
38:   C
39:           WRITE (1,15)
40:    15     FORMAT (' ENTER DAY, MONTH, YEAR SEPERATED BY COMMAS',/)
41:           READ (1,20)DAY,MONTH,YEAR
42:    20     FORMAT (I3,I3,I3)
43:           WRITE (1,25)
44:    25     FORMAT (' ENTER TIME (MILITARY: XXXX HOURS)',/)
45:           READ (1,30)HOUR
46:    30     FORMAT (I5)
47:           WRITE (1,35)
48:    35     FORMAT (' ENTER BAROMETER (INCHES OF MERCURY)',/)
49:           READ (1,40)BAROM
50:    40     FORMAT (F7.2)
```

```
     TESTRUN
 51:            WRITE (1,45)
 52:     45     FORMAT (' ENTER ROOM TEMPERATURE (DEGREES FAHRENHEIT)',/)
 53:            READ (1,50)TEMP
 54:     50     FORMAT (F6.1)
 55:   C
 56:   C ----   Echo date, time, barometer, and room temperature for
 57:   C ----   verific tion.  Offer option to correct faulty input.
 58:   C
 59:            WRITE (1,55)DAY,MONTH,YEAR
 60:     55     FORMAT (' DAY:',I3,'   MONTH:',I3,'   YEAR:',I3)
 61:            WRITE (1,60)HOUR
 62:     60     FORMAT (' TIME:',I5)
 63:            WRITE (1,65)BAROM
 64:     65     FORMAT (' BAROMETER:',F7.2,' INCHES OF MERCURY')
 65:            WRITE (1,70)TEMP
 66:     70     FORMAT (' ROOM TEMPERATURE:',F6.1,' DEGREES FAHRENHEIT')
 67:            WRITE (1,75)
 68:     75     FORMAT (///,'                    ARE THE INPUTS, ECHOED ABOVE,')
 69:
 70:            WRITE (1,80)
 71:     80     FORMAT ('                  CORRECT?  IF SO, ENTER A 1',/)
 72:            READ (1,85)CHECK
 73:     85     FORMAT (I1)
 74:            IF (CHECK.NE.1) GO TO 10
 75:   C
 76:   C ----   Following part of program calculates an average zero-input
 77:   C ----   reading for each transducer.  Average is obtained from 100
 78:   C ----   readings of each transducer.
 79:   C
 80:            WRITE (1,90)
 81:     90     FORMAT (///,' THIS PART OF THE PROGRAM OBTAINS AVERAGE')
 82:            WRITE (1,95)
 83:     95     FORMAT (' TRANSDUCER ZERO-INPUT READINGS.  WHEN TEST-')
 84:            WRITE (1,100)
 85:     100    FORMAT (' SECTION VELOCITY IS ZERO, HIT RETURN KEY')
 86:            WRITE (1,102)
 87:     102    FORMAT (' IN RESPONSE TO "PAUSE"',///)
 88:            PAUSE
 89:   C
 90:   C        Initialize all array elements to zero.
 91:   C
 92:     110    CONTINUE
 93:            DO 120 Z=1,16
 94:            AVSTAT(Z)=0.0
 95:     120    CONTINUE
 96:   C
 97:   C ----   Take 100 readings from each transducer, average them as shown
 98:   C ----   below, then write these averages to terminal. Also offer the
 99:   C ----   :tion to retake the average zero-input readings.
100:            ⊦ UNT=0
```

```
      TESTRUN
101:  C
102:            CALL STCLK
103:  C
104:            WRITE(1,7100)
105:   7100     FORMAT(///,' ',20X,'STARTING TO TAKE DATA',///)
106:            DO 7200 J=1,1800,18
107:               KOUNT=KOUNT+1
108:               CALL GETTIM(TIME)
109:               CHAN=0
110:               CALL AD(VALUE,CHAN,84)
111:               IDATA(J+1)=VALUE
112:               DO 7300 K=1,16
113:                  CHAN=K-1
114:                  CALL AD(VALUE,CHAN,80)
115:                  DI=K+J+1
116:                  IDATA(DI)=VALUE
117:   7300        CONTINUE
118:   7200     CONTINUE
119:            N=KOUNT*18
120:            DO 150 S=1,100
121:            DO 160 T=1,16
122:            CHAN=T-1
123:            CALL AD(VALUE,CHAN,80)
124:            AVSTAT(T)=AVSTAT(T)+(VALUE/100.0)
125:    160     CONTINUE
126:    150     CONTINUE
127:  C
128:  C
129:            WRITE (1,155)
130:    155     FORMAT (' AVERAGE ZERO-INPUT READINGS FOLLOW',/)
131:  C
132:            DO 180 W=1,16
133:            WRITE (1,165)W,AVSTAT(W)
134:    165     FORMAT (' TRANSDUCER',I3,' AVERAGE STATIC READING:',F6.0)
135:    180     CONTINUE
136:            WRITE (1,177)
137:    177     FORMAT (///,' TO PROCEED WITH THE PROGRAM, ENTER A 1',/)
138:            READ (1,178)XX
139:    178     FORMAT (I2)
140:            IF (XX.NE.1) GO TO 110
141:  C
142:  C
143:  C ----    Enter manometer reading and 90 and 0
144:  C ----    degree angle of attack voltages for experimental records.
145:  C ----    Test-section velocity is also computed as shown below.
146:  C
147:  C
148:            WRITE (1,185)
149:    185     FORMAT (//////,'*******************************NOW TURN ON THE
150:         + TUNNEL*******************************',//////)
```

```
      TESTRUN
151:   187    WRITE (1,190)
152:   190    FORMAT (' ENTER ROOM PRESS. MINUS TUNNEL STAT. PRESS.
153:       + (INCHES OF WATER)',/)
154:          READ (1,195)MANOM1
155:   195    FORMAT (F8.4)
156:          WRITE (1,200)
157:   200    FORMAT (' ENTER TUNNEL TOTAL PRESS. MINUS TUNNEL STATIC PRESS.
158:       + (INCHES OF WATER)',/)
159:          READ (1,195)MANOM2
160:   205    FORMAT (F8.4)
161:          WRITE (1,220)
162:   220    FORMAT (' ENTER 90 AND 0 DEGREE VOLTAGES, RESPECTIVELY',/)
163:          READ (1,225)P90,P0
164:   225    FORMAT (2F7.4)
165:          RHO=(BAROM*70.45)/(1716.0*(460.0+TEMP))
166:          TUNVEL=SQRT((2.0*(5.204*MANOM2))/RHO)
167:   C
168:   C ----  Echo manometer readings, tunnel velocity and
169:   C ----  90 and 0 degree angle of attack voltages for verification.
170:   C ----  offer option to correct faulty input.
171:   C
172:          WRITE (1,230)MANOM1
173:   230    FORMAT (' MANOMETER ONE: ',F8.4,' INCHES OF WATER')
174:          WRITE (1,233)MANOM2
175:   233    FORMAT (' MANOMETER TWO: ',F8.4,' INCHES OF WATER')
176:          WRITE (1,235)TUNVEL
177:   235    FORMAT (' TUNNEL VELOCITY: ',F7.2,' FT/SEC')
178:          WRITE (1,245)P90,P0
179:   245    FORMAT (' P90: ',F7.4,' VOLTS     P0: ',F7.4,' VOLTS')
180:          WRITE (1,75)
181:          WRITE (1,80)
182:          READ (1,85)CHEK
183:          IF (CHEK.NE.1) GO TO 187
184:   C
185:   C ----  The following part of the program writes pertinent
186:   C ----  information to file RAWDATA0DAT on disk.
187:   C
188:          CALL OPEN (3,'RAWDATA0DAT',2)
189:          WRITE (3,500)
190:   500    FORMAT (' DAY',10X,'MONTH',9X,'YEAR',9X,'TIME')
191:          WRITE (3,510)DAY,MONTH,YEAR,HOUR
192:   510    FORMAT (I3,11X,I3,11X,I3,9X,I5,/)
193:          WRITE (3,520)
194:   520    FORMAT (' TEMPERATURE',14X,'BAROMETER')
195:          WRITE (3,530)TEMP,BAROM
196:   530    FORMAT (2X,F6.1,18X,F7.2,/)
197:          WRITE (3,540)
198:   540    FORMAT (' MANOMETER 1',22X,'MANOMETER 2')
199:          WRITE (3,545)MANOM1,MANOM2
200:   545    FORMAT (2X,F8.4,25X,F8.4,/)
```

```
      TESTRUN
201:          WRITE (3,550)
202:   550    FORMAT (' TUNNEL VELOCITY',22X,'MOTOR VOLTAGE')
203:          WRITE (3NVEL,MOTVOL
204:   555    FORMAT (4X,F7.2,31X,/)
205:          WRITE (3,560)
206:   560    FORMAT (' 90 DEG. VOLTAGE',16X,'0 DEG. VOLTAGE')
207:          WRITE (3,570)P90,P0
208:   570    FORMAT (5X,F7.4,23X,F7.4,/)
209:          WRITE (3,580)
210:   580    FORMAT (' NUMBER OF PASSES',10X,'NUMBER OF IDATA ELEMENTS')
211:          WRITE (3,590)
212:   590    FORMAT (5X,'(KOUNT)',26X,'(N)')
213:          KOUNT=200
214:          N=3600
215:          WRITE (3,600)KOUNT,N
216:   600    FORMAT (3X,I6,26X,I6,//)
217:          WRITE (3,610)
218:   610    FORMAT (' AVERAGE ZERO-INPUT READINGS GIVEN BELOW',/)
219:          WRITE (3,620)AVSTAT(1),AVSTAT(2),AVSTAT(3),AVSTAT(4)
220:          WRITE (3,620)AVSTAT(5),AVSTAT(6),AVSTAT(7),AVSTAT(8)
221:          WRITE (3,620)AVSTAT(9),AVSTAT(10),AVSTAT(11),AVSTAT(12)
222:          WRITE (3,620)AVSTAT(13),AVSTAT(14),AVSTAT(15),AVSTAT(16)
223:   620    FORMAT (F9.3,5X,F9.3,5X,F9.3,5X,F9.3)
224:          WRITE (3,660)
225:   660    FORMAT (///)
226:          ENDFILE 3
227:   C
228:   C ----  Offer option to conduct only static runs
229:   C
230:          WRITE (1,247)
231:    247   FORMAT (//,' DO YOU WANT TO MAKE 1=DYNAMIC OR 2=STATIC RUNS?',/)
232:          READ(1,85)CHEK
233:          IF (CHEK.EQ.2) GOTO 2345
234:   C
235:   C ----  Initialize number or runs to zero, and then increment this
236:   C ----  number by one each run thereafter.
237:   C
238:          RUNS=0
239:    250   CONTINUE
240:          RUNS=RUNS+1
241:    255   CONTINUE
242:   C
243:          WRITE (1,257)RUNS
244:    257   FORMAT (////,' ********RETURN AIRFOIL TO ZERO ANGLE OF
245:        + ATTACK IN PREPARATION FOR RUN',I2,'********',////)
246:          NS=0
247:          KOUNT=0
248:          WRITE (1,260)
249:    260   FORMAT (' ENTER NUMBER OF SAMPLES (MULTIPLE OF 18,
250:        + 5040 MAXIMUM)',/)
```

```
      TESTRUN
  251:          READ (1,265)NS
  252:   265    FORMAT (I5)
  253:          WRITE (1,270)NS
  254:   270    FORMAT (//,' ',25X,'NS:',I5,//)
  255:  C
  256:  C ----  In the next segement, the operator is given the choice
  257:  C ----  between manual and automatic trigger.
  258:  C
  259:          WRITE (1,273)
  260:   273    FORMAT (' DO YOU WANT MANUAL OR AUTOMATIC TRIGGER?
  261:       + (1=AUTO, 2=MANUAL)',/)
  262:          READ (1,277)SELECT
  263:   277    FORMAT (I2)
  264:          IF (SELECT.NE.2) GO TO 281
  265:          PAUSE
  266:          GOTO 285
  267:  C
  268:  C ----  The program segement below is the automatic trigger.
  269:  C ----  The program stays in the 280 loop below until ZERANG
  270:  C ----  and VALUE differ by 2 or more digital counts.
  271:  C ----  When this occurs, due to rotation of the airfoil, the
  272:  C ----  program continues on to line number 285.
  273:  C
  274:   281    CALL AD(VALUE,0,84)
  275:          ZERANG=VALUE
  276:   280    CALL AD(VALUE,0,84)
  277:          SNAP=IABS(VALUE-ZERANG)
  278:          IF (SNAP.LE.1) GO TO 280
  279:  C
  280:  C ----  STCLK, below, will count up to 32,768 time clicks, each click
  281:  C ----  being .0010046 seconds long. Therefore, STCLK can only time
  282:  C ----  an event that lasts for no more than about 32 seconds.
  283:  C
  284:   285    CALL STCLK
  285:  C
  286:  C ----  The following part of the program reads and stores the time
  287:  C ----  obtained from subroutine GETTIM, as well as position and
  288:  C ----  pressure information obtained from the potentiometer and
  289:  C ----  pressure transducers, respectively.  This position and pressure
  290:  C ----  information is obtained through subroutine ADIO.
  291:  C
  292:          WRITE(1,290)
  293:   290    FORMAT(///,' ',20X,'STARTING TO TAKE DATA',///)
  294:          DO 320 J=1,NS,18
  295:          KOUNT=KOUNT+1
  296:          CALL GETTIM(TIME)
  297:          IDATA(J)=TIME
  298:          CHAN=0
  299:          CALL AD(VALUE,CHAN,84)
  300:          IDATA(J+1)=VALUE
```

```
      TESTRUN
301:          DO 300 K=1,16
302:          CHAN=K-1
303:          CALL AD(VALUE,CHAN,80)
304:          DI=K+J+1
305:          IDATA(DI)=VALUE
306:   300     CONTINUE
307:   320     CONTINUE
308:          WRITE (1,330)RUNS
309:   330     FORMAT (' ',15X,'DATA GATHERING COMPLETE FOR RUN',I2,//)
310:          WRITE (1,340)KOUNT
311:   340     FORMAT (' NUMBER OF PASSES = ',I6,//)
312:           N=KOUNT*18
313:          WRITE (1,343)N
314:   343    FORMAT (' NUMBER OF IDATA ELEMENTS= ',I6,//)
315:          VPD=(P90-P0)/90.0
316:          DTIM=(IDATA(2701)-IDATA(901))*(0.0010046)
317:          DPOSV=((IDATA(2702)-IDATA(902))/4096.0)*10.0
318:          DPOSD=DPOSV/VPD
319:          ROTRAT=DPOSD/DTIM
320:          WRITE (1,410)ROTRAT
321:   410    FORMAT (' AIRFOIL AVERAGE ROTATION RATE:',F6.2,' DEG/SEC',////)
322:   C
323:   C ----  Options are now offered to list the IDATA array at the
324:   C ----  terminal, to write this array to disk, and to repeat the
325:   C ----  data run.
326:   C
327:    344    WRITE(1,345)
328:    345     FORMAT(' DO YOU WANT TO LIST THE IDATA ARRAY?(Y=1)',//)
329:          READ(1,347)AA
330:    347    FORMAT (I2)
331:          IF (AA.NE.1)GO TO 350
332:          DO 420 XXX=180,N,180
333:          YYY=XXX-179
334:          WRITE (1,360)(IDATA(L),L=YYY,XXX)
335:    360    FORMAT (9I7)
336:    420    CONTINUE
337:          GOTO 344
338:    350    WRITE(1,355)
339:    355    FORMAT(' DO YOU WANT TO WRITE TO DISK?(Y=1)',//)
340:          READ (1,347)B
341:          IF (B.EQ.1) GO TO 390
342:    374    WRITE (1,375)RUNS
343:    375    FORMAT (' DO YOU WANT TO REPEAT RUN',I2,'? (Y=1)',//)
344:          READ (1,380)C
345:    380    FORMAT (I2)
346:          IF (C.EQ.1) GO TO 255
347:          IF (C.EQ.2) GO TO 4800
348:          GOTO 374
349:    390    CONTINUE
350:
```

```
C
C ----   The part of the program below writes the [illegible] data
C ----   to disk, in unformatted form, under the filename
C ----   RAWDATA1DAT, RAWDATA2DAT, [illegible], RAWDATA5DAT, depending
C ----   on the value of the variable RUNS. To view the data files
C ----   that are in unformatted form, use program [illegible]
C
         IF (RUNS.EQ.1) GO TO 710
         IF (RUNS.EQ.2) GO TO 720
         IF (RUNS.EQ.3) GO TO 730
         IF (RUNS.EQ.4) GO TO 740
         IF (RUNS.EQ.5) GO TO 750
C
   710   CONTINUE
         CALL OPEN (4,'RAWDATA1DAT',[illegible]
         WRITE (4) IDATA(I,J),I=1,N
         GO TO 760
   720   CONTINUE
         CALL OPEN (5,'RAWDATA2DAT',[illegible]
         WRITE (5) IDATA(I,J),I=1,N
         GO TO 760
   730   CONTINUE
         CALL OPEN (6,'RAWDATA3DAT',[illegible]
         WRITE (6) IDATA(I,J),I=1,N
         GO TO 760
   740   CONTINUE
         CALL OPEN (7,'RAWDATA4DAT'[illegible]
         WRITE (7) IDATA(I,J),I=1,N
         GO TO 760
   750   CONTINUE
         CALL OPEN (8,'RAWDATA5DAT'[illegible]
         WRITE (8) IDATA(I,J),I=1,N
         GO TO 760
   760   CONTINUE
         IF (RUNS.NE.[illegible]
         ENDFILE 4
         ENDFILE 5
         ENDFILE 6
         ENDFILE 7
         ENDFILE 8
  2345   CONTINUE
         WRITE [illegible]
  2346   FORMAT [illegible]
       + NORMAL [illegible]
         CALL OPEN [illegible]
         CALL OPEN [illegible]
C
C        [illegible]
C        data [illegible]
```

```
      TESTRUN
401:   2400   CONTINUE
402:          WRITE (1,2450)
403:   2450   FORMAT (' ENTER NS (MULTIPLE OF 18, LESS THAN OR
404:     +  EQUAL TO 5040)',/)
405:          READ (1,2150)NS
406:   2150   FORMAT (I4)
407:          KOUNT=0
408:          CNORM=0
409:          DO 5000 ZZZ=1,5
410:          KOUNT=0
411:          WRITE (1,2000)
412:   2000   FORMAT (////,' HIT RETURN TO START DATA COLLECTION',/)
413:          READ(1,8000)ICK
414:   8000   FORMAT(I3)
415:   C
416:   C      STCLK, below, will count up to 32,768 time clicks, each click
417:   C      being .0010046 seconds long. Therefore, STCLK can only time
418:   C      an event that lasts for no more than about 32 seconds.
419:   C
420:          CALL STCLK
421:   C
422:          WRITE(1,2100)
423:   2100   FORMAT(///,' ',20X,'STARTING TO TAKE DATA',///)
424:          DO 2200 J=1,NS,18
425:          KOUNT=KOUNT+1
426:          CALL GETTIM(TIME)
427:          IDATA(J)=TIME
428:          CHAN=0
429:          CALL AD(VALUE,CHAN,84)
430:          IDATA(J+1)=VALUE
431:          DO 2300 K=1,16
432:          CHAN=K-1
433:          CALL AD(VALUE,CHAN,80)
434:          DI=K+J+1
435:          IDATA(DI)=VALUE
436:   2300   CONTINUE
437:   2200   CONTINUE
438:          N=KOUNT*18
439:          WRITE (1,2500)N
440:   2500   FORMAT (' NUMBER OF IDATA ELEMENTS= ',I6,//)
441:   C
442:   C      Time average data
443:   C
444:          DO 2550 S=1,16
445:          IDATAT(S)=0.0
446:   2550   CONTINUE
447:          DO 2600 II=1,N,18
448:          DO 2700 JJ=3,18
449:          TT=II+JJ
450:          PKOUNT=KOUNT
```

```
      TESTRUN
451:            IDATAT(JJ-2)=((IDATA(TT-1))/RKOUNT)+IDATAT(JJ-2)
452:     2700   CONTINUE
453:     2600   CONTINUE
454:   C
455:   C ----   Compute the pressure coefficients
456:   C
457:            DO 2800 KK=1,16
458:            STICKY=AVSTAT(KK)-2048.0
459:            PRESS=(((IDATAT(KK)-STICKY)-2048.0)/2048.0)*(50.0/SENS(KK))
460:            CP(KK)=(PRESS+(MANOM1/27.68))/(MANOM2/27.68)
461:     2800   CONTINUE
462:   C
463:   C          ADJUSTMENTS FOR FAULTY TRANSDUCERS
464:   C
465:            CP(15)=CP(16)+(1.58/3.23)*(CP(14)-CP(16))
466:   C
467:   C ---- The next loop defines the pressure distribution on the upper
468:   C ---- surface of the airfoil, leading edge to trailing edge.
469:   C ---- Pressure coefficient is assumed to be zero at the trailing edge.
470:   C
471:            WRITE (1,2900)
472:     2900   FORMAT (' UPPER SURFACE PRESSURE COEFFICIENTS,
473:          + L.E. TO T.E., ARE GIVEN BELOW',)
474:            DO 3000 V=1,9
475:            CPU(V)=CP(V)
476:     3000   CONTINUE
477:            CPU(10)=CPU(9)+(CPU(9)-CPU(8))/.287*.098
478:            DO 3100 V=1,10
479:            WRITE (1,3200)V,CPU(V)
480:     3200   FORMAT (' CPU',I3,'=',F8.4)
481:     3100   CONTINUE
482:            READ(1,8001)ICK
483:   8001     FORMAT(I3)
484:   C
485:            WRITE (1,3300)
486:     3300   FORMAT (/,' LOWER SURFACE PRESSURE COEFFICIENTS,
487:          + L.E. TO T.E., ARE GIVEN BELOW')
488:            CPL(1)=CP(1)
489:            DO 3400 W=2,8
490:            DD=18-W
491:            CPL(W)=CP(DD)
492:     3400   CONTINUE
493:            CPL(9)=CPU(10)
494:            DO 3500 W=1,9
495:            WRITE (1,3600)W,CPL(W)
496:     3600   FORMAT (' CPL',I3,'=',F8.4)
497:     3500   CONTINUE
498:
499:   C
500:   C ---- The following loop integrates the upper pressure
```

```
ESTRUN
  501:  C ---- distribution using the trapezoidal rule.
  502:  C
  503:          AREAUT=0.0
  504:          DO 3700 X=1,9
  505:          LNGTHU=PORTU(X+1)-PORTU(X)
  506:          IF ((ABS(CPU(X+1)-CPU(X))).GT.(ABS((0.01)*CPU(X)))) GO TO 3800
  507:          AREAU=(0.5)*(CPU(X+1)+CPU(X))*LNGTHU
  508:   3800   IF ((ABS(CPU(X+1)-CPU(X))).LE.(ABS((0.01)*CPU(X)))) GO TO 4000
  509:          INTU=(PORTU(X)-PORTU(X+1))*CPU(X)/(CPU(X+1)-CPU(X))
  510:          IF (INTU.LT.LNGTHU) GO TO 3900
  511:          AREAU=(.5)*(CPU(X+1)+CPU(X))*LNGTHU
  512:          IF ((INTU).GE.(LNGTHU)) GO TO 4000
  513:   3900   AREAU=((.5)*INTU*CPU(X))+
  514:       +                  ((.5)*(LNGTHU-INTU)*CPU(X+1))
  515:   4000   AREAUT=AREAUT+AREAU
  516:   3700   CONTINUE
  517:  C
  518:  C ---- The following loop integrates the lower pressure
  519:  C ---- distribution using the trapezoidal rule.
  520:  C
  521:          AREALT=0.0
  522:          DO 4100 Y=1,8
  523:          LNGTHL=PORTL(Y+1)-PORTL(Y)
  524:          IF ((ABS(CPL(Y+1)-CPL(Y))).GT.(ABS((0.01)*CPL(Y)))) GO TO 4200
  525:          AREAL=(.5)*(CPL(Y+1)+CPL(Y))*LNGTHL
  526:          IF ((ABS(CPL(Y+1)-CPL(Y))).LE.(ABS((0.01)*CPL(Y)))) GO TO 4400
  527:   4200   INTL=(PORTL(Y)-PORTL(Y+1))*CPL(Y)/(CPL(Y+1)-CPL(Y))
  528:          IF ((INTL).LT.(LNGTHL)) GO TO 4300
  529:          AREAL=(.5)*(CPL(Y+1)+CPL(Y))*LNGTHL
  530:          IF ((INTL).GE.(LNGTHL)) GO TO 4400
  531:   4300   AREAL=((.5)*INTL*CPL(Y))+
  532:       +                  ((.5)*(LNGTHL-INTL)*CPL(Y+1))
  533:   4400   AREALT=AREALT+AREAL
  534:   4100   CONTINUE
  535:  C
  536:          NORMCO=AREALT-AREAUT
  537:          CNORM=CNORM+NORMCO/5.
  538:  C
  539:          WRITE (1,4500)NORMCO
  540:   4500   FORMAT (/,' NORMAL FORCE COEFFICIENT=',F8.5,/)
  541:  C
  542:  C ----  Option now offered to write to disk and continue run
  543:  C
  544:           DO 4550 J=1,16
  545:   4550    IDATA(J+2)=IDATAT(J)
  546:           DO 4560 J=1,18
  547:   4560    SDATA(ZZZ,J)=IDATA(J)
  548:   5000    CONTINUE
  549:           WRITE(1,4570)CNORM
  550:   4570    FORMAT(//,' AVERAGED NORMAL COEFFICIENT=',F8.5,/)
```

```
      TESTRUN
551:            WRITE(1,4575)
552:    4575    FORMAT(/,' DO YOU WANT TO WRITE TO DISK (Y=1) ')
553:            READ(1,4700)CHEK
554:            IF (CHEK.NE.1) GOTO 4599
555:            DO 4577 ZZZ=1,5
556:    4577    WRITE(9,360) (SDATA(ZZZ,L),L=1,18)
557:            WRITE(10,4580)IDATA(2),NORMCO
558:    4580    FORMAT(I5,F8.5,/)
559:    4599    WRITE (1,4600)
560:    4600    FORMAT (' DO YOU WANT TO CONTINUE THE RUN?  (Y=1)',/)
561:            READ (1,4700)CCC
562:    4700    FORMAT (I2)
563:            IF (CCC.EQ.1) GO TO 2400
564:            IF (CCC.NE.2) GOTO 4599
565:    4800    CONTINUE
566:            STOP
567:            END
```

```
DOS4A
 1:          PROGRAM DOS4A
 2:          INTEGER IDATA2(7200),NJ
 3:          INTEGER N,R,X,Y,V,W,S,I,J,L,AA,PP,QQ
 4:          INTEGER RR,SS,TT,UU,VV,WW,XX,YY,ZZ,RUN,TRAP,PAZZ,DIV,NUMEL
 5:          INTEGER ELEM1,ELEM2,DAY,MONTH,YEAR,HOUR,CHANG1,CHANG2
 6:          INTEGER DD,EE,FF,HH,LL,NN,MOOCOW,JJJ,ZOO
 7:          INTEGER MKOUNT
 8:          REAL PORTX(20),PORTY(20),CP(16),CPU(20),SENS(16)
 9:          REAL PRESS(16),REDAT(40),P90,P0,TEMP,BAROM,MANOM1,MANOM2
10:          REAL TUNVEL,MOTVOL,AVSTAT(16),ARNORM,ARMOM,RE,RHO,MU
11:          REAL VPD,AOA,AOAR,CL,CD,CNORM,CCHORD,TUNQ,LNGTHU,LNGTHL
12:          REAL AREAU,AREAL,DTIM,DPOSD,DPOSV,ROTRAT,NDRATE
13:          REAL REDATC(40),CMOM,ARN,ARM,ARC,ARCHOR
14:          REAL DETAN,DETBN,INCPL,INCPN,PI
15:  C
16:  C ---- Load transducer sensitivities (millivolts/psi)
17:          DATA SENS/197.0,170.3,173.0,227.5,178.0,179.0,189.0,
18:         +211.3,171.5,111.5,116.2,130.2,135.5,147.0,150.0,219.0/
19:  C
20:  C---    LOAD TRANSDUCER LOCATIONS ON UPPER SURFACE
21:          DATA PORTX/0.0,0.0250,0.0490,0.0980,0.131,0.197,0.328,0.615,
22:         +0.902,1.000,0.697,0.328,0.197,0.0980,0.0490,0.0330,0.016,0.0/
23:  C
24:  C ---- Load transducer locations for chord force (percent chord)
25:          DATA PORTY/0.0,0.0327,0.0440,0.0581,0.0637,0.0714,.0743,
26:         +0.0554,0.0178,0.0,0.0461,0.0743,0.0714,0.0581,0.0440,
27:         +0.0364,0.0262,0.0/
28:          WRITE (1,5)
29:      5   FORMAT (///,' *****THE DATA FILES TO BE REDUCED MUST BE ON
30:        + DISK DRIVE B AND MUST BE NAMED*****')
31:          WRITE (1,6)
32:      6   FORMAT (' *************RAWDATA0.DAT, RAWDATA1.DAT,. . . . . .,
33:        + RAWDATA5.DAT*************',///)
34:  C
35:  C ---- Read raw data from RAWDATA0DAT on drive B.
36:          CALL OPEN(3,'RAWDATA0DAT',2)
37:          READ (3,10)DAY,MONTH,YEAR,HOUR
38:     10   FORMAT (/,I3,11X,I3,11X,I3,9X,I5)
39:          READ (3,20)TEMP,BAROM
40:     20   FORMAT (//,2X,F6.1,18X,F7.2)
41:          READ (3,30)MANOM1,MANOM2
42:     30   FORMAT (//,2X,F8.4,25X,F8.4)
43:          READ (3,40)TUNVEL
44:     40   FORMAT (//,4X,F7.2,31X)
45:          READ (3,50)P90,P0
46:     50   FORMAT (//,5X,F7.4,23X,F7.4)
47:          READ (3,60)KOUNT,N
48:     60   FORMAT (///,3X,I6,26X,I6)
49:          READ (3,70)AVSTAT(1),AVSTAT(2),AVSTAT(3),AVSTAT(4)
50:          READ (3,75)AVSTAT(5),AVSTAT(6),AVSTAT(7),AVSTAT(8)
 1: *
```

```
      DOS4A
   51:          READ (3,75)AVSTAT(9),AVSTAT(10),AVSTAT(11),AVSTAT(12)
   52:          READ (3,75)AVSTAT(13),AVSTAT(14),AVSTAT(15),AVSTAT(16)
   53:     70   FORMAT (////,F9.3,5X,F9.3,5X,F9.3,5X,F9.3)
   54:     75   FORMAT (F9.3,5X,F9.3,5X,F9.3,5X,F9.3)
   55:          ENDFILE 3
   56:          VPD=(P90-P0)/90.0
   57:  C
   58:          RUN=0
   59:    470   CONTINUE
   60:          RUN=RUN+1
   61:          WRITE(1,5000) RUN
   62:    5000  FORMAT('  RUN = ',I3)
   63:          IF (RUN.EQ.1) GO TO 490
   64:          IF (RUN.EQ.2) GO TO 510
   65:          IF (RUN.EQ.3) GO TO 525
   66:          IF (RUN.EQ.4) GO TO 535
   67:          IF (RUN.EQ.5) GO TO 545
   68:    490   CONTINUE
   69:          CALL OPEN(4,'RAWDATA1DAT',2)
   70:          READ(4)(IDATA2(L),L=1,N)
   71:          ENDFILE 4
   72:          GO TO 550
   73:    510   CONTINUE
   74:          CALL OPEN(5,'RAWDATA2DAT',2)
   75:          READ(5)(IDATA2(L),L=1,N)
   76:          ENDFILE 5
   77:          GO TO 550
   78:    525   CONTINUE
   79:          CALL OPEN(6,'RAWDATA3DAT',2)
   80:          READ(6)(IDATA2(L),L=1,N)
   81:          ENDFILE 6
   82:          GO TO 550
   83:    535   CONTINUE
   84:          CALL OPEN(7,'RAWDATA4DAT',2)
   85:          READ(7)(IDATA2(L),L=1,N)
   86:          ENDFILE 7
   87:          GO TO 550
   88:    545   CONTINUE
   89:          CALL OPEN(8,'RAWDATA5DAT',2)
   90:          READ(8)(IDATA2(L),L=1,N)
   91:          ENDFILE 8
   92:    550   CONTINUE
   93:  C
   94:    650   CONTINUE
   95:  C
   96:  C ---- The steps below compute Reynolds number, tunnel "Q"
   97:  C ---- and volts per degree for the run.
   98:  C
   99:          IF (RUN.GT.1) GOTO 895
  100:          RHO=(BAROM*70.45)/(1716.0*(460+TEMP))
```

```
      DOS4A
101:          MU=(2.270*(10.0**(-8.0))*((460.0+TEMP)**1.5))/(460.0+TEMP+198.6)
102:          RE=(RHO*TUNVEL*1.016)/MU
103:          TUNQ=(0.5)*RHO*(TUNVEL**2)
104:    C
105:    C ---- The following writes pertinent information to disk file
106:    C ---- REDUDATADAT as a heading.
107:    C
108:          CALL OPEN(10,'REDUDATADAT',2)
109:          WRITE (10,800)
110:     800  FORMAT (' DAY',10X,'MONTH',9X,'YEAR',9X,'TIME')
111:          WRITE (10,810)DAY,MONTH,YEAR,HOUR
112:     810  FORMAT (I3,11X,I3,11X,I3,9X,I5,/)
113:          WRITE (10,820)
114:     820  FORMAT (' TEMPERATURE',14X,'BAROMETER')
115:          WRITE (10,830)TEMP,BAROM
116:     830  FORMAT (2X,F6.1,18X,F7.2,/)
117:          WRITE (10,840)
118:     840  FORMAT (' MANOMETER 1',22X,'MANOMETER 2')
119:          WRITE (10,845)MANOM1,MANOM2
120:     845  FORMAT (2X,F8.4,25X,F8.4,/)
121:          WRITE (10,850)
122:     850  FORMAT (' TUNNEL VELOCITY',22X,'MOTOR VOLTAGE')
123:          WRITE (10,855)TUNVEL
124:     855  FORMAT (4X,F7.2,31X,/)
125:          WRITE (10,880)
126:     880  FORMAT (' REYNOLDS NUMBER',25X,'TUNNEL "Q"')
127:          WRITE (10,890)RE,TUNQ
128:     890  FORMAT (4X,E11.4,30X,F6.3,/)
129:          DO 895 HH=1,16
130:          WRITE (10,897)HH,AVSTAT(HH)
131:     897  FORMAT (' AVERAGE ZERO-INPUT READING, TRANSDUCER',I3,' =',F6.0)
132:     895  CONTINUE
133:          WRITE(10,1100)
134:    C
135:    C ---- One pass through the DO 100 J=1,N,18 loop computes one
136:    C ---- point in the CN (normal force coefficient) versus ALPHA curve.
137:    C
138:          MKOUNT=KOUNT-1
139:          DO 1000 J=1,MKOUNT
140:          NJ=(J-1)*18
141:          DO 100  I=1,18
142:          NN=I+NJ
143:          REDAT(I)=IDATA2(NN)
144:          REDAT(I+18)=IDATA2(NN+18)
145:      100 CONTINUE
146:    C
147:    C ---- The loop below subtracts the average zero input readings
148:    C ---- (AVSTAT) from each appropriate IDATAT element.
149:    C
150:          DO 200 I=3,18
```

```
      ' DOS4A
  151:          REDAT(I)=REDAT(I)-AVSTAT(I-2)
  152:          REDAT(I+18)=REDAT(I+18)-AVSTAT(I-2)
  153:   200    CONTINUE
  154:  C
  155:  C ---- Operations in the following loop correct for the finite
  156:  C ---- time between samples using a linear interpolation. Time
  157:  C ---- between passes must be sufficiently small or the linear
  158:  C ---- interpolation will be invalid.
  159:  C
  160:          DO 300 R=1,18
  161:          REDATC(R)=REDAT(R+18)-(REDAT(R+18)-REDAT(R))*(R-1)/18.0
  162:   300    CONTINUE
  163:  C
  164:  C ---- The following loop converts digital quantities to degrees
  165:  C ---- (angle of attack) and psi (sensed differential pressure).
  166:  C
  167:  C ---- The AOA conversion below assumes the A/D board is strapped
  168:  C ---- for the 0-10 volt unipolar input range. The amp on the
  169:  C ---- board is set for a gain of 1, so any input to the board
  170:  C ---- greater than 10 volts will saturate the A/D conversion system.
  171:  C
  172:          AOA=(((REDATC(2)/4096.0)*10.0)-P0)/VPD
  173:          TIME=REDATC(1)
  174:  C
  175:  C ---- The PRESS conversion below assumes the A/D board is strapped
  176:  C ---- for the (-5)-(+5) volt bipolar input range, where the input
  177:  C ---- (from the transducers, is first amplified through an
  178:  C ---- amplifier of gain 100. So any input greater than +/-50 milli-
  179:  C ---- volts will saturate the A/D conversion system.
  180:  C
  181:          DO 400  S=1,16
  182:          PRESS(S)=(REDATC(S+2)/2048.0)*50.0/SENS(S)
  183:          CP(S)=(PRESS(S)+(MANOM1/27.68))/(MANOM2/27.68)
  184:   400    CONTINUE
  185:  C
  186:  C ---- The next loop defines the pressure distribution on the
  187:  C ---- airfoil, leading edge to trailing edge, and back to leading
  188:  C ---- edge.
  189:  C
  190:          DO 405  V=1,9
  191:          CPU(V)=CP(V)
  192:   405    CONTINUE
  193:  C
  194:          CPU(10)=CPU(9)+(CPU(9)-CPU(8))/.287*.098
  195:  C
  196:          DO 410  V=10,16
  197:          CPU(V+1)=CP(V)
  198:   410    CONTINUE
  199:  C
  200:          CPU(18)=CPU(1)
```

```
      DOS4A
  201:  C
  202:  C
  203:  C ---- The following loop integrates the normal force and moment
  204:  C ---- distribution using the trapezoidal rule.
  205:  C
  206:        ARNORM=0.0
  207:        ARMOM=0.0
  208:  C
  209:  C
  210:        DO 2000  I=1,9
  211:        ARN=.5*(PORTX(I+1)-PORTX(I))*(CPU(I)+CPU(I+1))
  212:        ARM=.5*(PORTX(I+1)-PORTX(I))*(PORTX(I)*CPU(I)+PORTX(I+1)*
  213:       +   CPU(I+1))
  214:  C
  215:        ARNORM=ARNORM-ARN
  216:        ARMOM=ARMOM-ARM
  217:   2000 CONTINUE
  218:  C
  219:  C
  220:        DO 2500  I=10,17
  221:        ARN=.5*ABS(PORTX(I+1)-PORTX(I))*(CPU(I)+CPU(I+1))
  222:        ARM=.5*ABS(PORTX(I+1)-PORTX(I))*(PORTX(I)*CPU(I)+PORTX(I+1)*
  223:       +   CPU(I+1))
  224:  C
  225:        ARNORM=ARNORM+ARN
  226:        ARMOM=ARMOM+ARM
  227:   2500 CONTINUE
  228:  C
  229:        CNORM=ARNORM
  230:        CMOM=-ARMOM+0.25*CNORM
  231:  C
  232:  C ---- The following loop integrates the chord force
  233:  C ---- distribution using the trapezoidal rule.
  234:  C
  235:        ARCHOR=0.00
  236:  C
  237:        DO 3000  I=1,6
  238:        ARC=.5*(PORTY(I+1)-PORTY(I))*(CPU(I)+CPU(I+1))
  239:        ARCHOR=ARCHOR+ARC
  240:   3000 CONTINUE
  241:  C
  242:        DO 3500  I=7,10
  243:        ARC=.5*ABS(PORTY(I+1)-PORTY(I))*(CPU(I)+CPU(I+1))
  244:        ARCHOR=ARCHOR-ARC
  245:   3500 CONTINUE
  246:  C
  247:        DO 3750  I=11,17
  248:        ARC=.5*ABS(PORTY(I+1)-PORTY(I))*(CPU(I)+CPU(I+1))
  249:        ARCHOR=ARCHOR+ARC
  250:   3750 CONTINUE
```

```
      DOS4A
250:   3750  CONTINUE
251:  C
252:  C
253:        CCHORD=ARCHOR
254:  C
255:  C
256:        PI=3.14159
257:        AOAR=AOA*PI/180.0
258:        CD=CNORM*SIN(AOAR)+CCHORD*COS(AOAR)
259:        CL1=CNORM*COS(AOAR)
260:        WRITE(10,900)TIME,AOA,CL1,CD,CMOM
261:   900  FORMAT(F5.0,5F9.4)
262:   1000 CONTINUE
263:        WRITE(10,1100)
264:   1100 FORMAT(//)
265:        IF(RUN.LT.5) GO TO 470
266:        STOP
267:        END
    *
```

ADIO

```
 1:             .Z80
 2:             ENTRY   AD
 3:  ;          A/D SERVICE ROUTINE
 4:  ;          FORTRAN CALLABLE
 5:  ;          CALL AD(VALUE,CHAN,BASE)
 6:  ;
 7:  ;          GET ONE SAMPLE FROM THE CHAN'TH CHANNEL
 8:  ;          ON THE A/D BOARD WITH BASE ADDRESS 'BASE'
 9:  ;
10:  AD:        LD      (VALUE),HL
11:             LD      (CHAN),DE
12:             LD      (BASE),BC
13:             EX      DE,HL   ;HL->CHAN
14:             LD      A,(HL)  ;GET CHAN NO.
15:             LD      HL,(BASE)
16:             LD      C,(HL)  ;GET BASE I/O ADDRESS TO C REG FOR OUTING
17:             OUT     (C),A   ;MODE 0 TO CHAN NO.
18:                             ;USES BASE ADDRESS IN C REG
19:             INC     C       ;POINT TO START CONVERSION PORT
20:             LD      A,0
21:             OUT     (C),A   ;START CONVERSION
22:             DEC     C       ;POINT TO BASE REGISTER
23:  NRDY:      IN      A,(C)   ;GET STATUS
24:             AND     080H    ;BIT 7 IS STATUS, =1 IS BUSY
25:             JR      NZ,NRDY ;NOT ALL 0'S => BUSY
26:             INC     C       ;POINT TO BASE ADD+1
27:             INC     C       ;POINT TO DRL
28:             IN      A,(C)   ;LOW BYTE OF VALUE
29:             LD      E,A
30:             INC     C       ;POINT TO DRH
31:             IN      A,(C)   ;HIGH BYTE OF VALUE
32:             AND     0FH     ;MASK OUT HIGH NIBBLE
33:             LD      D,A     ;DE=VALUE
34:             LD      HL,(VALUE)      ;HL->WHERE TO PUT VALUE
35:             LD      (HL),E  ;PUT LOW BYTE OF VALUE
36:             INC     HL
37:             LD      (HL),D  ;THAT GIVES THE CALLER THE VALUE
38:  ;
39:             RET
40:  ;
41:  VALUE:     DW      0       ;STORAGE FOR ADDRESS OF VALUE
42:  CHAN:      DW      0       ;STORAGE FOR ADDRESS OF CHANNEL NO
43:  BASE:      DW      0       ;STORAGE FOR ADDRESS OF BASE ADDRESS
44:  ;
45:             .Z80
46:             ENTRY DA
47:  ;          CALL DA(VAL,CHAN,BASE)
48:  ;          CHAN IS 0
49:  ;          BASE IS 72(BASE 10)
50:  DA:        LD      A,(DE)          ;GET CHAN
```

```
        ADIO
51:             ADD     A,A             ;DOUBLE IT
52:             INC     A               ;ADD ONE
53:             PUSH    HL              ;SAVE VAL
54:             PUSH    BC              ;
55:             POP     HL              ;HL=>BASE
56:             LD      C,(HL)          ;C=LOW BYTE OF BASE
57:             ADD     A,C             ;
58:             LD      C,A             ;C=LOW BYTE VALUE OF PORT
59:             POP     HL              ;GET VAL
60:             LD      A,(HL)          ;GET LOW BYTE
61:             OUT     (C),A           ;PUT LOW BYTE
62:             DEC     C               ;C=HIGH BYTE PORT
63:             INC     HL              ;HL=>HI BYTE
64:             LD      A,(HL)          ;GET HI BYTE
65:             OUT     (C),A           ;PUT HI BYTE
66:             RET
67:             END
```

```
        STCLK
ENTRY STCLK
.Z80
STCLK:  LD A,017H  ; CHANNEL 1 CTRL WD =TIME/16
        OUT (079H),A
        LD A,09AH  ;TIME CONSTANT
        OUT (079H),A
        LD A,057H  ;CHANNEL 2 CNTRL WD=CTR
        OUT (07AH),A
        LD A,0FFH  ;TIME CONSTANT=256(BASE 10)
        OUT (07AH),A
        LD A,057H  ;CHANNEL 3 CNTRL WD=CTR
        OUT (07BH),A
        LD A,0FFH  ;TIME CONSTANT
        OUT (07BH),A
        JP 0       ;SYSTEM REENTRY POINT
        END STCLK
```

```
    GETTIM
ENTRY GETTIM
.Z80
GETTIM:
        PUSH    HL      ;SAVE DEST ADDRESS
        IN      A,(00AH)
        LD      E,A
        IN      A,(00BH)
        LD      D,A
        LD      HL,0FFFFH       ;MAX COUNT
        XOR     A       ;CLEAR CARRY
        SBC     HL,DE   ;SUBTR CURRENT COUNT FROM MAX COUNT
        EX      DE,HL   ;TIME TO DE
        POP     HL      ;GET ADDRESS
        LD      (HL),E
        INC     HL
        LD      (HL),D
        RET
        END
```

PRINTER

```
10 REM PARALLEL PRINTER PATCH FOR PORTS &E, &F
20 POKE &HF907,&H7F
30 POKE &HF912,&HC3
40 POKE &HF913,&H0
50 POKE &HF914,&HFE
60 POKE &HFE00,&HC3
70 POKE &HFE01,&H7E
80 POKE &HFE02,&H3E
90 POKE &HFE03,&H1
100 POKE &HFE04,&HD3
110 POKE &HFE05,&H7F
120 POKE &HFE06,&H3E
130 POKE &HFE07,&H0
140 POKE &HFE08,&HD3
150 POKE &HFE09,&H7F
160 POKE &HFE0A,&H3E
170 POKE &HFE0B,&HFF
180 POKE &HFE0C,&H3D
190 POKE &HFE0D,&HC2
200 POKE &HFE0E,&HC
210 POKE &HFE0F,&HFE
220 POKE &HFE10,&HC9
230 SYSTEM
```

VITA

Eric J. Stephen was born on 30 September 1959 in Portland, Indiana. After graduation from Jay County High School in 1977, he was accepted into AFROTC at Purdue University in West Lafayette, Indiana. He graduated in 1981 with a Bachelor of Science Degree in Aeronautical and Astronautical Engineering. His first engineering assignment was to the Air Force Wright Aeronautical Laboratories, where he worked as a Composite Design and Fabrication Engineer, working mostly with graphite/epoxy materials. In May of 1985, he entered the School of Engineering at the Air Force Institute of Technology.

Permanent Address: 106 Mangold Drive

Portland, IN 47371

END

5-87

DTIC